ISSN 1881-7831 Online ISSN 1881-784X

DD&T

Drug Discoveries & Therapeutics

Volume 8, Number 3
June, 2014

IRCA BSSA

IACMHR

www.ddtjournal.com

DD&T
Drug Discoveries & Therapeutics

ISSN: 1881-7831
Online ISSN: 1881-784X
CODEN: DDTRBX
Issues/Year: 6
Language: English
Publisher: IACMHR Co., Ltd.

Drug Discoveries & Therapeutics is one of a series of peer-reviewed journals of the International Research and Cooperation Association for Bio & Socio-Sciences Advancement (IRCA-BSSA) Group and is published bimonthly by the International Advancement Center for Medicine & Health Research Co., Ltd. (IACMHR Co., Ltd.) and supported by the IRCA-BSSA and Shandong University China-Japan Cooperation Center for Drug Discovery & Screening (SDU-DDSC).

Drug Discoveries & Therapeutics publishes contributions in all fields of pharmaceutical and therapeutic research such as medicinal chemistry, pharmacology, pharmaceutical analysis, pharmaceutics, pharmaceutical administration, and experimental and clinical studies of effects, mechanisms, or uses of various treatments. Studies in drug-related fields such as biology, biochemistry, physiology, microbiology, and immunology are also within the scope of this journal.

Drug Discoveries & Therapeutics publishes Original Articles, Brief Reports, Reviews, Policy Forum articles, Case Reports, News, and Letters on all aspects of the field of pharmaceutical research. All contributions should seek to promote international collaboration in pharmaceutical science.

Editorial Board

Editorial and Head Office:

Pearl City Koishikawa 603,
2-4-5 Kasuga, Bunkyo-ku,
Tokyo 112-0003, Japan
Tel.: +81-3-5840-9697
Fax: +81-3-5840-9698
E-mail: office@ddtjournal.com

Drug Discoveries & Therapeutics

Editorial and Head Office

Pearl City Koishikawa 603, 2-4-5 Kasuga, Bunkyo-ku,
Tokyo 112-0003, Japan

Tel: +81-3-5840-9697, Fax: +81-3-5840-9698
E-mail: office@ddtjournal.com
URL: www.ddtjournal.com

Editorial Board Members

CONTENTS

Volume 8, Number 3, 2014

Review

Brief Report

Original Articles

Case Report

Commentary

CONTENTS (*Continued*)

Review

DOI: 10.5582/ddt.2014.01026

Perspectives on a combined test of multi serum biomarkers in China: Towards screening for and diagnosing hepatocellular carcinoma at an earlier stage

Keming Zhang[1], Peipei Song[2,*], Jianjun Gao[2], Gaohua Li[1], Xin Zhao[1], Shaogeng Zhang[1]

[1] *Department of Hepatobiliary Surgery, 302 Hospital of Chinese PLA, Beijing, China;*
[2] *Hepato-Biliary-Pancreatic Surgery Division, Graduate School of Medicine, The University of Tokyo, Tokyo, Japan.*

Summary **China has 50% of the worldwide hepatocellular carcinoma (HCC) cases, and the HBV-related cases accounts for approximately 85%. Over the past few decades, although a series of standardized management methods for HCC has been implemented in China, most HCC patient in China still suffered from advanced-stage disease, in consequence, reducing the opportunity of curable treatment that can be offered to achieve long-term disease-free survival for HCC patient. Accordingly, strategies including screening and diagnose HCC at an earlier stage are urgently needed in China. In this study, the current status, challenges, and prospects of early detection of HCC in China have been analyzed. The result indicated the need for using multi serum biomarkers for early HCC detection. During the past ten years, the research on the clinical usefulness of novel serum biomarkers of des-γ-carboxy-prothrombin (DCP), Dickkopf-1 (DKK1) and Midkine (MDK) in early HCC detection for Chinese patients found that the novel serum biomarker can complete the measurement of α-fetoprotein (AFP) in the diagnosis process of HCC, particularly for the patient with negative AFP with/or at an early stage. More large-scale, multi-center studies are expected to be performed in China to provide further evidence, and using novel and reliable serum biomarkers to complement AFP as a new trend is expected to be extensively used in clinical practice to facilitate early detection for those patients with HCC in China.**

Keywords: α-fetoprotein (AFP), des-γ-carboxyprothrombin (DCP), HCC, sensitivity, tumor marker

1. Introduction

Liver cancer is the fifth most common cancer and the second leading cause of cancer-related deaths worldwide, with a reported cases of 782,000 each year (*1*). As the most common type of liver cancer, hepatocellular carcinoma (HCC) is prevalent in Asian countries, accounting for 75-80% cases reported globally (*2,3*). HCC is prevalent in males, the male incidence rates of the following countries or districts in Asia are over 25/100,000 (persons): mainland China (58/100,000), Taiwan (53/100,000), South Korea (45/100,000), Thailand (33.4/100,000), and Hong Kong (29.9/100,000) of particular note is the fact that China alone accounts for 50% of HCC cases worldwide (*4,5*). Currently, HCC become the second and third leading cause of cancer-related deaths respectively in males and in females in China (Table 1) (*6,7*), and the HCC's incidence has increased in the past few decades caused by the high prevalence of its main etiological agents, chronic hepatitis B virus (HBV) infections (*8-10*). In fact, 93 million HBV carriers are Chinese, accounting for 2/3 of such patients worldwide, and about 20 million of these people have chronic HBV infection (*11,12*).

Evidence has shown that surgical resection and liver transplantation may offer the best opportunity for treating HCC yet are only available to early-detected patients (*13-16*). The normal overall 5-year survival rate is 40%, but with a liver resection to treat early HCC, the 5-year survival rate rise to 60-70% (*17,18*). Over the past few decades, a series of standardized management methods for HCC has been implemented

**Address correspondence to:*
Dr. Peipei Song, Hepato-Biliary-Pancreatic Surgery Division, Graduate School of Medicine, The University of Tokyo, 7-3-1Hongo, Bunkyo-ku, Tokyo 113-8655, Japan.
E-mail: ppsong-tky@umin.ac.jp

Table 1.The current status to screen for and diagnose HCC in China

Items	Current status in China
Prevalence	The second most common cancer in urban areas and most common in rural areas; with an overall prevalence rate of 26-32/10,000, even up to 70-80/10,000 in some areas (*5,11*)
Mortality	The second leading cause of cancer-related deaths in males and the third leading cause of cancer-related deaths in females; with a total mortality rate of 26.26/100,000 (*11*)
Etiological factors	85% of patients with HBV infection, 10% of patients with HCVinfection, and a small minority involve HBV and HCV (*8,9*)
Major at-risk population	People with HBV infection; 93 million HBV carriers, 20 millionof these with chronic HBV Infection (*11,12*)
Screening and surveillance	No government-funded screening and surveillance program for HCC high-risk population screening and surveillance (*10*)
Screening and Diagnostic algorithm	The test of ultrasonography and AFP every 6 months for the population ages 35-40 at risk for developing HCC (*6*)
Treatment algorithm	Comprehensive therapy predominantly in the form of surgery (*7*)
Early detection	Most patients with HCC present with advanced-stage disease (*10*)

by China Government, and the Expert Consensus on the Treatment Standards for Hepatic Carcinoma, the Chinese Guidelines on HCC, was drafted in 2009 (*19*). Currently, standard treatment for HCC in China is comprehensive therapy predominantly in the form of surgery (*7,20*). As clinical techniques have developed in China, new techniques have also become available, such as laparoscopic surgery and minimally invasive robotic surgery. However, most HCC patient in China still suffered from advanced-stage disease (*10*), thus reducing the chance of curable treatment. Accordingly, strategies to screen for and diagnose HCC at an earlier stage are urgently needed in China when curable interventions can be offered to achieve long-term disease-free survival for HCC patient (*21*).

2. The current strategies to screen for and diagnose HCC in China

2.1. *Screening high-risk population for developing HCC*

Evidence showed that screening high-risk HBV- or HCV-related chronic liver diseases population may improve the rate of early HCC detection and curative treatment. It has been found by a systematic literature review involving over three thousand papers included in PubMed database between 2001 and 2011 (*22*), and it has also been shown by several cohort studies (*23-25*).

Unlike in the USA, European countries, and other Asian countries such as Japan where HCV is the most significant etiological factor for developing HCC (*26*), the HBV-related cases accounts for approximately 85% while only 10% are HCV-related and a small minority involve HBV and HCV in China (*8,9*). Thus, people with HBV are the largest risk population for developing HCC in China.

Globally, many guidelines for HCC treatment recommend HCC screening and surveillance, including the guidelines established by the American Association for the Study of Liver Disease (AASLD) (*27*), the National Comprehensive Cancer Network (NCCN) (*28*), and the Asian Pacific Association for the Study of the Liver (APASL) (*29*). In Asia, Japan and South Korea have implemented their own nationwide screening and surveillance program for the HCC high-risk population. In Japan, as early as 2002, the Japanese Ministry of Health, Labor, and Welfare started a national 5-year program to screen for HCV and HBV infection among people over 40 years of age, given the high prevalence of HCV infection in this age group (*30*). With the support of this program, 9 million people had been screened until the end of 2006, 112,000 scanning objects were found infected HCV and 110,000 were found infected HBV (*31*). Since most high-risk patients were closely followed, more than 60% of cases had detected HCC nodules in the early stage in Japan (*32,33*).

Similarly, a screening and surveillance program has also established in Taiwan. The program focuses on screening patients with cirrhosis every 3-6 months and patients with no cirrhosis every 6-12 months (*10,34*). However, there is no such program funded by government for HCC high-risk population screening in China, including Hong Kong (*10*). As a result, a well thought-out strategy for screening high-risk populations with HBV-related chronic liver disease is urgently needed in China to enhance the early detection of HCC.

2.2. *Serum biomarkers for screening and diagnosis of HCC*

Screening and diagnosis tools should have an acceptable accuracy and cost. In general, imaging tools have been

widely used in the USA and European countries, while serum biomarkers are widely used in HCC screening and diagnosis in Asia. Diagnostic imaging techniques include ultrasonography, computed tomography (CT), and magnetic resonance imaging (MRI). According to a systematic review, ultrasonography has a 60% sensitivity and a 97% specificity, CT has a 68% sensitivity and a 93% specificity, and MRI has a 81% sensitivity and a 85% specificity (*35*). Ultrasound is the most common imaging tool used in the screening process for HCC thanks to is the features such as simple, inexpensive, non-invasive, and allows real-time observation. However, a successful ultrasound-detection relies on the expertise of the physician, the available of ultrasound equipment, and the echo texture of the liver. So the actual sensitivity and specificity of ultrasound-detection is difficult to evaluate due to the lack of standard in China (*36,37*).

Serum biomarkers are striking prospective alternative tools for screening and early diagnosis of HCC thanks to the non-invasive, objective, and reproducible assessments they would enabled (*38*). According to the Chinese Guidelines on HCC, ultrasonography and α-fetoprotein (AFP) measurement are recommended to be performed every 6 months for the people ages between 35 and 40 at risk for developing HCC (*6*). Currently, the serum biomarker AFP is considered as a useful and practicable tool for the screening and early diagnosis of HCC in China. The clinical usefulness of AFP in China has been ascertained by a trial that with a randomized control in 2004 which involved 18,816 Chinese patients aged between 35 and 59 with HBV infection or a history of chronic hepatitis (*39*). However, the sensitivity of AFP is unsatisfactory (25-65%) at the commonly used cut-off (20 ng/mL), especially in the detection of early-stage HCC (*40,41*), up to 50% of HCC patients have an AFP level below 20 ng/mL. Elevated levels of AFP could also be found in non-malignant chronic liver disease patients, including 15-58% with chronic hepatitis and 11-47% with liver cirrhosis (*42-44*).

Besides, there are many diagnostic difficulties in clinical practice, such as cases with high AFP level, but no space occupying lesion by imaging finding, cases with negative AFP, less than 1 cm or no HCC featured lesion by imaging finding (*7*). Thus, AFP cannot be used as a sole tool to screening and diagnose HCC. The novel and dependable serum biomarkers to complement AFP are urgently needed to be discovered in order to improve the clinical outcomes.

3. The future perspective on using multi serum biomarkers in early HCC detection in China

3.1. *The combined test of AFP, AFP-L3, and DCP*

Besides AFP, there are two other serum biomarkers – lens culinaris agglutinin-reactive fraction of AFP (AFP-L3), and des-γ-carboxyprothrombin (DCP, also known as prothrombin induced by vitamin K absence-II, PIVKA-II) – that have been studied worldwide to explore for clinical usefulness in HCC screening and diagnosis, and has been used in some countries (*45-48*). According to HCC Guidelines in Japan, ultrasonography and measurement of AFP, AFP-L3, or DCP should be performed every 3-4 months in the highest-risk group (HBV- or HCV-related liver cirrhosis patients) and every 6-month in the high-risk group (patients with HBV- or HCV-related chronic liver disease or liver cirrhosis due to other causes) (*49,50*). Currently, AFP, AFP-L3, and DCP are used widely and routinely as a tool for screening HCC in Japan, and these tests are covered by Japan's national health insurance as the serum biomarkers to screen for HCC in clinical settings.

Worldwide, a number of researches have carried out at DCP. In 1984, Liebman *et al*.(*51*) first reported DCP in the plasma of 90% of patients with HCC. Since then, substantial evidence has been assembled through numerous clinical trials, and studies have demonstrated the clinical usefulness of serum DCP levels to screen for and diagnose patients with HCC (*48,52,53*). Multiple reports have found that the combined testing of DCP and AFP have a sensitivity of 47.5-94.0% and specificity of 53.3-98.5% in HCC early detection (Table 2) (*45,46,48,53-67*).

Meanwhile, many researchers recommend that DCP could also be used in assessing the progression of HCC, including serving as an HCC recurrence indicator after curative therapy, a good predictor of the vascular invasion presence and could be used to select liver transplants' recipients, and could facilitate the research of new chemotherapeutic strategies for treating HCC (*68-74*). However, currently, DCP is approved in Japan, Korea and Indonesia (*75*), yet has not been approved in China until now.

3.2. *Evidence for exploration of using DCP in early HCC detection in China*

Evidence has shown that the test that combine DCP and AFP could achieve a better sensitivity and specificity in HCC early detection, and the testing of DCP has been widely used for many HCV-related HCC cases, such as in Japan. But in China, 85% of HCC cases have HBV infection. So, is DCP applicable as a screening and diagnostic tool in China? What about its sensitivity and specificity in Chinese HCC cases? Furthermore, what is its clinical usefulness in assessing HCC progression? According to evidence-based medicine (EBM), systematic evaluation needs to be performed to assess the screening and diagnostic value of DCP in Chinese patients with HCC.

In China, such a study was conducted in 2002 to

Table 2.The exploration of clinical usefulness of using serum biomarker DCP to complement AFP in HCC early detection*

Marker	Cut-off value	Sensitivity[a]	Specificity[a]	PPV[a]	NPV[a]
DCP + AFP (*54*)	8 mAU/mL, 20 ng/mL	90.0% (90/100)	*N*	*N*	*N*
DCP + AFP (*55*)	16 mAU/mL, 20 ng/mL	87.3% (55/63)	84.0% (158/188)	64.7% (55/85)	95.2% (158/166)
DCP + AFP (*56*)	40 mAU/mL, 20 ng/mL	83.5% (76/91)	*N*	*N*	*N*
DCP + AFP (*57*)	40 mAU/mL, 20 ng/mL	86.7% (52/60)	*N*	*N*	*N*
DCP + AFP (*58*)	40 mAU/mL, 20 ng/mL	78.3% (94/120)	58.9% (53/90)	71.8% (94/131)	67.1% (53/79)
DCP + AFP (*62*)	40 mAU/mL, 20 ng/mL	83.6% (51/61)	68.2% (45/66)	70.8% (51/72)	81.8% (45/55)
DCP + AFP (*63*)	40 mAU/mL, 20 ng/mL	83.3% (204/245)	77.2% (206/267)	77.0% (204/265)	83.4% (206/247)
DCP + AFP (*59*)	40 mAU/mL, 200 ng/mL	78.3% (83/106)	*N*	*N*	*N*
DCP + AFP (*45*)	80 mAU/mL, 40 ng/mL	65.5% (19/29)	84.5% (596/705)	14.8% (19/128)	98.3% (596/606)
DCP + AFP (*64*)	90 mAU/mL, 45 ng/mL	84.4% (130/154)	*N*	*N*	*N*
DCP + AFP (*60*)	100 mAU/mL, 100 ng/mL	72.4% (55/76)	*N*	*N*	*N*
DCP + AFP (*60*)	100 mAU/mL, 300 ng/mL	63.2% (48/76)	*N*	*N*	*N*
DCP + AFP (*48*)	150 mAU/mL, 20 ng/mL	86% (-/-)[b]	63% (-/-)[b]	*N*	*N*
DCP + AFP (*48*)	619 mAU/mL, 27 ng/mL	74% (-/-)[b]	87% (-/-)[b]	*N*	*N*
DCP + AFP (*64*)	0.8 ng/mL, 45 ng/mL	88.3% (136/154)	*N*	*N*	*N*
DCP + AFP (*53*)	20.24 ng/mL, 15 ng/mL	94.0% (47/50)	80.5% (33/41)	85.5% (47/55)	91.7% (33/36)
DCP + AFP (*65*)	0.1 μg/mL, 20 ng/mL	92.9% (65/70)	53.3% (24/45)	75.6% (65/86)	82.8% (24/29)
DCP + AFP (*65*)	0.1 mg/mL, 400 ng/mL	85.7% (60/70)	82.2% (37/45)	88.2% (60/68)	78.7% (37/47)
DCP + AFP (*66*)	40 mAU/ml, 20 ng/ml	78.3% (47/60)	56.7% (17/30)	*N*	*N*
DCP + AFP (*54*)	8 mAU/mL, 20 ng/mL	66.7% (18/27)	*N*	*N*	*N*
DCP + AFP (*55*)	16 mAU/mL, 20 ng/mL	82.9% (29/35)	84.0% (158/188)	49.2% (29/59)	96.3% (158/164)
DCP + AFP (*58*)	40 mAU/mL, 20 ng/mL	59.4% (-/-) b	58.9% (53/90)	*N*	*N*
DCP + AFP (*48*)	150 mAU/mL, 20 ng/mL	78% (-/-)[b]	62% (-/-)[b]	*N*	*N*
DCP + AFP (*48*)	598 mAU/mL, 11 ng/mL	70% (-/-)[b]	80% (-/-)[b]	*N*	*N*
DCP + AFP (*55*)	16 mAU/mL, 20 ng/mL	61.5% (8/13)	84.0% (158/188)	21.1% (8/38)	96.9% (158/163)
DCP + AFP (*56*)	40 mAU/mL, 20 ng/mL	83.7% (36/43)	*N*	*N*	*N*
DCP + AFP (*67*)	40 mAU/mL, 200 ng/mL	47.5% (29/61)	98.5% (132/134)	93.5% (29/31)	80.5% (132/164)
DCP + AFP-L3 (*61*)	40 mAU/mL, 10%	41.7% (15/36)	89.8% (44/49)	75.0% (15/20)	67.7% (44/65)
DCP + AFP-L3 (*46*)	40 mAU/mL, 10%	66.7% (14/21)	89.5% (51/57)	70.0% (14/20)	87.9% (51/58)
DCP + AFP-L3 (*67*)	40 mAU/mL, 10%	54.1% (33/61)	97.8% (131/134)	91.7% (33/36)	82.4% (131/159)

* In all studies indicated, patients with chronic hepatitis and/or liver cirrhosis were designated as the comparative non-HCC patient group. [a] Sensitivity = True positive (TP) / (TP + Falsenegative (FN)), Specificity = True negative (TN) / (TN + False positive (FP)), Positive predictive value (PPV) = TP / TP + FP, Negative predictive value (NPV) = TN / TN + FN. [b] The patient distribution was not noted. *N*, Not noted or not investigated.

determine DCP and AFP levels in 60 patients with HCC and 30 patients with cirrhosis but no HCC (*66*), results showed that the combined testing of DCP and AFP could achieve a sensitivity of 78.3%, which is higher than that of DCP alone (51.7%) and AFP alone (56.7%). Another study to assess the clinical usefulness of DCP involving 120 Chinese patients with HCC and 90 patients with cirrhosis was reported in 2003 (*58*), and results also showed that the combined tests of DCP and AFP had a sensitivity of 78.3%, which is higher than that of DCP (53.3%) and AFP alone (58.3%).

Moreover, a large-scale, multi-center study of DCP's usefulness in early HCC detection was also launched in Chongqing, Beijing, and Tianjin of China in 2012 (*11*). As part of the study, the test was conducted in one of the centers - the Southwest Hospital, Third Military Medical University in Chongqing - involving 336 patients with HCC (80% have HBV infection) and 252 patients with liver diseases other than HCC. Results showed that there is no significant correlation between serum levels of DCP and AFP (R^2 = 0.0179); DCP had a total sensitivity of 74% while a combination of DCP and AFP had a sensitivity of 84%, which is higher than either DCP or AFP alone (*7,11*). Besides, DCP resulted in a specificity of 56% with a cut-off value of 40 mAU/mL and 94% with a cut-off value of 100 mAU/mL (*32*).

These studies found that the combined tests of DCP and AFP could improve sensitivity for detecting Chinese HCC cases, thus suggesting that DCP is a useful serum biomarker in Chinese patients for HCC screening and early diagnosis. Such evidence provides a better perspective for using DCP in HCC early detection in China. However, more large-scale, multi-center studies are expected to be performed in China to provide further evidence of the clinical usefulness of serum biomarker DCP in early HCC detection, especially with long-term surveillance and follow-up to provide strong data-support and verification.

3.3. *Research advances in other serum biomarkers for early HCC detection in China*

In recent years, there are also many studies on the clinical usefulness of other serum biomarkers in early HCC detection, including Golgi protein-73 (GP73), glypican-3 (GPC3), gamma-glutamyltransferase (GGTII), and so on. Most recently, research on

Dickkopf-1 (DKK1) and Midkine (MDK) as diagnostic serum biomarkers has raised concern in China.

Serum DKK1 as a biomarker in HCC diagnosis Published in 2012, a large-scale, multi-centre study assessed serum DKK1 for HCC diagnosis in 1,284 participants (831 in the test cohort and 453 in the validation cohort) in China (*76,77*). Results showed that serum's levels of DKK1 were significantly higher in HCC patients than in all controls; serum DKK1 had greater AUC, sensitivity, and specificity values than did AFP in patients with HCC compared with chronic HBV infection and cirrhosis controls; DKK1 maintained high diagnostic accuracy for AFP negative HCC patients, including early-stage HCC patients; raised concentrations of DKK1 in serum could distinguish HCC from chronic HBV infection and cirrhosis; measurement of DKK1 and AFP together improved diagnostic accuracy against HCC versus all controls compared with any test alone.

Serum MDK as a biomarker in HCC diagnosis Published in 2013, a study that involved three independent cohorts with a total of 933 participants including 388 HCC cases and 545 different controls enrolled from different medical centers (*78*). Results showed that MDK levels were significantly elevated in HCC tissues as well as serum samples; serum MDK for HCC diagnosis showed an obviously higher sensitivity compared with AFP (86.9% *vs*.51.9%) with similar specificities (83.9% *vs*.86.3%); even in very early-stage HCC, the sensitivity of MDK is significant higher than AFP (80% *vs*. 40%); in those AFP-negative HCC cases, the sensitivity could reach as high as 89.2%; and serum MDK level was significantly decreased in HCC patients after curative resection and re-elevated when tumor relapsed.

Both of the two studies suggested that the novel serum biomarkers of DKK1 and MDK can complete the measurement of AFP in the diagnosis process of HCC, particularly for those negative AFP patients and/or at an early stage. However, these studies were small-scale. According to the guidelines on phases of evaluating an early detection biomarker for cancer developed by the National Cancer Institute's Early Detection Research Network (*79*), further validation using larger cohort of serum HCC samples with hepatitis B and hepatitis C infectious liver disease, nonalcoholic fatty liver disease (NAFLD), and alcohol-induced liver disease (ALD) from multiple centers in a prospective, randomized controlled trial is needed to provide further evidence in China.

In conclusion, research and exploration for using multi serum biomarkers in early HCC detection has raised concern in China. Using novel and reliable serum biomarkers to complement AFP as a new trend is expected to be extensively used in China to facilitate screening for and diagnosing HCC at an earlier stage and improve clinical outcomes.

References

1. World Health Organization. GLOBOCAN 2012: Estimated Cancer Incidence, Mortality and Prevalence Worldwide in 2012. *http://globocan.iarc.fr/Pages/fact_sheets_cancer.aspx* (accessed May 20, 2014)
2. Jemal A, Bray F, Center MM, Ferlay J, Ward E, Forman D. Global cancer statistics. CA Cancer J Clin. 2011; 61:69-90.
3. Venook AP, Papandreou C, Furuse J, de Guevara LL. The incidence and epidemiology of hepatocellular carcinoma: a global and regional perspective. The oncologist. 2010; 15 Suppl 4:5-13.
4. Asia-Pacific Working Party on Prevention of Hepatocellular C. Prevention of hepatocellular carcinoma in the Asia-Pacific region: Consensus statements. Journal of gastroenterology and hepatology. 2010; 25:657-663.
5. Yuen MF, Hou JL, Chutaputti A, Asia Pacific Working Party on Prevention of Hepatocellular C. Hepatocellular carcinoma in the Asia pacific region. Journal of gastroenterology and hepatology. 2009; 24:346-353.
6. Chinese Anti-Cancer Association Society of Liver Cancer, Chinese Society of Clinical Oncology, Chinese Society of Hepatology Liver Cancer Study Group. The expert consensus on the treatment standards for hepatocellular carcinoma. Digestive Disease and Endoscopy. 2009; 3:40-51.
7. Song P, Feng X, Zhang K, Song T, Ma K, Kokudo N, Dong J, Tang W. Perspectives on using des-γ-carboxyprothrombin (DCP) as a serum biomarker: Facilitating early detection of hepatocellular carcinoma in China. Hepatobiliary Surg Nutr. 2013; 2:227-231.
8. Tanaka M, Katayama F, Kato H, Tanaka H, Wang J, Qiao YL, Inoue M. Hepatitis B and C virus infection and hepatocellular carcinoma in China: A review of epidemiology and control measures. J Epidemiol. 2011; 21:401-416.
9. Yuen MF, Hou JL, Chutaputti A. Hepatocellular carcinoma in the Asia pacific region. J Gastroenterol Hepatol. 2009; 24:346-353.
10. Kudo M, Han KH, Kokudo N, Cheng AL, Choi BI, Furuse J, Izumi N, Park JW, Poon RT, Sakamoto M. Liver Cancer Working Group report. Jpn J Clin Oncol. 2010; 40 Suppl 1:i19-27.
11. Song P, Feng X, Zhang K, Song T, Ma K, Kokudo N, Dong J, Yao L, Tang W. Screening for and surveillance of high-risk patients with HBV-related chronic liver disease: promoting the early detection of hepatocellular carcinoma in China. Biosci Trends. 2013; 7:1-6.
12. Zhang C, Zhong Y, Guo L. Strategies to prevent hepatitis B virus infection in China: immunization, screening, and standard medical practices. Biosci Trends. 2013; 7:7-12.
13. Qin LX, Tang ZY. Recent progress in predictive biomarkers for metastatic recurrence of human hepatocellular carcinoma: A review of the literature. J Cancer Res Clin Oncol. 2004; 130:497-513.
14. Ji J, Shi J, Budhu A, *et al*. MicroRNA expression, survival, and response to interferon in liver cancer. N Engl J Med. 2009; 361:1437-1447.
15. Llovet JM, Di Bisceglie AM, Bruix J, Kramer BS, Lencioni R, Zhu AX, Sherman M, Schwartz M, Lotze M, Talwalkar J, Gores GJ. Design and endpoints of clinical trials in hepatocellular carcinoma. J Natl Cancer Inst. 2008; 100:698-711.

16. Akamatsu N, Sugawara Y. Primary biliary cirrhosis and liver transplantation. Intractable Rare Dis Res 1: 66-80,2012.
17. Gao JJ, Song PP, Tamura S, Hasegawa K, Sugawara Y, Kokudo N, Uchida K, Orii R, Qi FH, Dong JH, Tang W. Standardization of perioperative management on hepato-biliary-pancreatic surgery. Drug Discov Ther. 2012; 6:108-111.
18. Llovet JM, Burroughs A, Bruix J. Hepatocellular carcinoma. Lancet. 2003; 362:1907-1917.
19. Song P, Tang W, Tamura S, Hasegawa K, Sugawara Y, Dong J, Kokudo N. The management of hepatocellular carcinoma in Asia: A guideline combining quantitative and qualitative evaluation. Biosci Trends. 2010; 4:283-287.
20. Feng XB, Zheng SG, Xia F, Ma KS, Wang SG, Bie P, Dong JH. Classification and management of hepatolithiasis: A high-volume, single-center's experience. Intractable Rare Dis Res 1: 151-156, 2012.
21. Forner A, Llovet JM, Bruix J. Hepatocellular carcinoma. Lancet. 2012; 379:1245-1255.
22. Song P, Tobe RG, Inagaki Y, Kokudo N, Hasegawa K, Sugawara Y, Tang W. The management of hepatocellular carcinoma around the world: A comparison of guidelines from 2001 to 2011. Liver Int. 2012; 32:1053-1063.
23. Yuen MF, Cheng CC, Lauder IJ, Lam SK, Ooi CG, Lai CL. Early detection of hepatocellular carcinoma increases the chance of treatment: Hong Kong experience. Hepatology. 2000; 31:330-335.
24. Bolondi L, Sofia S, Siringo S, Gaiani S, Casali A, Zironi G, Piscaglia F, Gramantieri L, Zanetti M, Sherman M. Surveillance programme of cirrhotic patients for early diagnosis and treatment of hepatocellular carcinoma: a cost effectiveness analysis. Gut. 2001; 48:251-259.
25. Danta M, Barnes E, Dusheiko G. The surveillance and diagnosis of hepatocellular carcinoma. Eur J Gastroenterol Hepatol. 2005; 17:491-496.
26. Byam J, Renz J, Millis JM. Liver transplantation for hepatocellular carcinoma. Hepatobiliary Surg Nutr. 2013; 2: 22-30.
27. Bruix J, Sherman M. Management of hepatocellular carcinoma. Hepatology. 2005; 42:1208-1236.
28. Benson AB, 3rd, Abrams TA, Ben-Josef E, *et al*. NCCN clinical practice guidelines in oncology: hepatobiliary cancers. J Natl Compr Canc Netw. 2009; 7:350-391.
29. Omata M, Lesmana LA, Tateishi R, *et al*. Asian Pacific Association for the Study of the Liver consensus recommendations on hepatocellular carcinoma. Hepatol Int. 2010; 4:439-474.
30. Yoshizawa H, Tanaka J: A national project for the management of viral hepatitis toward prevention of hepatocellular carcinoma in Japan; in Morrissey RF (ed): International Kilmer Conference Proceedings. Laval, Polyscience Publications, vol 8, pp 247-264, 2004.
31. Yoshizawa H, Tanaka J, Miyakawa Y. National prevention of hepatocellular carcinoma in Japan based on epidemiology of hepatitis C virus infection in the general population. Intervirology. 2006; 49:7-17.
32. Song PP, Gao JJ, Inagaki Y, Kokudo N, Hasegawa K, Sugawara Y, Tang W. Biomarkers: Evaluation of screening for and early diagnosis of hepatocellular carcinoma in Japan and China. Liver Cancer. 2013;2: 31-39.
33. Izumi N. Diagnostic and treatment algorithm of the Japanese society of hepatology: a consensus-based practice guideline. Oncology. 2010; 78 Suppl 1:78-86.
34. Chen TH, Chen CJ, Yen MF, Lu SN, Sun CA, Huang GT, Yang PM, Lee HS, Duffy SW. Ultrasound screening and risk factors for death from hepatocellular carcinoma in a high risk group in Taiwan. Int J Cancer. 2002; 98:257-261.
35. Colli A, Fraquelli M, Casazza G, Massironi S, Colucci A, Conte D, Duca P. Accuracy of ultrasonography, spiral CT, magnetic resonance, and alpha-fetoprotein in diagnosing hepatocellular carcinoma: a systematic review. Am J Gastroenterol. 2006; 101:513-523.
36. Aghoram R, Cai P, Dickinson JA. Alpha-foetoprotein and/or liver ultrasonography for screening of hepatocellular carcinoma in patients with chronic hepatitis B. Cochrane Database Syst Rev. 2012; 9:CD002799.
37. Amarapurkar D, Han KH, Chan HL, Ueno Y. Application of surveillance programs for hepatocellular carcinoma in the Asia-Pacific Region. J Gastroenterol Hepatol. 2009; 24:955-961.
38. Forner A, Bruix J. Biomarkers for early diagnosis of hepatocellular carcinoma. Lancet Oncol. 2012; 13:750-751.
39. Zhang BH, Yang BH, Tang ZY. Randomized controlled trial of screening for hepatocellular carcinoma. J Cancer Res Clin Oncol. 2004; 130:417-422.
40. Farinati F, Marino D, De Giorgio M, Baldan A, Cantarini M, Cursaro C, Rapaccini G, Del Poggio P, Di Nolfo MA, Benvegnu L, Zoli M, Borzio F, Bernardi M, Trevisani F. Diagnostic and prognostic role of alpha-fetoprotein in hepatocellular carcinoma: both or neither? Am J Gastroenterol. 2006; 101:524-532.
41. El-Serag HB, Marrero JA, Rudolph L, Reddy KR. Diagnosis and treatment of hepatocellular carcinoma. Gastroenterology. 2008; 134:1752-1763.
42. Daniele B, Bencivenga A, Megna AS, Tinessa V. Alpha-fetoprotein and ultrasonography screening for hepatocellular carcinoma. Gastroenterology. 2004; 127:S108-112.
43. Taketa K. Alpha-fetoprotein: Reevaluation in hepatology. Hepatology. 1990; 12:1420-1432.
44. Johnson PJ. The role of serum alpha-fetoprotein estimation in the diagnosis and management of hepatocellular carcinoma. Clin Liver Dis. 2001; 5:145-159.
45. Ishii M, Gama H, Chida N, Ueno Y, Shinzawa H, Takagi T, Toyota T, Takahashi T, Kasukawa R. Simultaneous measurements of serum alpha-fetoprotein and protein induced by vitamin K absence for detecting hepatocellular carcinoma. South Tohoku District Study Group. Am J Gastroenterol. 2000; 95:1036-1040.
46. Shimauchi Y, Tanaka M, Kuromatsu R, Ogata R, Tateishi Y, Itano S, Ono N, Yutani S, Nagamatsu H, Matsugaki S, Yamasaki S, Tanikawa K, Sata M. A simultaneous monitoring of Lens culinaris agglutinin A-reactive alpha-fetoprotein and des-gamma-carboxy prothrombin as an early diagnosis of hepatocellular carcinoma in the follow-up of cirrhotic patients. Oncol Rep. 2000; 7:249-256.
47. Durazo FA, Blatt LM, Corey WG, Lin JH, Han S, Saab S, Busuttil RW, Tong MJ. Des-gamma-carboxyprothrombin, alpha-fetoprotein and AFP-L3 in patients with chronic hepatitis, cirrhosis and hepatocellular carcinoma. J Gastroenterol Hepatol. 2008; 23:1541-1548.
48. Marrero JA, Feng Z, Wang Y, *et al*. Alpha-fetoprotein,

des-gamma carboxyprothrombin, and lectin-bound alpha-fetoprotein in early hepatocellular carcinoma. Gastroenterology. 2009; 137:110-118.
49. Clinical Practice Guidelines for Hepatocellular Carcinoma - The Japan Society of Hepatology 2009 update. Hepatol Res. 2010; 40 Suppl 1:2-144.
50. Makuuchi M, Kokudo N, Arii S, Futagawa S, Kaneko S, Kawasaki S, Matsuyama Y, Okazaki M, Okita K, Omata M, Saida Y, Takayama T, Yamaoka Y. Development of evidence-based clinical guidelines for the diagnosis and treatment of hepatocellular carcinoma in Japan. Hepatol Res. 2008; 38:37-51.
51. Liebman HA, Furie BC, Tong MJ, Blanchard RA, Lo KJ, Lee SD, Coleman MS, Furie B. Des-gamma-carboxy (abnormal) prothrombin as a serum marker of primary hepatocellular carcinoma. N Engl J Med. 1984; 310:1427-1431.
52. Volk ML, Hernandez JC, Su GL, Lok AS, Marrero JA. Risk factors for hepatocellular carcinoma may impair the performance of biomarkers: A comparison of AFP, DCP, and AFP-L3. Cancer Biomark. 2007; 3:79-87.
53. Beale G, Chattopadhyay D, Gray J, Stewart S, Hudson M, Day C, Trerotoli P, Giannelli G, Manas D, Reeves H. AFP, PIVKAII, GP3, SCCA-1 and follisatin as surveillance biomarkers for hepatocellular cancer in non-alcoholic and alcoholic fatty liver disease. BMC Cancer. 2008; 8:200.
54. Soga K, Watanabe T, Aikawa K, Toshima M, Shibasaki K, Aoyagi Y. Serum des-gamma-carboxyprothrombin level by a modified enzyme immunoassay method in hepatocellular carcinoma: Clinical significance in small hepatocellular carcinoma. Hepatogastroenterology. 1998; 45:1737-1741.
55. Ikoma J, Kaito M, Ishihara T, Nakagawa N, Kamei A, Fujita N, Iwasa M, Tamaki S, Watanabe S, Adachi Y. Early diagnosis of hepatocellular carcinoma using a sensitive assay for serum des-gamma-carboxy prothrombin: A prospective study. Hepatogastroenterology. 2002; 49:235-238.
56. Mita Y, Aoyagi Y, Yanagi M, Suda T, Suzuki Y, Asakura H. The usefulness of determining des-gamma-carboxy prothrombin by sensitive enzyme immunoassay in the early diagnosis of patients with hepatocellular carcinoma. Cancer. 1998; 82:1643-1648.
57. Okuda H, Nakanishi T, Takatsu K, Saito A, Hayashi N, Watanabe K, Magario N, Yokoo T, Naraki T. Measurement of serum levels of des-gamma-carboxy prothrombin in patients with hepatocellular carcinoma by a revised enzyme immunoassay kit with increased sensitivity. Cancer. 1999; 85:812-818.
58. Cui R, He J, Zhang F, Wang B, Ding H, Shen H, Li Y, Chen X. Diagnostic value of protein induced by vitamin K absence (PIVKAII) and hepatoma-specific band of serum gamma-glutamyl transferase (GGTII) as hepatocellular carcinoma markers complementary to alpha-fetoprotein. Br J Cancer. 2003; 88:1878-1882.
59. Tanaka Y, Kashiwagi T, Tsutsumi H, Nagasawa M, Toyama T, Ozaki S, Naito M, Ishibashi K, Azuma M. Sensitive measurement of serum abnormal prothrombin (PIVKA-II) as a marker of hepatocellular carcinoma. Hepatogastroenterology. 1999; 46:2464-2468.
60. Nakao A, Suzuki Y, Isshiki K, Kimura Y, Takeda S, Kishimoto W, Nonami T, Harada A, Takagi H. Clinical evaluation of plasma abnormal prothrombin (des-gamma-carboxy prothrombin) in hepatobiliary malignancies and other diseases. Am J Gastroenterol. 1991; 86:62-66.
61. Nomura F, Ishijima M, Kuwa K, Tanaka N, Nakai T, Ohnishi K. Serum des-gamma-carboxy prothrombin levels determined by a new generation of sensitive immunoassays in patients with small-sized hepatocellular carcinoma. Am J Gastroenterol. 1999; 94:650-654.
62. Wang CS, Lin CL, Lee HC, Chen KY, Chiang MF, Chen HS, Lin TJ, Liao LY. Usefulness of serum des-gamma-carboxy prothrombin in detection of hepatocellular carcinoma. World J Gastroenterol. 2005; 11:6115-6119.
63. Kim do Y, Paik YH, Ahn SH, Youn YJ, Choi JW, Kim JK, Lee KS, Chon CY, Han KH. PIVKA-II is a useful tumor marker for recurrent hepatocellular carcinoma after surgical resection. Oncology. 2007; 72 Suppl 1:52-57.
64. Lamerz R, Runge M, Stieber P, Meissner E. Use of serum PIVKA-II (DCP) determination for differentiation between benign and malignant liver diseases. Anticancer Res. 1999; 19:2489-2493.
65. Deyashiki Y, Nishioka Y, Takahashi K, Kosaka Y, Suzuki K. Evaluation of des-gamma-carboxy prothrombin as a marker protein of hepatocellular carcinoma. Cancer. 1989; 64:2546-2551.
66. Cui R, Wang B, Ding H, Shen H, Li Y, Chen X. Usefulness of determining a protein induced by vitamin K absence in detection of hepatocellular carcinoma. Chin Med J (Engl). 2002; 115:42-45.
67. Sassa T, Kumada T, Nakano S, Uematsu T. Clinical utility of simultaneous measurement of serum high-sensitivity des-gamma-carboxy prothrombin and Lens culinaris agglutinin A-reactive alpha-fetoprotein in patients with small hepatocellular carcinoma. Eur J Gastroenterol Hepatol. 1999; 11:1387-1392.
68. Tang W, Miki K, Kokudo N, Sugawara Y, Imamura H, Minagawa M, Yuan LW, Ohnishi S, Makuuchi M. Des-gamma-carboxy prothrombin in cancer and non-cancer liver tissue of patients with hepatocellular carcinoma. Int J Oncol. 2003; 22:969-975.
69. Yuan LW, Tang W, Kokudo N, Sugawara Y, Karako H, Hasegawa K, Aoki T, Kyoden Y, Deli G, Li YG, Makuuchi M. Measurement of des-gamma-carboxy prothrombin levels in cancer and non-cancer tissue in patients with hepatocellular carcinoma. Oncol Rep. 2004; 12:269-273.
70. Tang W, Kokudo N, Sugawara Y, Guo Q, Imamura H, Sano K, Karako H, Qu X, Nakata M, Makuuchi M. Des-gamma-carboxyprothrombin expression in cancer and/or non-cancer liver tissues: association with survival of patients with resectable hepatocellular carcinoma. Oncol Rep. 2005; 13:25-30.
71. Inagaki Y, Tang W, Makuuchi M, Hasegawa K, Sugawara Y, Kokudo N. Clinical and molecular insights into the hepatocellular carcinoma tumour marker des-gamma-carboxyprothrombin. Liver Int. 2011; 31:22-35.
72. Inagaki Y, Xu HL, Hasegawa K, Aoki T, Beck Y, Sugawara Y, Tang W, Kokudo N. Des-gamma-carboxyprothrombin in patients with hepatocellular carcinoma and liver cirrhosis. J Dig Dis. 2011; 12:481-488.
73. Inagaki Y, Qi F, Gao J, Qu X, Hasegawa K, Sugawara Y, Tang W, Kokudo N. Effect of c-Met inhibitor SU11274 on hepatocellular carcinoma cell growth. Biosci Trends. 2011; 5:52-56.
74. Gao JJ, Inagaki Y, Xue X, Qu XJ, Tang W. c-Met: A

potential therapeutic target for hepatocellular carcinoma. Drug Discov Ther. 2011; 5:2-11.
75. Song PP, Gao JJ, Kokudo N, Dong JH, Tang W. "Knowledge into action" Exploration of an appropriate approach for constructing evidence-based clinical practice guidelines for hepatocellular carcinoma. Biosci Trends. 2012; 6:147-152.
76. Shen Q, Fan J, Yang XR, *et al*. Serum DKK1 as a protein biomarker for the diagnosis of hepatocellular carcinoma: A large-scale, multicentre study. Lancet Oncol. 2012; 13:817-826.
77. Peter A, Prieto, Charles H, Cha. DKK1 as a serum biomarker for hepatocellular carcinoma. Hepatobiliary Surg Nutr. 2013; 2:127-128.
78. Zhu WW, Guo JJ, Guo L, *et al*. Evaluation of Midkine as a Diagnostic Serum Biomarker in Hepatocellular Carcinoma. Clin Cancer Res. 2013; 19:3944-3954.
79. Pepe MS, Etzioni R, Feng Z, Potter JD, Thompson ML, Thornquist M, Winget M, Yasui Y. Phases of biomarker development for early detection of cancer. J Natl Cancer Inst. 2001; 93:1054-1061.

(Received April 3, 2014; Revised May 26, 2014; Accepted May 31, 2014)

Brief Report

DOI: 10.5582/ddt.2014.01012

Synthesis and biological evaluation of novel indoline-2,3-dione derivatives as antitumor agents

Pengzhan Li[1], Yanmei Tan[1], Guyue Liu[2], Yang Liu[1], Jianzhen Liu[1], Yanzhen Yin[1], Guisen Zhao[1,*]

[1] *Department of Medicinal Chemistry, Key Laboratory of Chemical Biology (Ministry of Education), School of Pharmaceutical Sciences, Shandong University, Ji'nan, Shandong, China;*
[2] *Department of Pharmacology, Shenyang Pharmaceutical University, Shenyang, China.*

Summary **A new series of 1,5-disubstituted indolin-2,3-diones was synthesized and their inhibition of the growth of a human acute promyelocytic leukemia (HL-60) cell line was evaluated. These compounds had promising inhibition of HL-60 cell growth *in vitro*. Results indicated that compounds with a benzyl substituent at the N-1 position on the indolin-2,3-dione ring had more potent antiproliferative activity than those with a (4-fluorobenzyl) amino-2-oxoethyl substituent at the N-1 position. Among the compounds synthesized, compound 8l inhibited half of cell growth at a concentration of 0.07 μM and compound 8p did so at a concentration of 0.14 μM. These compounds may serve as lead compounds for further optimization in order to develop novel anticancer agents.**

Keywords: Indoline-2,3-diones, anticancer agent, HL-60 human leukemia cells

1. Introduction

Indole derivatives have attracted considerable attention in medicinal chemistry because of their pharmacological activities (*1,2*). During drug design, substituted indoles are considered a "privileged scaffold" for numerous pharmacologically active lead compounds because of their substantial affinity for many receptors (*3,4*). Isatin (indoline-2, 3-dione, **1**, Figure 1), one of the simplest indole derivatives, has led to numerous analogues with a wide range of biological properties, including anti-cancer activity (*5-9*). Indirubin (**2**, Figure 1), the active ingredient in the traditional Chinese medicine preparation Danggui Longhui Wan used to treat myelocytic leukemia, is reported to have antiproliferative action against human cancer cells by inhibiting the genes or proteins that regulate cell cycle progression; indirubin arrests the G2/M phase, although its mechanism of action in cells is not fully understood (*10*). Inhibited growth induced by indirubin-3-oxime (**3**, Figure 1) is associated with induction of cyclin-dependent kinase inhibitor p21, inhibition of cyclin D1, and activation of caspase-3 (*11*). Indirubin derivatives are reported to inhibit signal transducer and activator of transcription 3 (Stat3) signaling and induce apoptosis in human cancer cells (*12*). Indoline-2,3-dione might be used as a privileged scaffold to design a variety of therapeutic molecules, and many indoline-2,3-dione derivatives have been studied as antitumor agents (*13-18*). Among the reported indoline-2,3-dione derivatives, 5,7-dibromo-1-(naphthalen-1-yl methyl)indoline-2,3-dione (**4**, Figure 1) has potent anti-tumor properties with

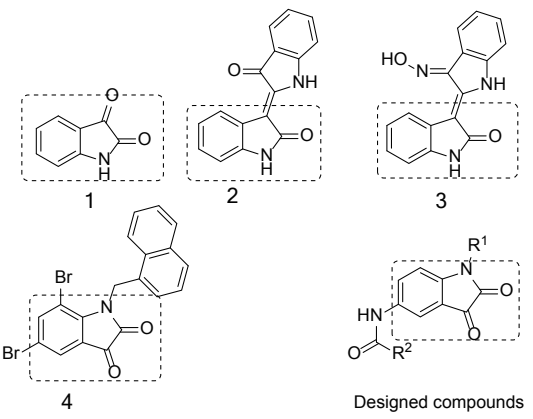

Figure 1. Structures of indoline-2,3-dione derivatives and designed compounds

**Address correspondence to:*
Dr. Guisen Zhao, Department of Medicinal Chemistry, School of Pharmaceutical Sciences, Shandong University, 44 Wenhuaxi Rd, Ji'nan, Shandong 250012, China.
E-mail: guisenzhao@sdu.edu.cn

an IC_{50} value of 0.19 mM against human monocyte-like histiocytic lymphoma (U937) cells (*19*). Thus, the current study introduced different substituents at the N-1 and C-5 positions on the indoline-2,3-dione ring in order to synthesize a series of novel 1,5-disubstituted indoline-2,3-diones and evaluate their antiproliferative activity on HL-60 human leukemia cells.

2. Materials and Methods

2.1. *Chemistry*

The synthesis of target compounds is shown in Diagram 1. The starting material, indolin-2,3-dione (**1**) was purchased from Aladdin Industrial Corporation, Shanghai, China. Intermediate **5** was produced from compound **1** using fuming nitric acid as a nitrating agent and sulfuric acid as a solvent. Intermediate **6** was prepared by treating **5** with 2,2-dimethylpropane-1,3-diol with catalysis by *p*-toluenesulfonic acid. The key intermediate **7** was obtained from **6** that had reacted with 2-chloro-*N*-(4-fluorobenzyl) acetamide (or benzyl chloride) under alkaline conditions *via* electrophilic substitution. With Pd/C (10%, w/w) as the catalyst, the nitro group in intermediate **7** was converted to an amino group by hydrogenation. The resulting compound was allowed to react with acyl chloride in the presence of anhydrous potassium carbonate to yield acylated products, and then the acylated products were converted to target compound **8** by deprotection under acidic conditions.

2.2. *Cell line*

Human acute promyelocytic leukemia (HL-60) cells (obtained from the American Type Culture Collection) were cultured in RPMI 1640 medium. The medium consisted of 10% heat-inactivated fetal bovine serum (FBS) (Gibco®, Invitrogen, Carlsbad, CA, USA), 100 IU/mL penicillin, 100 μg/mL streptomycin, and 1 mmol/L L-glutamine. Cells were incubated in a humid atmosphere of 5% CO_2 at 37°C.

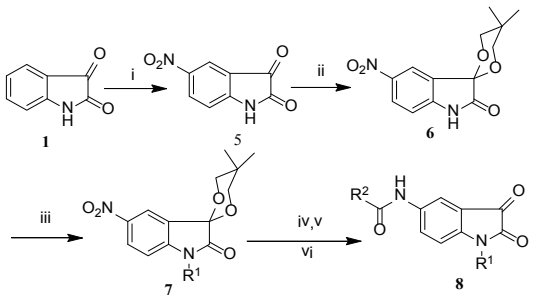

Diagram 1. Synthesis of target compounds. Reagents and conditions. (i) Fuming nitric acid and sulfuric acid; –10-0°C, 1 h; (ii) 2,2-dimethylpropane-1,3-diol, *p*-toluenesulfonic acid, and cyclohexane; reflux, 14 h; (iii) 2-chloro-*N*-(4-fluorobenzyl)acetamide or benzyl chloride, dimethylformamide, and potassium carbonate; 85°C, 40 min; (iv) H_2 and 10% Pd/C; room temperature, 4 h; (v) Acyl chloride and potassium carbonate; 0°C - room temperature, 2 h; (vi) Hydrochloric acid and acetic acid; 30°C, 12 h.

2.3. *Cell viability assay using the trypan blue exclusion method*

Trypan blue was ground with a small amount of distilled water, diluted with double-distilled water to 4%, filtered, and then stored at 37°C. The stock solution was diluted to 0.4% with PBS when used. HL-60 cells (1×10^5/mL) were seeded in 12-well plates with a volume of 2 mL in each well. A single cell suspension was prepared after incubation with different concentrations of target compounds. The single cell suspension (50 mL) and the trypan blue solution (0.4 %, 50 mL) were mixed well and observed for up to 3 min under a microscope. Dead cells stained blue while living cells did not. The numbers of dead cells and living cells were calculated with a hemocytometer and cell viability was expressed as the percentage of viable cells.

3. Results and Discussion

The extent to which compounds **8a-8p** inhibited HL-60 cell growth was measured and results are shown in Table 1. Results indicated that compounds with a benzyl substituent (R^1) at the N-1 position on the indolin-2,3-dione ring (**8k-8p**) had more potent antiproliferative activity against HL-60 cells than those with a (4-fluorobenzyl)amino-2-oxoethyl substituent at the N-1 position (**8a-8j**). The effect of the substituent (R^2) on inhibiting HL 60 cell growth depended on the substituent (R^1) at the N-1 position on the indolin-2,3-dione ring. When R^1 was a 4-fluorobenzylamino-2-oxoethyl group, compounds with an aryl group (R^2) (**8a-8g**) had greater inhibition than those with an aliphatic group (**8h** and **8i**). When R^1 was a benzyl group at the N-1 position, compounds with either an aryl group (**8k-8n**) or an aliphatic group (**8o-8p**) had antiproliferative activity with IC_{50} values of less than 1.1 μM. Among compounds **8k-8p** that have a benzyl group at the N-1 position on the indolin-2,3-dione ring, **8l** with a phenyl acetamide group at the C-5 position inhibited HL-60 cell growth the most with an IC_{50} value of 0.07 μM. The next most potent inhibitor of growth was **8p**, which had an IC_{50} value of 0.14 μM and a cyclopropane carboxamide group at the C-5 position.

In conclusion**,** sixteen 1,5-disubstituted indolin-2,3-diones were synthesized and their inhibition of HL-60 cell growth was evaluated. Findings indicated that compounds with a benzyl substituent at the N-1 position on the indolin-2,3-dione ring had more potent inhibition of HL-60 cell growth than those with a 4-fluorobenzylamino-2-oxoethyl substituent at the N-1 position. Among the compounds with a benzyl substituent group at the N-1 position, the most potent inhibitors of HL-60 cell growth were compound **8l**, which had a phenyl acetamide group at the C-5 position, and compound **8p**, which had a cyclopropane carboxamide group at the C-5 position. The mechanisms by which these compounds inhibited growth are being investigated.

Table 1. Inhibition of HL-60 cell growth by target compounds

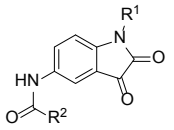

Designation	R^1	R^2	IC_{50} (μM)[a]
8a	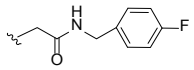		4.8
8b	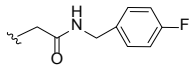		7.2
8c	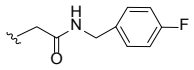	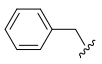	7
8d	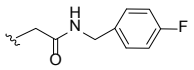	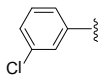	3.4
8e	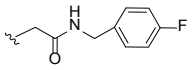	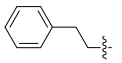	8.8
8f	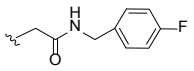	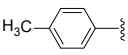	NT[b]
8g	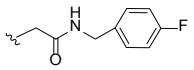	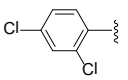	9.2
8h	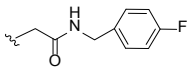		15.6
8i	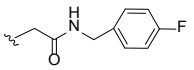		15.4
8j	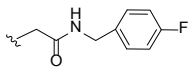		19.3
8k	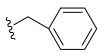		0.98
8l	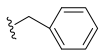	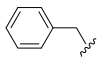	0.07
8m	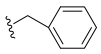	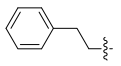	0.63
8n	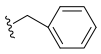	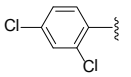	1.1
8o	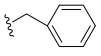		0.7
8p	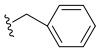		0.14

[a] IC_{50} indicates the concentration of each compound required for a 50% decrease in cell viability. [b] Not tested.

Acknowledgement

This work was supported by a grant from the National Natural Science Foundation of China (grant no. 21272140) and the Shandong Natural Science Foundation (grant no. ZR2011HM042).

References

1. Humphrey GR, Kuethe JT. Practical methodologies for the synthesis of indoles. Chem Rev. 2006; 106:2875-2911.
2. Brancale A, Silvestri R. Indole, a core nucleus for potent inhibitors of tubulin polymerization. Med Res Rev. 2007; 27:209-238.
3. Evans BE, Rittle KE, Bock MG, et al. Methods for drug discovery: Development of potent, selective, orally effective cholecystokinin antagonists. J Med Chem. 1988; 31:2235-2246.
4. Horton DA, Bourne GT, Smythe ML. The combinatorial synthesis of bicyclic privileged structures or privileged substructures. Chem Rev. 2003; 103:893-930.
5. Pandeya SN, Smitha S, Jyoti M, Sridhar SK. Biological activities of isatin and its derivatives. Acta Pharm. 2005; 55:27-46.
6. Sharma VM, Prasanna P, Seshu VA, et al. Novel indolo[2,1-b]quinazoline analogues as cytostatic agents: Synthesis, biological evaluation and structure–activity relationship. Bioorg Med Chem Lett. 2002; 12:2303-2307.
7. Moon MJ, Lee SK, Lee JW, Song WK, Kim SW, Kim JI, Cho C, Choi SJ, Kim YC. Synthesis and structure–activity relationships of novel indirubin derivatives as potent anti-proliferative agents with CDK2 inhibitory activities. Bioorg Med Chem. 2006; 14:237-246.
8. Abadi AH, Abou-Seri SM, Abdel-Rahman DE, Klein C, Lozach O, Meijer L. Synthesis of 3-substituted-2-oxoindole analogues and their evaluation as kinase inhibitors, anticancer and antiangiogenic agents. Eur J Med Chem. 2006; 41:296-305.
9 Gursoy A, Karali N. Synthesis and primary cytotoxicity evaluation of 3-[[(3-phenyl-4(3H)-quinazolinone-2-yl) mercaptoacetyl]hydrazono]-1H-2- indolinones. Eur J Med Chem. 2003; 38:633-643.
10. Marko D, Schatzle S, Friedel A, Genzlinger A, Zankl H, Meijer L, Eisenbrand G. Inhibition of cyclin-dependent kinase 1 (CDK1) by indirubin derivatives in human tumour cells. Br J Cancer. 2001; 84:283-289.
11. Kameswaran TR, Ramanibain R. Indirubin-3-monooxime induced cell cycle arrest and apoptosis in Hep-2 human laryngeal carcinoma cells. Biomed Pharmacother. 2009; 63:146-154.
12. Nam S, Buettner R, Turkson J, Kim D, Cheng JO, Muehlbever S, Hippe F, Vatter S, Merz KH, Eisenbrand G, Jove R. Indirubin derivatives inhibit stat3 signaling and induce apoptosis in human cancer cells. Proc Natl Acad Sci U S A. 2005; 102:5998-6003.
13. Hoessel R, Leclerct S, Endicott JA, Nobel ME, Lawrie A, Tunnah P, Leost M, Damiens E, Marie D, Marko D, Niederberger E, Tang WC. Indirubin, the active constituent of a Chinese antileukaemia medicine, inhibits cyclin dependent kinases. Nat Cell Biol. 1999; 5:60-67.
14. Marko D, Schatzle S, Friedel A, Genzlinger A, Zankl H, Meijer L, Eisenbrand G. Inhibition of cyclin dependent kinase1 (CDK1) by indirubin derivatives in human tumour cel1s. Br J Cancer. 2001; 84:283-289.
15. Wang ZH, Li WY, Li FL, Zhang L, Hua WY, Cheng JC, Yao ZQ. Synthesis and antitumor activity of 7-azaindirubin. Chin Chem Lett. 2009; 20:542-544.
16. Libnow S, Methling K, Hein M, Michalik D, Harms M, Wende K, Flemming A, Kockerling M, Reinke H, Bednarski PJ, Lalk M Langera P. Synthesis of indirubin-N'-glycosides and their anti-proliferative activity against

human cancer cell lines. Bioorg Med Chem. 2008; 16:5570-5583.
17. Luk KC, Simcox ME, Schutt A, Rowan K, Thompson T, Chen Y, Kammlott U, DePinto W, Dunten P, Dermatakis A. A new series of potent oxindole inhibitors of CDK2. Bioorg Med Chem Lett. 2004; 14:913-917.
18. Dermatakis A, Luk KC, DePinto W. Synthesis of potent oxindole CDK2 inhibitors. Bioorg Med Chem. 2003; 11:1873-1881.
19. Matesic L, Locke JM, Bremner JB, Pvne SG, Skropeta D, Ranson M, Vine KL. N-phenethyl and N-naphthylmethyl isatins and analogues as in vitro cytotoxic agents. Bioorg Med Chem. 2008; 16:3118-3124.

(Received February 13, 2014; Revised May 1, 2014; Accepted May 23, 2014)

Appendix

Proton nuclear magnetic resonance (^{1}H-NMR) spectra and carbon nuclear magnetic resonance (^{13}C-NMR) spectra were determined with a Bruker Avance ATC600 instrument at 600 MHz with tetramethylsilane (TMS) as the internal standard. The chemical shifts (δ) were reported in parts per million (ppm) and were relative to the central peak of the solvent, which was DMSO-d_6 or $CDCl_3$. Coupling constants (J) are given in Hz. Reported ^{1}H-NMR data are as follows: chemical shift, multiplicity (s = singlet, d = doublet, t = triplet, q = quartet, br = broad, or m = multiplet), coupling constants, and number of protons. Infrared (IR) spectra were measured with a Nicolet Nexus 470FT-IR spectrometer and are expressed in cm^{-1}. Mass spectra (MS) were measured with an API 4000, and high resolution mass (HRMS) spectra were recorded with an LTQ Orbitrap mass spectrometer. The melting points were determined with a Büchi capillary melting point apparatus and are uncorrected. Unless otherwise noted, all materials were obtained from commercial suppliers and were used without further purification.

1. Procedure for preparation of intermediate 5

Fuming nitric acid (3.0 mL, 0.065 mol) was added dropwise to a solution of indoline-2,3-dione (7.35g, 0.05 mol) in sulfuric acid (50 mL) under 0°C. The mixture was stirred for 1 h at 0°C and then slowly poured into 500 mL of crushed ice. The precipitate was filtered, washed three times with water, and then dried to yield intermediate **5.**

*5-nitroindoline-2,3-dione (**5**).* Yield: 78%; light yellow power; mp: 257.8-258.5°C. ^{1}H-NMR (DMSO-d_6) δ: 11.67 (s, 1H, NH), 8.44 (m, 1H, Ar-H), 8.21 (s, 1H, Ar-H), 7.09 (d, J = 8.4 Hz, 1H, Ar-H).

2. Procedure for preparation of intermediate 6

5-nitroindoline-2,3-dione (3.5 g, 0.018 mol), *p*-toluenesulfonic acid (0.4 g), and neopentyl glycol (3.8 g, 0.018 mol) were successively added and dissolved in cyclohexane (80 mL). The mixture was heated to 80°C for 14 h. The reaction mixture was cooled to room temperature and then filtered. The precipitate was sequentially washed with saturated sodium carbonate solution and water and then further purified by column chromatography with petroleum ether/ethyl acetate (6:1 to 3:1) to yield intermediate **6**.

*5,5-Dimethyl-5'-nitrospiro[[1,3]dioxane-2,3'-indolin]-2'-one (**6**).* Yield: 88%; white solid; mp: 212.3-214.1°C. ^{1}H-NMR (DMSO-d_6) δ: 11.21 (s, 1H, NH), 8.28 (dd, J_1 = 9.0 Hz, J_2 = 1.8 Hz, 1H, Ar-H), 8.08 (d, J = 1.8 Hz, 1H, Ar-H), 7.04 (d, J = 8.4 Hz, 1H, Ar-H), 4.49 (d, J = 9.6 Hz, 2H, CH_2), 3.55 (d, J = 10.8 Hz, 2H, CH_2), 1.35 (s, 3H, CH_3), 0.90 (s, 3H, CH_3).

3. General procedure for preparation of intermediate 7

2-Chloro-*N*-(4-fluorobenzyl) acetamide or benzyl chloride (4.3 mmol) was added to a solution of intermediate **6** (1.0 g, 3.6 mmol) and anhydrous potassium carbonate (1 g, 7.2 mmol) in dried dimethylformamide (10 mL). The mixture was heated to 85°C for 40 min and then cooled to room temperature. The reaction mixture was poured into ice water (100 mL) and a precipitate was produced. The precipitate was then filtered, washed with water, and further purified by column chromatography with petroleum ether/ ethyl acetate (6:1 to 1:1) to yield **7**.

*2-(5,5-Dimethyl-5'-nitro-2'-oxospiro[[1,3]dioxane-2,3'-indolin]-1'-yl)-N-(4- fluorobenzyl)acetamide (**7a**).* Yield: 75%; white solid; mp: 231.9-232.1°C. ^{1}H-NMR ($CDCl_3$) δ: 8.33 (d, J = 1.8 Hz, 1H, Ar-H), 8.31 (dd, J = 8.4 Hz, J = 2.4 Hz, 1H, Ar-H), 7.19 (dd, J_1 =12 Hz, J_2 = 8.4 Hz, 2H, Ar-H), 7.00 (t, J = 8.4 Hz, 2H, Ar-H), 6.96 (d, J = 8.4 Hz, 1H , Ar-H), 6.10 (s, 1H, N-H), 4.59 (d, J = 11.4 Hz, 2H, CH_2), 4.41 (d, J = 5.4 Hz, 2H, CH_2), 4.35 (s, 2H, CH_2), 3.55 (d, J = 10.8 Hz, 2H, CH_2), 1.56 (s, 3H, CH_3), 0.90 (s, 3H, CH_3). MS (ESI) *m/z*: 444.5 $[M+H]^+$.

*1'-benzyl-5,5-dimethyl-5'-nitrospiro[[1,3]dioxane-2,3'-indolin]-2'-one (**7b**).* Yield: 63%; Pale yellow solid; mp: 154.4-155.4°C. ^{1}H-NMR ($CDCl_3$) δ: 8.31 (d, J = 2.4 Hz, 1H, Ar-H), 8.18 (dd, J_1 = 9.0 Hz, J_2 = 2.4 Hz, 1H, Ar-H), 7.35 (t, J = 7.2 Hz, 2H, Ar-H), 7.30 (t, J = 7.2 Hz, 1H, Ar-H), 7.26 (t, J = 3.0 Hz, 2H, Ar-H), 6.71 (d, J = 8.4 Hz, 1H, Ar-H), 4.88 (s, 2H, CH_2), 4.73 (d, J = 11.4 Hz, 2H, CH_2), 3.57 (d, J = 11.4 Hz, 2H, CH_2), 1.45 (s, 3H, CH_3), 0.92 (s, 3H, CH_3). MS (ESI) *m/z*: 369.2 $[M+H]^+$.

4. General procedure for preparation of compound 8

Intermediate **7** (2.26 mmol) and 10% Pd/C (0.4g, 10%) were added to 50 mL of distilled ethyl acetate. The mixture reacted with hydrogen for 4 h at room

temperature and then the reaction mixture was filtered. Anhydrous potassium carbonate (0.34 g, 2.5 mmol) was added to the filtrate, and then acyl chloride (2.5 mmol) was added dropwise at 0°C. After the resulting solution was stirred for 2 h at room temperature, the mixture was filtered. The organic phase was washed successively with 5% sodium hydroxide (3 × 15mL), 3% hydrochloric acid (3 × 15mL), and saturated brine (3 × 15 mL) and then evaporated in a vacuum to yield a white solid., Glacial acetic acid (63 mL) and hydrochloric acid (7 mL) were added to the solid. The mixture was stirred overnight at 30°C and then poured into distilled water (50 mL), and a precipitate was produced. The precipitate was filtered and purified by recrystallization in 95% ethanol to yield compound **8**.

*N-(1-(2-(4-Fluorobenzylamino)-2-oxoethyl)-2,3-dioxoindolin-5-yl)benzamide (**8a**)*. Yield: 89%; purple solid; mp: 305.3-306.5°C. ^{1}H-NMR (DMSO-d_6) δ: 10.39 (s, 1H, NH), 8.77 (t, J = 6.0 Hz, 1H, NH), 8.05 (d, J = 2.4 Hz, 1H, Ar-H), 7.97 (d, J = 7.2 Hz, 2H, Ar-H), 7.94 (dd, J_1 = 8.4 Hz, J_2 = 2.4 Hz, 1H, Ar-H),7.61 (t, 1H, J = 7.2 Hz, Ar-H), 7.55 (t, J = 7.8 Hz, 2H, Ar-H), 7.26 (t, J = 8.4 Hz, 2H, Ar-H), 7.14 (t, J = 9.0 Hz, 2H, Ar-H), 7.09 (d, J = 8.4 Hz, 1H, Ar-H), 4.40 (s, 2H, CH_2), 4.29 (d, J = 6.0 Hz, 2H, CH_2). ^{13}C-NMR (DMSO-d_6) δ: 183.43, 166.59, 165.60, 162.43, 160.82, 159.07, 146.60, 135.52, 134.88, 132.21, 130.02, 129.54, 129.48, 128.90, 128.90 128.07, 128.07, 118.10, 116.89, 115.51, 115.36, 111.27, 43.13, 41.81. IR (KBr, cm^{-1}): υ_{NH}: 3,409.78, 3,282.05; $\upsilon_{=CH}$: 3,066.89; υ_{CH2}: 2,929.70; $\upsilon_{C=O}$: 1,740.92, 1,659.42; $\upsilon_{C=C}$: 1,625.12, 1,606.10, 1,547.80, 1,510.18, 1,495.13, 1,454.36; δ_{CH}: 1,361.73, 1,310.36; $\gamma_{=CH}$: 823.81, 708.86. HRMS (ESI) *m/z* calculated for $C_{24}H_{19}F_1N_3O_4$ [M+H]$^+$: 432.1354, found 432.1347.

*N-(1-(2-(4-Fluorobenzylamino)-2-oxoethyl)-2,3-dioxoindolin-5-yl) furan-2- carboxamide (**8b**)*. Yield: 41%; Purple solid; mp: 309.5-312.2°C. ^{1}H-NMR (DMSO-d_6) δ: 10.37 (s, 1H, NH), 8.76 (t, J = 5.4 Hz, 1H, NH), 7.99 (s, 1H, FU-H), 7.97 (s, 1H, Ar-H), 7.91 (d, J = 6.6 Hz, 1H, Ar-H), 7.33 (d, J = 3.0 Hz, 1H, FU-H), 7.25 (t, J = 7.8 Hz, 2H, Ar-H), 7.13 (t, J = 8.4 Hz, 2H, Ar-H), 7.08 (d, J = 8.4 Hz, 1H, Ar-H), 6.72 (s, 1H, FU-H), 4.38 (s, 2H, CH_2), 4.28 (d, J = 6.0 Hz, 2H, CH_2). IR (KBr, cm^{-1}): υ_{NH}: 3,366.07, 3,283.56; $\upsilon_{=CH}$: 3,116.07; υ_{CH2}: 2,929.99; $\upsilon_{C=O}$: 1,742.21, 1,671.43, 1,651.30; $\upsilon_{C=C}$: 1,626.82, 1,607.51, 1,584.76, 1,553.03, 1,510.75, 1,494.39; δ_{CH}: 1,426.20, 1,362.83, 1,341.25, 1,316.50; υ_{C-O}: 1,225.46; $\gamma_{=CH}$: 1,009.95, 829.14, 760.00. HRMS (ESI) *m/z* calculated for $C_{22}H_{17}F_1N_3O_5$ [M+H]$^+$: 422.1147, found 422.1141.

*N-(1-(2-(4-Fluorobenzylamino)-2-oxoethyl)-2,3-dioxoindolin-5-yl) phenylacetamide (**8c**)*. Yield: 92%; orange-red solid; mp: 263.7-265.3°C. ^{1}H-NMR (DMSO-d_6) δ: 10.32 (s, 1H, NH), 8.74 (t, J = 6.0 Hz, 1H, NH), 7.89 (d, J = 1.8 Hz, 1H, Ar-H), 7.70 (dd, J_1 = 8.4 Hz, J_2 = 1.8 Hz, 1H, Ar-H), 7.33 (d, J = 4.2 Hz, 4H, Ar-H), 7.25 (m, 3H, Ar-H), 7.12 (t, J = 8.4 Hz, 2H, Ar-H), 7.02 (d, J = 7.8 Hz, 1H, Ar-H), 4.36 (s, 2H, CH_2), 4.26 (d, J = 6.0 Hz, 2H, CH_2), 3.64 (s, 2H, CH_2). ^{13}C-NMR (DMSO-d_6) δ: 183.44, 169.70, 166.58, 162.43, 160.82, 159.00, 146.28, 136.17, 135.59, 129.55, 129.55, 129.53, 129.48, 128.77, 128.77, 128.74, 127.04, 118.12, 115.60, 115.49, 115.35, 111.40, 43.61, 43.19, 41.80. IR (KBr, cm^{-1}): υ_{NH}: 3,295.80; $\upsilon_{=CH}$: 3,064.79; υ_{CH2}: 2,935.13; $\upsilon_{C=O}$: 1,740.64, 1,659.85; $\upsilon_{C=C}$: 1,623.61, 1,606.65, 1,552.75, 1,510.47, 1,493.13, 1,453.99; δ_{CH}: 1,359.98; $\gamma_{=CH}$: 825.00, 728.32, 695.99. HRMS (ESI) *m/z* calculated for $C_{25}H_{21}F_1N_3O_4$ [M+H]$^+$: 446.1511, found 446.1504.

*N-(1-(2-(4-Fluorobenzylamino)-2-oxoethyl)-2,3-dioxoindolin-5-yl)-3-chloro- benzamide (**8d**)*. Yield: 81%; pink solid; mp: 310.3-311.2°C. ^{1}H-NMR (DMSO-d_6) δ: 10.48 (s, 1H, NH), 8.77 (t, J = 6.6 Hz, 1H, NH), 8.02 (s, 2H, Ar-H), 7.92 (d, J = 7.8 Hz, 2H, Ar-H), 7.69 (d, J = 7.8 Hz, 1H, Ar-H), 7.59 (t, J = 7.8 Hz, 1H, Ar-H), 7.25 (t, J = 7.8 Hz, 2H,Ar-H), 7.14 (t, J = 9.0 Hz, 2H, Ar-H),7.10 (d, J = 8.4 Hz,1H, Ar-H), 4.40 (s, 2H, CH_2), 4.28 (d, J = 6.0 Hz, 2H, CH_2). ^{13}C-NMR (DMSO-d_6) δ: 183.38, 166.57, 164.43, 162.43, 160.82, 159.04, 146.76, 136.82, 135.20, 133.72, 132.00, 130.88, 130.08, 129.53, 129.48, 127.81, 126.90, 118.10, 116.95, 115.50, 115.36, 111.30, 43.21, 41.81. IR (KBr, cm^{-1}): υ_{NH}: 3,386.50, 3,291.67; $\upsilon_{=CH}$: 3,067.66; υ_{CH2}: 2,931.61; $\upsilon_{C=O}$: 1,740.97, 1,653.98; $\upsilon_{C=C}$: 1,622.64, 1,607.07, 1,547.56, 1,510.85, 1,493.14, 1,453.60; δ_{CH}: 1,360.11, 1,314.51; $\gamma_{=CH}$: 819.38, 738.47. HRMS (ESI) *m/z* calculated for $C_{24}H_{18}Cl_1F_1N_3O_4$ [M+H]$^+$: 466.0964, found 466.0959.

*N-(1-(2-(4-Fluorobenzylamino)-2-oxoethyl)-2,3-dioxoindolin-5-yl)-3- phenylpropanamide (**8e**)*. Yield: 78%; Orange-red solid; mp: 264.1-265.8°C. ^{1}H-NMR (DMSO-d_6) δ: 10.06 (s, 1H, NH), 8.74 (t, J = 6.0 Hz, 1H, NH), 7.88 (s, 1H, Ar-H), 7.65 (d, J = 7.2 Hz, 1H, Ar-H), 7.28 (t, J = 7.8 Hz, 2H, Ar-H), 7.25 (m, 4H, Ar-H), 7.18 (t, J = 7.2 Hz, 1H, Ar-H), 7.12 (t, J = 8.4 Hz, 2H, Ar-H), 7.01 (d, J = 9.0 Hz, 1H, Ar-H), 4.35 (s, 2H, CH_2), 4.27 (d, J = 5.4 Hz, 2H, CH_2), 2.91 (t, J = 7.8 Hz, 2H, CH_2), 2.62 (t, J = 7.8 Hz, 2H, CH_2). ^{13}C-NMR (DMSO-d_6) δ: 183.48, 170.95, 166.58, 162.42, 160.82, 158.99, 146.14, 141.48, 135.60, 129.53, 129.48, 128.77, 128.77, 128.68, 128.68, 128.59, 126.42, 118.10, 115.53, 115.48, 115.35, 111.37, 43.17, 41.79, 38.32, 31.21. IR (KBr, cm^{-1}): υ_{NH}: 3,336.21, 3,297.32; $\upsilon_{=CH}$: 3,063.99; υ_{CH2}: 2,928.64; $\upsilon_{C=O}$: 1,741.08, 1,655.82; $\upsilon_{C=C}$: 1,623.72, 1,606.97, 1,551.06, 1,510.67, 1,493.11, 1,454.12; δ_{CH}: 1,357.92, 1,302.92; $\gamma_{=CH}$: 824.89, 752.43, 699.35. HRMS (ESI) *m/z* calculated for $C_{26}H_{23}F_1N_3O_4$ [M+H]$^+$: 460.1667, found 460.1659.

*N-(1-(2-(4-Fluorobenzylamino)-2-oxoethyl)-2,3-dioxoindolin-5-yl)-4- methylbenzamide (**8f**)*. Yield: 75%; purple solid; mp: 299.2-300.6°C. ^{1}H-NMR (DMSO-d_6) δ: 10.30 (s, 1H, NH), 8.77 (t, J = 5.4 Hz, 1H, NH), 8.04 (s, 1H, Ar-H), 7.94 (d, J = 8.4 Hz, 1H,

Ar-H), 7.89 (d, J = 7.8 Hz, 2H, Ar-H), 7.35 (d, J = 7.8 Hz, 2H, Ar-H), 7.25 (t, J = 7.2 Hz, 2H, Ar-H), 7.14 (t, J = 8.4 Hz, 2H, Ar-H),7.08 (d, 1H, J = 8.4 Hz, Ar-H), 4.39 (s, 2H, CH_2), 4.28 (d, J = 5.4 Hz, 2H, CH_2), 2.39 (s, 3H, Ar-CH_3). ^{13}C-NMR (DMSO-d_6) δ: 183.16, 166.58, 165.75, 162.42, 160.82, 159.06, 146.53, 142.26, 135.58, 131.97, 130.00, 129.53, 129.48, 129.41, 129.41, 128.10, 128.10, 118.09, 116.87, 115.50, 115.36, 111.24, 43.20, 41.78, 21.46. IR (KBr, cm^{-1}): υ_{NH}: 3,411.85, 3,288.56; $\upsilon_{=CH}$: 3,066.50; υ_{CH2}: 2,924.11; $\upsilon_{C=O}$: 1,740.74, 1,657.81; $\upsilon_{C=C}$: 1,625.25, 1,608.70, 1,551.81, 1,509.61, 1,498.29, 1,452.81; δ_{CH}: 1,362.94, 1,324.94, 1,308.45; $\gamma_{=CH}$: 842.44, 745.99. HRMS (ESI) *m/z* calculated for $C_{25}H_{21}F_1N_3O_4$ $[M+H]^+$: 446.1511, found 446.1505.

*N-(1-(2-(4-Fluorobenzylamino)-2-oxoethyl)-2,3-dioxoindolin-5-yl)-2,4-dichloro-benzamide (**8g**)*. Yield: 84%; orange-red solid; mp: 304.7-305.3°C. ^{1}H-NMR (DMSO-d_6) δ: 10.69 (s, 1H, NH), 8.75 (t, J = 6.0 Hz, 1H, NH), 7.97 (d, J = 1.8 Hz, 1H, Ar-H), 7.81 (dd, J_1 = 8.4 Hz, J_2 = 1.8 Hz, 1H, Ar-H), 7.80 (d, J = 1.8 Hz, 1H, Ar-H), 7.67 (d, J = 8.4 Hz, 1H, Ar-H), 7.58 (dd, J_1 = 7.8 Hz, J_2 = 1.8 Hz, 1H, Ar-H), 7.25 (dd, J_1 = 8.4 Hz, J_2 = 5.4 Hz, 2H, Ar-H), 7.13 (t, J = 9.6 Hz, 2H, Ar-H), 7.08 (d, J = 9.0 Hz, 1H, Ar-H), 4.39 (s, 2H, CH_2), 4.28 (d, J = 6.0 Hz, 2H, CH_2). ^{13}C-NMR (DMSO-d_6) δ: 183.33, 166.53, 164.50, 162.42, 160.82, 159.04, 146.82, 135.75, 135.53, 135.02, 131.73, 130.83, 129.74, 129.54, 129.48, 129.20, 127.97, 118.22, 116.02, 115.50, 115.36, 111.52, 43.21, 41.79. IR (KBr, cm^{-1}): υ_{NH}: 3,241.44; $\upsilon_{=CH}$: 3,055.05; υ_{CH2}: 2,973.71; $\upsilon_{C=O}$: 1,729.76, 1,657.14; $\upsilon_{C=C}$: 1,622.08, 1,603.25, 1,583.27, 1,556.63, 1,537.15, 1,509.54, 1,496.91, 1,456.35; δ_{CH}: 1,363.94, 1,337.78, 1,320.71; $\gamma_{=CH}$: 836.38, 818.75, 780.98, 682.46. HRMS (ESI) *m/z* calculated for $C_{24}H_{17}Cl_2F_1N_3O_4$ $[M+H]^+$: 500.0575, found 500.0563.

*N-(1-(2-(4-Fluorobenzylamino)-2-oxoethyl)-2,3-dioxoindolin-5-yl)cyclopropane carboxamide (**8h**)*. Yield: 71%; pink solid; mp: 285.3-286.4°C. ^{1}H-NMR (DMSO-d_6) δ: 10.34 (s, 1H, NH), 8.75 (t, J = 6.0 Hz, 1H, NH), 7.89 (d, J = 1.8 Hz, 1H, Ar-H), 7.69 (dd, J_1 = 9.0 Hz, J_2 = 2.4 Hz, 1H, Ar-H), 7.24 (t, J = 6.6 Hz, 2H, Ar-H), 7.13 (t, J = 8.4 Hz, 2H, Ar-H), 7.02 (d, J = 7.8 Hz, 1H, Ar-H), 4.36 (s, 2H, CH_2), 4.27 (d, J = 6.6 Hz, 2H, CH_2), 1.73 (t, J = 6.6 Hz, 1H, CH), 0.81 (d, J = 7.2 Hz, 4H, CH_2). ^{13}C-NMR (DMSO-d_6) δ: 183.50, 172.17, 166.59, 162.42, 160.81, 158.99, 146.04, 135.78, 129.52, 129.47, 128.46, 118.10, 115.45, 115.46, 115.35, 111.36, 43.16, 41.78, 14.98, 7.74, 7.74. IR (KBr, cm^{-1}): υ_{NH}: 3,345.65, 3,261.80; $\upsilon_{=CH}$: 3,052.49; υ_{CH2}: 2,942.81; $\upsilon_{C=O}$: 1,735.03, 1,655.16; $\upsilon_{C=C}$: 1,623.94, 1,604.93, 1,542.29, 1,511.22, 1,494.16, 1,459.03; δ_{CH}: 1,359.77, 1,342.21; $\gamma_{=CH}$: 839.71, 822.92, 748.66, 714.68. HRMS (ESI) *m/z* calculated for $C_{21}H_{19}F_1N_3O_4$ $[M+H]^+$: 396.1354, found 396.1348.

*N-(1-(2-(4-Fluorobenzylamino)-2-oxoethyl)-2,3-dioxoindolin-5-yl)pivalamide (**8i**)*. Yield: 63%; orange-red solid; mp: 260.4-261.9°C. ^{1}H-NMR (DMSO-d_6) δ: 9.34 (s, 1H, NH), 8.75 (t, J = 6.0 Hz, 1H, NH), 7.91 (dd, J_1 = 8.4 Hz, J_2 = 1.8 Hz,1H,Ar-H), 7.88 (d, J = 2.4 Hz, 1H, Ar-H), 7.24 (t, J = 7.2 Hz, 2H, Ar-H), 7.14 (d, J = 8.4 Hz, 1H, Ar-H), 7.13 (t, J = 9.6 Hz, 2H, Ar-H), 4.36 (s, 2H, CH_2), 4.27 (d, J = 6.0 Hz,1H,CH_2), 1.23 (s,9H,CH_3). ^{13}C-NMR (DMSO-d_6) δ: 183.50, 177.01, 166.58, 162.42, 160.82, 159.01, 146.26, 135.72, 130.02, 129.51, 129.46, 117.94, 116.94, 115.48, 115.35, 110.03, 43.17, 41.79, 39.50, 27.58, 27.58, 27.58. IR (KBr, cm^{-1}): υ_{NH}: 3,265.79; $\upsilon_{=CH}$: 3,074.19; υ_{CH3}: 2,968.59, 2,872.71; $\upsilon_{C=O}$: 1,746.57, 1,671.78, 1,652.98; $\upsilon_{C=C}$: 1,624.86, 1,605.91, 1,534.80, 1,509.89, 1,493.55, 1,452.28; δ_{CH}: 1,367.79, 1,335.79, 1,307.98; $\gamma_{=CH}$: 901.66, 810.87, 712.86, 660.87. HRMS (ESI) *m/z* calculated for $C_{22}H_{23}F_1N_3O_4$ $[M+H]^+$: 412.1667, found 442.1663.

*N-(1-(2-(4-Fluorobenzylamino)-2-oxoethyl)-2,3-dioxoindolin-5-yl)-2-hydroxybenzamide (**8j**)*. Yield**:** 78%; orange-red solid; mp: 308.7-309.4°C. ^{1}H-NMR (DMSO-d_6) δ: 11.73 (s, 1H, Ar-OH), 10.45 (s, 1H, NH), 8.76 (t, J = 5.4 Hz, 1H, NH), 7.99 (d, J = 2.4 Hz, 1H, Ar-H), 7.94 (d, J = 7.8 Hz, 1H, Ar-H), 7.87 (dd, J_1 = 9.0 Hz, J_2 = 2.4 Hz, 1H, Ar-H), 7.45 (t, J = 10.2 Hz, 1H, Ar-H), 7.25 (m, 2H, Ar-H), 7.14 (t, J = 6.0 Hz, 2H, Ar-H), 7.10 (d, J = 8.4 Hz, 1H, Ar-H), 6.98 (m, 2H, Ar-H), 4.40 (s, 2H, CH_2), 4.29 (d, J = 6.0 Hz, 2H, CH_2). ^{13}C-NMR (DMSO-d_6) δ: 183.33, 167.52, 166.58, 162.425, 160.82, 159.05, 159.02, 147.00, 134.41, 134.26, 130.75, 129.52, 129.47, 129.34, 119.48, 118.17, 117.70, 117.62, 117.60, 115.51, 115.37, 111.34, 43.22, 41.791. IR (KBr, cm^{-1}): υ_{OH}: 3,311.80; $\upsilon_{=CH}$: 3,082.92; $\upsilon_{C=O}$: 1,739.57, 1,666.67, 1,644.81; $\upsilon_{C=C}$: 1,627.13, 1,606.39, 1,558.03, 1,509.98, 1,496.31, 1,444.51; δ_{CH}: 1,329.79, 1,313.73; $\gamma_{=CH}$: 831.30, 757.81. HRMS (ESI) *m/z* calculated for $C_{24}H_{19}F_1N_3O_5$ $[M+H]^+$: 446.1511, found 446.1504.

*N-(1-Benzyl-2,3-dioxoindolin-5-yl)benzamide (**8k**)*. Yield: 77%; vermilion solid; mp: 197.2-198.1°C. ^{1}H-NMR (DMSO-d_6) δ: 10.30 (s, 1H, NH), 7.89 (d, J = 2.4 Hz, 1H, Ar-H), 7.63 (dd, J_1 = 8.4 Hz, J_2 = 2.4 Hz, 1H, Ar-H), 7.41 (d, J = 7.2 Hz, 2H, Ar-H), 7.33 (m, 4H, Ar-H), 7.28 (t, J = 7.2 Hz, 2H, Ar-H), 7.25 (m, 2H, Ar-H), 6.93 (d, J = 8.4 Hz, 1H, Ar-H), 4.88 (s, 2H, CH_2). ^{13}C-NMR (DMSO-d_6) δ: 183.64, 165.94, 158.93, 146.51, 135.97, 135.50, 134.90, 132.17, 129.85, 129.10, 129.10, 128.87, 128.87, 128.06, 128.06, 127.98, 127.81, 127.81, 118.03, 117.00, 111.62, 43.40. IR (KBr, cm^{-1}): υ_{NH}: 3,345.43; $\upsilon_{=CH}$: 3,061.69, 3,031.09; $\upsilon_{C=O}$: 1,738.95, 1,680.98; $\upsilon_{C=C}$: 1,624.14, 1,605.06, 1,548.19, 1,491.44, 1,453.53; δ_{CH}: 1,346.93; $\gamma_{=CH}$: 827.86, 767.62, 719.86, 697.76. HRMS (ESI) *m/z* calculated for $C_{22}H_{17}N_2O_3$ $[M+H]^+$: 357.1234, found 357.1247.

*N-(1-Benzyl-2,3-dioxoindolin-5-yl)-2-phenyl-acetamide (**8l**)*. Yield: 63%; vermilion solid; mp: 237.5-238.1°C. ^{1}H-NMR (DMSO-d_6) δ: 10.30 (s, 1H, NH), 7.88 (d, J = 1.8 Hz, 1H, Ar-H), 7.63 (dd, J_1 = 8.4 Hz, J_2 = 2.4 Hz, 1H, Ar-H), 7.42 (d, J = 7.2 Hz, 2H, Ar-H), 7.32 (m, 4H, Ar-H), 7.28 (t, J = 7.2 Hz, 2H, Ar-H),

7.24 (m, 2H, Ar-H), 6.93 (d, J = 8.4 Hz, 1H, Ar-H), 4.88 (s, 2H, CH_2), 3.62 (s, 2H, CH_2). ^{13}C-NMR (DMSO-d_6) δ: 183.62, 169.64, 158.86, 146.21, 136.17, 135.96, 135.51, 129.51, 129.51, 129.08, 129.08, 128.77, 128.77, 128.56, 127.97, 127.77, 127.77, 127.03, 118.09, 115.71, 111.76, 43.58, 43.35. IR (KBr, cm^{-1}): υ_{NH}: 3,411.39; $\upsilon_{=CH}$: 3,062.87; $\upsilon_{C=O}$: 1,738.62, 1,652.37; $\upsilon_{C=C}$: 1,623.88, 1,605.09, 1,579.75, 1,543.55, 1,493.95, 1,454.39; δ_{CH}: 1,332.28, 1,308.90; $\gamma_{=CH}$: 834.59, 796.04, 700.39. HRMS (ESI) *m/z* calculated for $C_{23}H_{19}N_2O_3$ $[M+H]^+$: 371.1390, found 371.1408.

*N-(1-Benzyl-2,3-dioxoindolin-5-yl)-3-phenylpropanamide (**8m**)*. Yield: 68%; purple solid; mp: 224.2-225.1°C. ^{1}H-NMR (DMSO-d_6) δ: 10.03 (s, 1H, NH), 7.88 (d, J = 2.4 Hz, 1H, Ar-H), 7.58 (dd, J_1 = 8.4 Hz, J_2 = 2.4 Hz, 1H, Ar-H), 7.42 (d, J = 7.2 Hz, 2H, Ar-H), 7.34 (t, J = 7.2 Hz, 2H, Ar-H), 7.28 (m, 3H, Ar-H), 7.23 (d, J = 7.2 Hz, 2H, Ar-H), 7.17 (t, J = 7.2 Hz, 1H, Ar-H), 6.92 (d, J = 7.8 Hz, 1H, Ar-H), 4.88 (s, 2H, CH_2), 2.90 (t, J = 7.8 Hz, 2H, CH_2), 2.60 (t, J =8.4 Hz, 2H, CH_2). ^{13}C-NMR (DMSO-d_6) δ: 183.68, 170.02, 158.85, 146.08, 141.47, 135.95, 135.57, 129.08, 129.08, 128.75, 128.75, 128.66, 128.66, 128.47, 127.97, 127.78, 127.78, 126.39, 118.03, 115.68, 111.71, 43.36, 38.28, 31.20. IR (KBr, cm^{-1}): υ_{NH}: 3,360.01; $\upsilon_{=CH}$: 3,062.68, 3,027.27; υ_{CH2}: 2,966.01, 2,929.00, 2,863.15; $\upsilon_{C=O}$: 1,735.82, 1,679.20; $\upsilon_{C=C}$: 1,626.21, 1,605.59, 1,558.72, 1,491.25, 1,454.00; δ_{CH}: 1,354.90, 1,330.60; $\gamma_{=CH}$: 828.33, 751.50, 717.10, 696.51. HRMS (ESI) *m/z* calculated for $C_{24}H_{21}N_2O_3$ $[M+H]^+$: 385.1547, found 385.1563.

*N-(1-Benzyl-2,3-dioxoindolin-5-yl)-2,4-dichlorobenzamide (**8n**)*. Yield: 68%; pink solid; mp: 268.3-269.7°C. ^{1}H-NMR (DMSO-d_6) δ: 10.67 (s, 1H, NH), 7.97 (d, J = 1.8 Hz, 1H, Ar-H), 7.78 (d, J = 1.8 Hz, 1H, Ar-H), 7.74 (dd, J_1 = 8.4 Hz, J_2 = 1.8 Hz, 1H, Ar-H), 7.64 (d, J = 7.8 Hz, 1H, Ar-H), 7.57 (dd, J_1 = 8.4 Hz, J_2 = 1.8 Hz, 1H, Ar-H), 7.43 (d, J = 7.8 Hz, 2H, Ar-H), 7.35 (t, J = 7.2 Hz, 2H, Ar-H), 7.29 (t, J = 7.2 Hz, 1H, Ar-H), 6.98 (d, J = 8.4 Hz, 1H, Ar-H), 4.91 (s, 2H, CH_2). ^{13}C-NMR (DMSO-d_6) δ: 183.52, 164.46, 158.90, 146.74, 135.88, 135.75, 135.50, 134.99, 131.73, 130.80, 129.70, 129.08, 129.08, 129.03, 127.98, 127.94, 127.78, 127.78, 118.17, 116.15, 111.85, 43.40. IR (KBr, cm^{-1}): υ_{NH}: 3,274.61; $\upsilon_{=CH}$: 3,087.49, 3,062.10; $\upsilon_{C=O}$: 1,740.80, 1,721.83, 1,655.88; $\upsilon_{C=C}$: 1,624.58, 1,601.71, 1,583.30, 1,555.92, 1,533.52, 1,490.68, 1,452.88; δ_{CH}: 1,349.20, 1,330.00, 1,308.67; $\gamma_{=CH}$: 836.63, 779.15, 720.75, 700.82. HRMS (ESI) *m/z* calculated for $C_{22}H_{15}Cl_2N_2O_3$ $[M+H]^+$: 425.0454, found 425.0472.

*N-(1-Benzyl-2, 3-dioxoindolin-5-yl) pivalamide (**8o**)*. Yield: 60%; purple solid; mp: 233.4-234.6°C. ^{1}H-NMR (DMSO-d_6) δ: 9.31 (s, 1H, NH), 7.88 (d, J = 1.8 Hz, 1H, Ar-H), 7.73 (dd, J_1 = 8.4 Hz, J_2 = 2.4 Hz, 1H, Ar-H), 7.42 (d, J = 7.2 Hz, 2H, Ar-H), 7.34 (t, J = 7.2 Hz, 2H, Ar-H), 7.28 (t, J = 7.2 Hz, 1H, Ar-H), 6.92 (d, J = 8.4 Hz, 1H, Ar-H), 4.88 (s, 2H, CH_2), 1.19 (s, 9H, CH_3). ^{13}C-NMR (DMSO-d_6) δ: 183.69, 177.03, 158.92, 146.18, 135.99, 135.66, 129.80, 129.06, 129.06, 127.94, 127.73, 127.73, 117.93, 117.03, 111.43, 43.32, 39.50, 27.56, 27.56, 27.56. IR (KBr, cm^{-1}): υ_{NH}: 3,413.43; $\upsilon_{=CH}$: 3,060.11; υ_{CH3}: 2,967.60, 2,869.76; $\upsilon_{C=O}$: 1,728.23, 1,677.41; $\upsilon_{C=C}$: 1,619.06, 1,604.10, 1,538.36, 1,491.97, 1,453.15; δ_{CH}: 1,398.83, 1,335.23, 1,314.85; $\gamma_{=CH}$: 831.45, 788.33, 749.15, 717.95, 697.87. HRMS (ESI) *m/z* calculated for $C_{20}H_{21}N_2O_3$ $[M+H]^+$: 337.1547, found 337.1572.

*N-(1-Benzyl-2,3-dioxoindolin-5-yl)cyclopropanecarboxamide (**8p**)*. Yield: 79%; pink solid; mp: 249.5-250.2°C. ^{1}H-NMR (DMSO-d_6) δ: 10.30 (s, 1H, NH), 7.88 (d, J = 2.4 Hz, 1H, Ar-H), 7.62 (dd, J_1 = 8.4 Hz, J_2 = 2.4 Hz, 1H, Ar-H), 7.42 (d, J = 7.2 Hz, 2H, Ar-H), 7.34 (t, J = 7.8 Hz, 2H, Ar-H), 7.28 (t, J = 7.8 Hz, 1H, Ar-H), 6.92 (d, J = 8.4 Hz, 1H, Ar-H), 4.88 (s, 2H, CH_2), 1.71 (m, 1H, CH), 0.79 (d, J = 6.0 Hz, 4H, CH_2). ^{13}C-NMR (DMSO-d_6) δ: 183.69, 172.14, 158.85, 145.96, 135.98, 135.74, 129.07, 129.07, 128.32, 127.96, 127.78, 127.78, 118.05, 115.62, 111.71, 43.36, 14.95, 7.72, 7.72. IR (KBr, cm^{-1}): υ_{NH}: 3,340.81; $\upsilon_{=CH}$: 3,059.31; υ_{CH2}: 2,925.08; $\upsilon_{C=O}$: 1,739.43, 1,714.20, 1,680.28; $\upsilon_{C=C}$: 1,621.56, 1,606.07, 1,553.06, 1,491.32, 1,454.23; δ_{CH}: 1,397.01, 1,351.43, 1,336.26, 1,301.19; γ_{CH}: 841.29, 822.95, 790.28, 718.39, 698.72. HRMS (ESI) *m/z* calculated for $C_{19}H_{17}N_2O_3$ $[M+H]^+$: 321.1234, found 321.1213.

Original Article

DOI: 10.5582/ddt.2014.01028

Synthesis and crystal structure of 6-fluoro-3-hydroxypyrazine-2-carboxamide

Fangyuan Shi[1], Zongtao Li[2], Lingjin Kong[2], Yuanchao Xie[1], Tao Zhang[2,*], Wenfang Xu[1,*]

[1] *Department of Medicinal Chemistry, School of Pharmaceutical Sciences, Shandong University, Ji'nan, Shandong, China;*
[2] *Shandong Qidu Pharmaceutical Co., Ltd., Zibo, Shandong, China.*

Summary **As a RNA polymerase inhibitor, 6-fluoro-3-hydroxypyrazine-2-carboxamide commercially named favipiravir has been proved to have potent inhibitory activity against RNA viruses *in vitro* and *in vivo*. A four-step synthesis of the compound is described in this article, amidation, nitrification, reduction and fluorination with an overall yield of about 8%. In addition, we reported the crystal structure of the title compound. The molecule is almost planar and the intramolecular O−H···O hydrogen bond makes a 6-member ring. In the crystal, molecules are packing governed by both hydrogen bonds and stacking interactions.**

Keywords: Synthesis, crystal structure, hydrogen bond, π-π stacking interactions

1. Introduction

There is much interest in RNA polymerase inhibitors for their potential contributions in the treatment of the influenza (*1-3*). One inhibitor, 6-fluoro-3-hydroxypyrazine-2-carboxamide named favipiravir was first prepared by Y. Furuta and coworkers (*4*), and has been proved to have potent inhibitory activity against RNA viruses *in vitro* and *in vivo* (*5-8*). The previously reported synthetic procedure is shown in Scheme 1 involving seven steps starting from 3-aminopyrazine-2-carboxylic acid. However, in the ammoniated step, it involves the catalysis of tris(dibenzylideneacetone) dipalladium and (*S*)-(-)-2,2'-bis(diphenylphosphino)-1,1'-binaphthyl (BINAP), which are very expensive. The last step proceeds poorly with a low (4.3%) isolated yield, making the overall yield approximately 0.44%. This sythesitc process is hardly suitable for large-scale production. Therefore, in order to improve the yield and reduce the cost, we report a modified procedure that boosts the overall yield over 20-fold with four steps in this article. We also report the crystal structure of the compund for the first time.

**Address correspondence to:*
Dr. Wenfang Xu, Department of Medicinal Chemistry, School of Pharmaceutical Sciences, Shandong University, 44, West Culture Road, Ji'nan, Shandong 250012, China.
E-mail: wenfxu@gmail.com

2. Materials and Methods

2.1. *Materials*

Solvent for anhydrous reaction should be processed before use. ^{1}H-NMR spectra were determined on a Brucker Avance 300 spectrometer or 600 using tetramethylsilane (TMS) as an internal standard. The solvents for NMR were DMSO-d^6 (δ 2.5 for ^{1}H), CD_3Cl_3 (δ 7.3 for ^{1}H). HRMS analysis was provided by Agilent 6520 Q-TOF LC/MS spectrometer (Agilent, Germany). All reactions were monitored by thin-layer chromatography (TLC) on 25.4 × 76.2 mm silica gel plates (GF-254). Silica gel used for column chromatography was 200~300 mesh. Melting points were determined on an electrothermal melting point apparatus and were uncorrected.

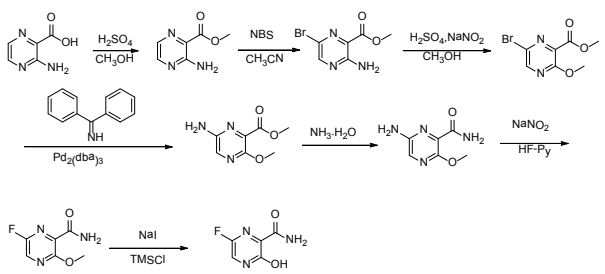

Scheme1. Synthesis of 6-fluoro-3-hydroxypyrazine-2-carboxamide reported in the reference.

2.2. *Synthesis*

2.2.1. *Preparation of 3-hydroxypyrazine-2-carboxamide*

To a suspension of 3-hydroxypyrazine-2-carboxylic acid (1.4 g, 10 mmol) in 150 mL MeOH, $SOCl_2$ was added dropwise at 40°C with magnetic stirring for 6 h resulting in a bright yellow solution. The reaction was then concentrated to dryness. The residue was dissolved in 50 mL 25% aqueous ammonia and stirred overnight to get a suspension. The precipitate was collected and dried. The solid yellow-brown crude product was recrystallization with 50 mL water to get the product as pale yellow crystals (1.1 g, 78%). mp = 263-265°C. ^{1}H-NMR (300 MHz, DMSO): δ 13.34 (brs, 1H, OH), 8.69 (s, 1H, pyrazine H), 7.93-8.11 (m, 3H, pyrazine H, $CONH_2$). HRMS (ESI): *m/z* $[M + H]^+$ calcd for $C_5H_6N_3O_2^+$: 140.0460; found: 140.0457.

2.2.2. *Preparation of 3-hydroxy-6-nitropyrazine-2-carboxamide*

In the solution of 3-hydroxypyrazine-2-carboxamide (1.0 g, 7 mmol) in 6 mL concentrate sulfuric acid under ice-cooling, potassium nitrate (1.4 g, 14 mmol) was added. After stirring at 40°C for 4 h, the reaction mixture was poured into 60 mL water. The product was collected by filtration as yellow solid (0.62 g, 48%). mp = 250-252°C. ^{1}H-NMR (600 MHz, DMSO): δ 12.00-15.00 (br, 1H, OH), 8.97 (s, 1H, pyrazine H), 8.32 (s, 1H, $CONH_2$), 8.06 (s, 1H, $CONH_2$). ^{13}C-NMR (75 MHz, DMSO): δ 163.12, 156.49, 142.47, 138.20, 133.81. HRMS (ESI): *m/z* $[M + H]^+$ calcd for $C_5H_5N_4O_4^+$: 185.0311; found: 185.0304.

2.2.3. *Preparation of 6-amino-3-hydroxypyrazine-2-carboxamide*

3-Hydroxy-6-nitropyrazine-2-carboxamide (0.6 g, 3.3 mmol) and a catalytic amount of raney nickel were suspended in MeOH, then hydrazine hydrate was added dropwise. The resulting solution was refluxed 2 h, cooled, filtered with diatomite, and then MeOH is evaporated in vacuo to get the crude product as dark brown solid without further purification (0.4 g, 77%). HRMS (ESI): *m/z* $[M + H]^+$ calcd for $C_5H_7N_4O_2^+$: 155.0569; found:155.0509.

2.2.4. *Preparation of 6-fluoro-3-hydroxypyrazine-2-carboxamide*

To a solution of 6-amino-3-hydroxypyrazine-2-carboxamide (0.4 g, 2.6 mmol) in 3 mL 70% HF-pyridine aqueous at -20°C under nitrogen atmosphere, sodium nitrate (0.35 g, 5.2 mmol) was added. After stirring 20 min, the solution was warmed to room temperature for another one hour. Then 20 mL ethyl acetate/water (1:1) were added, after separation of the upper layer, the aqueous phase is extracted with four 20 mL portions of ethyl acetate. The combined extracts are dried with anhydrous magnesium sulfate and concentrated to dryness to get crude product as oil. The crude product was purified by chromatography column as white solid (0.12 g, 30%). mp = 178-180°C. ^{1}H-NMR (600 MHz, DMSO): δ 12.34 (brs, 1H, OH), 8.31 (d, 1H, pyrazine H, J = 8.0 Hz), 7.44 (s, 1H, $CONH_2$), 5.92 (s, 1H, $CONH_2$). ^{13}C-NMR (75 MHz, DMSO): δ 168.66, 159.69, 153.98, 150.76, 135.68. HRMS (ESI): *m/z* $[M + H]^+$ calcd for $C_5H_5FN_3O_2^+$: 158.0366; found: 158.0360.

2.3. *Single X-ray crystallography*

6-Fluoro-3-hydroxypyrazine-2-carboxamide (0.2 g) was dissolved in methanol (50 mL) at room temperature. Colorless crystals of this compound were obtained through slow evaporation after two weeks. A colorless single crystal with dimension 0.37 × 0.29 × 0.27 mm^3 was selected for indexing and data collection at 150 Kon aNonius-based Kappa Bruker diffractrometer equipped with a charge-coupled de vice (CCD) area detector and Mo Kα (k = 0.7107 Å) radiation. The structures were solved by direct methods using the program SHELXS-97 and refined by full-matrix least-square refinementon F2 using the program SHELXL-97. All H atoms were placed in geometrically calculated positions and refined using a riding model with C-H = 0.93 Å (for CH); 0.86 Å (for NH_2 groups) and 0.82 Å (for OH), their isotropic displacement parameters were set to 1.2 times (1.5 times for OH) the equivalent displacement parameter of their parent atoms. Crystal data: $C_5H_4FN_3O_2$, Mr = 157.11, orthorhombic, $Pna2_1$, Z = 4, a = 9.1106(8), b = 14.7619(14), c = 4.6910(4) Å, α = β = γ = 90º, V = 630.89 (10) $Å^3$, T = 296 K, F(000) = 320, u = 0.15 mm^{-1}, Dx = 1.654 Mg m^{-3}. 7031 reflections were corrected, 832 unique (R_{int} = 0.0195). R_1 = 0.0294, wR_2 = 0.0825. Further details of the crystallographic data can be found in the supporting information (CCDC deposition number 969968).

3. Results and Discussion

The low yield and high cost for the synthesis of favipiravir is attributed to the complicated process and expensive cytalyst in the ammoniated step. 3-Hydroxypyrazine-2-carboxylic acid (compound **1**) could be purchased or synthsized from 3-aminopyrazine-2-carboxylic acid (*9*), which is a common intermediate in orgainc synthesis. In our synthetic route, compound **1** was first esterified and amidated to give compound **2**, followed by nitration with potassium nitrate. During the reduction stept, we carried out several different methods. Hydrogen reduction proceeded poorly with a low (30%) yield and produced a large number of by-products. Reaction with zinc and

ammonia produced a large number of brown solid, which were difficult to purity and led to the failure of fluorination. The raney nickel went well with higher (77%) yield and fewer by-products. In the last fluorination step, it was found that about an hour after the reaction started, the yield decrease with reaction time. If the reaction time exceed 12 h, there would be no product existed. Overall, the target compound was prepared with a yield of about 8%, as shown in Scheme 2.

Slow evaporation of a solution of the title compound in methanol gave single crystals that were suitable for X-ray diffraction. It crystallized in the orthorhombic space group $Pna2_1$. In the title compound, $C_5H_4FN_3O_2$, the molecule is almost planar (r.m.s. deviation for the non-H atoms = 0.014 Å) and an intramolecular O–H···O hydrogen bond closes a 6-member ring (Figure 1), which can also prevent the keto-enol tautomerism of C3 position.

In the crystal, the molecules arrange in a prism structure, and are linked into chains by N–H···O hydrogen bonds and N–H···N hydrogen bonds (Figure 2). The characteristics of these bonds are given in Table 1. The molecules arrange in two nearly vertical (θ = 87.12°) orientations, forming a cavity structure. Each pyrazine ring is both a hydrogen bond donor and acceptor, and these interactions work cooperatively to lock the molecules together. All bond length and angles are in the normal range.

From the crystal structure we find that the neighboring pyrazine ring are nearly-parallel (θ = 2.81), with a vander Waals distance of about 3.23 Å. The arrangement of aromatic (π) systems predicts that between molecules, π-π stacking interactions exist. We note the structure also displays displacement with a distance of about 3.08 Å. As we all know, π-π electron interaction is an important force, which is roughly proportional to the area of π-overlap. Of course, displacement of π-systems can diminish the repulsion (*10*). These characteristics show that the crystal structure is packing governed by both hydrogen bonds and stacking interactions.

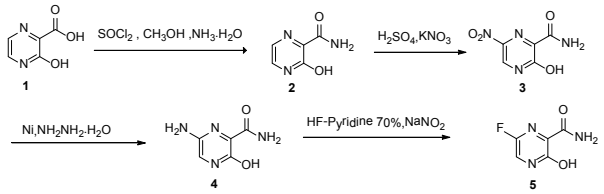

Scheme 2. Synthesis of 6-fluoro-3-hydroxypyrazine-2-carboxamide.

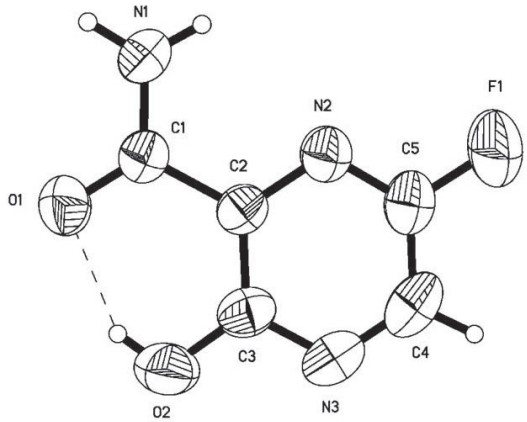

Figure 1. ORTEP plot of the 6-fluoro-3-hydroxypyrazine-2-carboxamide.

4. Conclusion

We have presented a new method for the synthesis of 6-fluoro-3-hydroxypyrazine-2-carboxamide, which is more effective and economical relative to the one previously reported. Upon crystallization, we find the molecule is almost planar and exist an intramolecular O–H···O hydrogen bond. Molecules are linked into chains by hydrogen bonds and the neighboring pyrazine ring display π-π stacking interactions (offset face-to-face). These arrangements show that the crystal structure is packing governed by both hydrogen bonds and stacking interactions, arranging in two nearly vertical orientations and forming a cavity structure.

Acknowledgements

This work was financially supported by the National Nature Science Foundation of China (No. 21172134), the Doctoral Foundation of Ministry of Education of China (No.20110131110037) and National Scientific and Technological Major Project of Ministry of Science and Technology of China (Grant No. 2011ZX09401-015).

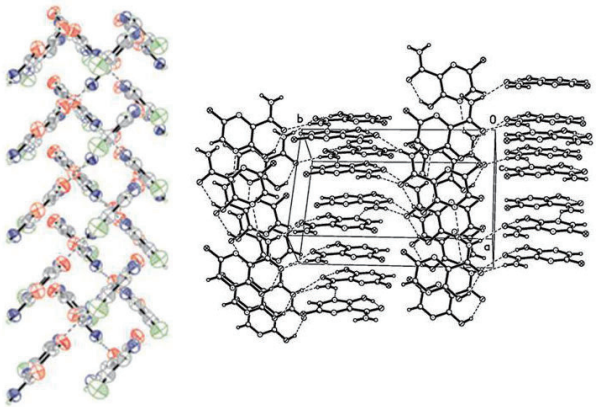

Figure 2. Crystal structure of 6-fluoro-3-hydroxypyrazine-2-carboxamide.

Table 1. Hydrogen bonds geometry (Å,°)

D–H···*A*	*D*–H	H–*A*	*D*–*A*	*D*–H···*A*
N1–H1B···N3^{i}	0.86	2.34	3.000 (2)	134
N1–H1*A*···O1^{ii}	0.86	2.06	2.9099 (18)	170
O2–H2···O1	0.82	1.88	2.591 (2)	144

Symmetry codes: (i) x−1/2, −y+1/2, z−1; (ii) −x+1, −y+1, z−1/2.

References

1. Nistal-Villan E, Garcia-Sastre A. New prospects for the rational design of antivirals. Nat Med. 2009; 15:1253-1254.
2. Krug RM, Aramini JM. Emerging antiviral targets for influenza A virus. Trends pharmacol Sci. 2009; 30:269-277.
3. Shi F, Xie Y, Shi L, Xu W. Viral RNA polymerase: A promising antiviral target for influenza A virus. Curr Med Chem. 2013; 20:3923-3934.
4. Furuta Y, Takahashi K. Nitrogenous heterocyclic carboxamide derivatives or salts thereof and antiviral agents containing both. WO 00/10569[P]. 2001-04-07.
5. Furuta Y, Gowen BB, Takahashi K, Shiraki K, Smee DF, Barnard DL. Favipiravir (T-705), a novel viral RNA polymerase inhibitor. Antiviral Res. 2013; 100:446-454.
6. Furuta Y, Takahashi K, Shiraki K, Sakamoto K, Smee DF, Barnard DL, Gowen BB, Julander JG, Morrey JD. T-705 (favipiravir) and related compounds: Novel broad-spectrum inhibitors of RNA viral infections. Antiviral Res. 2009; 82:95-102.
7. Furuta Y, Takahashi K, Kuno-Maekawa M, Sangawa H, Uehara S, Kozaki K, Nomura N, Egawa H, Shiraki K. Mechanism of action of T-705 against influenza virus. Antimicrob. Agents Chemother. 2005; 49:981-986.
8. Gowen BB, Wong MH, Jung KH, Sanders AB, Mendenhall M, Bailey KW, Furuta Y, Sidwell RW. In vitro and in vivo activities of T-705 against arenavirus and bunyavirus infections. Antimicrobial Agents Chemother. 2007; 51:3168-3176.
9. Caldwell JJ, Veillard N, Collins I. Design and synthesis of 2(1H)-pyrazinones as inhibitors of protein kinases. Tetradron. 2012; 68:9713-9728.
10. Głoˊwka ML, Martynowski D, Kozàowska K. Stacking of six-membered aromatic rings in crystals. J Mol Struct. 1999; 474:81-89.

(Received June 21, 2014; Accepted June 27, 2014)

Original Article

DOI: 10.5582/ddt.2014.01024

Effectiveness of Chinese prescription Kangen-karyu for dyslipidemia, using 3T3-L1 adipocytes and type 2 diabetic mice

Chan Hum Park[1], Dong Young Rhyu[2], Jeong Sook Noh[3], Chul Min Park[2], Takako Yokozawa[1,4,*]

[1] *College of Korean Medicine, Daegu Haany University, Daegu, Republic of Korea;*
[2] *College of Natural Sciences and Institute of Korean Traditional Medicine Industry, Mokpo National University, Jeonnam, Republic of Korea;*
[3] *Department of Food Science & Nutrition, Tongmyong University, Busan, Republic of Korea;*
[4] *Graduate School of Science and Engineering for Research, University of Toyama, Toyama, Japan.*

Summary **The Chinese prescription Kangen-karyu, comprised of six crude drugs, has received much attention due to its numerous biological activities. The present study was conducted to examine whether Kangen-karyu has an ameliorative effect on dyslipidemia. The effect of Kangen-karyu was evaluated using 3T3-L1 adipocytes, and also *db/db* mice as an experimental model for diabetic dyslipidemia. Kangen-karyu significantly inhibited adipocyte differentiation and lipid accumulation. Kangen-karyu also down-regulated the mRNA levels of peroxisome proliferator-activated receptor (PPAR)γ, sterol regulatory element-binding protein (SREBP)-1c, and fatty acid synthase, and the protein levels of aP2 and PPARγ, which indicates that Kangen-karyu inhibited adipogenesis during adipocyte differentiation, and may have potential anti-dyslipidemia effects. In addition, the administration of Kangen-karyu reduced hyperlipidemia in *db/db* type 2 diabetic mice through a decline in the serum levels of lipids, and an improvement of lipoprotein profiles. The enhanced hepatic triglyceride level of the *db/db* mice was significantly reduced by Kangen-karyu administration through the down-regulation of SREBP-1 and lipogenic enzymes in the liver. These findings indicate that Kangen-karyu exerts anti-dyslipidemia effects in adipocytes and type 2 diabetic *db/db* mice.**

Keywords: Kangen-karyu, 3T3-L1 adipocyte, *db/db* mouse, dyslipidemia

1. Introduction

Metabolic syndrome is a multi-component disorder characterized by hypertriglyceridemia, hyperglycemia, abdominal obesity and hypertension, and is closely linked to type 2 diabetes mellitus (*1,2*). The etiology of metabolic syndrome involves the complex interaction between genetic, metabolic, and environmental factors (*3*). Obesity is well recognized as the most important health problem related to the genesis of metabolic syndrome, and the rising incidence of this disease throughout the world has generated interest in the underlying mechanisms involved in these pathologies (*4*).

**Address correspondence to:*
Dr. Takako Yokozawa, Graduate School of Science and Engineering for Research, University of Toyama, 3190 Gofuku, Toyama 930-8555, Japan.
E-mail: yokozawa@inm.u-toyama.ac.jp

Obesity is caused by an imbalance between energy intake and expenditure that may lead to the pathological growth of adipocytes (*5*). Adipocytes play a central role in regulating adipose mass and obesity. Increased adipose mass in obesity is not only caused by adipose tissue hypertrophy, but also by adipose tissue hyperplasia, which triggers the transformation of preadipocytes into adipocytes (*6,7*). Thus, adipocyte differentiation and the amount of fat accumulation are associated with development of obesity. On the other hand, dysfunctional lipid metabolism is a key component in the development of metabolic syndrome, a very common condition characterized by dyslipidemia, insulin resistance, abdominal obesity, and hypertension, which are all related to an elevated risk of type 2 diabetes mellitus (*8*). The liver is an important organ for maintaining lipid metabolism and homeostasis, since it can store (*via* lipogenesis) or release (as lipoprotein) lipid fuels. Triglycerides (TG) are involved in the ectopic accumulation of lipid

stores in the liver and are associated with a number of diseases, such as metabolic syndrome and type 2 diabetes.

Anti-obesity drugs such as orlistat, sibutramine, and topiramate have been used to treat obesity (*9*). However, these drugs have many side effects, including dry mouth, anorexia, insomnia, and gastrointestinal distress (*10*). Due to the adverse side effects associated with many anti-obesity drugs, recent drug trials have focused on herbal medicines (*11*). Under the guidelines of the US Food and Drug Administration, botanical drugs can be developed faster and more cheaply than conventional single-entity pharmaceuticals. Thus, there are many botanicals that might provide safe, natural, and cost-effective alternatives to synthetic drugs. Recent studies have found that natural bioactive compounds can be used to treat obesity in 3T3-L1 adipocytes and in an obese mouse model.

Kangen-karyu (Guan-Yuan-Ke-Li), a crude drug developed from a traditional Chinese prescription consisting of six herbs (Paeoniae Radix, Cnidii Rhizoma, Carthami Flos, Cyperi Rhizoma, Aucklandiae Radix, and Salviae Miltiorrhizae Radix), has been clinically used as a treatment for cardiovascular diseases, such as angina pectoria and cerebrovascular diseases. Kangen-karyu shows biological activity, such as an anti-aging effect, the inhibition of platelet aggregation, a hypotensive effect, and the recovery of learning and memory impairment induced by senescence (*12-15*). In addition, we have reported that Kangen-karyu showed favorable ameliorative effects on fructose-induced metabolic syndrome, such as hyperglycemia, hyperlipidemia, and hypertension, through the reduction of TG and cholesterol levels with the regulation of hepatic sterol regulatory element-binding protein (SREBP)-1 expression, and also exhibited protective effects against diet-induced hypercholesterolemia in rats (*16,17*). We also reported the beneficial effect of Kangen-karyu on hyperlipidemia in streptozotocin-induced type 1 diabetic rats (*18*). These results suggest that Kangen-karyu can ameliorate metabolic disorders such as dyslipidemia and diabetes mellitus. Therefore, this study was designed to determine whether Kangen-karyu affects the differentiation of 3T3-L1 preadipocytes into adipocytes and the mechanism related to its differentiation. We also investigated the effect of Kangen-karyu on diabetic dyslipidemia. For this, *db/db* mice were used as an experimental model for diabetic dyslipidemia. The *db/db* mice develop diabetes mellitus due to a failure to respond to leptin, resulting from a mutation in their receptor gene expressed in the hypothalamus, although gene expression and leptin secretion are markedly augmented in these mice, resulting in leptin resistance (*19*). The *db/db* mice were also characterized by obesity, sustained hyperglycemia, and hyperlipidemia as a result of destroyed leptin receptors (*20*).

2. Materials and Methods

2.1. *Materials*

Dulbecco's modified Eagle's medium (DMEM), fetal calf serum (FCS), penicillin, streptomycin, and phosphate-buffered saline (PBS) were purchased from HyClone Laboratories (Logan, UT, USA). 3-(4,5-Dimethylthiazol-2-yl)-2,5-diphenyl tetrazolium bromide (MTT), insulin, dexamethasone, 3-isobutyl-1-methylxanthine (IBMX), oil red O, 2-mercapthoethanol, protease inhibitor cocktail, and β-actin were purchased from Sigma-Aldrich (St Louis, MO, USA). Primary antibodies against peroxisome proliferator-activated receptor (PPAR)γ, PPARα, and SREBP-1c were purchased from Santa Cruz Biotechnology (Santa Cruz, CA, USA). Similarly, secondary antibodies for mouse (peroxidase-conjugated affinipure goat anti-mouse IgG) and rabbit (peroxidase-conjugated affinipure goat anti-rabbit IgG) were purchased from Jackson ImmunoResearch Laboratories (Baltimore, USA). The protein molecular weight marker was obtained from Thermo Scientific (Rockford, IL, USA). The nitrocellulose membrane for Western blotting was purchased from Bio-Rad Laboratories (Richmond, CA, USA). Western blot chemiluminescent substrate was purchased from Imgenex (San Diego, CA, USA). Radioimmunoprecipitation assay buffer was purchased from Biosesang (Seoul, Korea). ECL Western Blotting Detection Reagents were purchased from GE Health Care (Piscataway, NJ, USA). All solvents, chemicals, and reagents were of analytical grade and purchased from Sigma-Aldrich unless otherwise specified.

2.2. *Preparation of Kangen-karyu extract*

The composition of Kangen-karyu used in this study is shown in Table 1. Kangen-karyu was as follows (values indicate proportions of each ingredient, expressed in parts per whole): Paeoniae Radix 2, Cnidii Rhizoma 2, Carthami Flos 2, Cyperi Rhizoma 1, Aucklandiae Radix 1, Salviae Miltiorrhizae Radix 4. These six crude drugs were boiled gently in 25 times their volume of water at 100°C for 1 h. After filtration, the solution was evaporated under reduced pressure to give an extract at a yield of 44%, by weight, of the

Table 1. Composition of Kangen-karyu

Common name	Botanical name	Family name
Paeoniae Radix	*Paeonia lactiflora* PALLAS	Paeoniaceae
Cnidii Rhizoma	*Cnidium officinale* MAKINO	Umbelliferae
Carthami Flos	*Carthamus tinctorius* L.	Compositae
Cyperi Rhizoma	*Cyperus rotundus* L.	Cyperaceae
Aucklandiae Radix	*Aucklandia lappa* DCNE.	Compositae
Salviae Miltiorrhizae Radix	*Salvia miltiorrhiza* BUNGE	Labiatae

starting materials. The extract was dissolved in 50% aqueous ethanol with sonication, and filtered through a Cosmonice filter (PVDF, 0.45 μm; Nakalai Tesque, Kyoto, Japan). Reverse-phase high-performance liquid chromatography was performed using a Cosmosil $5C_{18}$-AR II column (250 × 4.6 mm i.d.; Nakalai Tesque) with elution gradients of 4-30% (39 min) and 30-75% (15 min) CH_3CN in 50 mM H_3PO_4 at a flow rate of 0.8 mL/min. The UV absorbance from 200 to 400 nm was monitored with a Jasco MD-910 photodiode array detector (Jasco, Tokyo, Japan). All assigned peaks were identified by carrying out co-injection tests with authentic samples and comparing with UV spectral data. The major compounds detected were paeoniflorin, pentagalloyl glucose, rosmarinic acid, lithospermic acid, and lithospermic acid B. A voucher specimen has been deposited in the herbarium of the University of Toyama.

2.3. *Culture cell experiments*

2.3.1. *Cell culture and differentiation*

3T3-L1 preadipocytes obtained from the American Type Culture Collection (Manassas, VA, USA) were cultured in DMEM containing 10% FCS, 100 μg/mL streptomycin, 100 U/mL penicillin, 44 mM $NaHCO_3$, and 1 mM sodium pyruvate at 37°C under a 5% CO_2 atmosphere. To induce differentiation, 3T3-L1 preadipocytes were cultured until confluence was reached (day 0), and the culture medium was replaced with a fresh induction medium containing 5 μg/mL insulin, 0.5 mM IBMX, and 1 μM dexamethasone in DMEM with 10% FCS for 2 days. The medium was then replaced with a differentiation medium containing 5 μg/mL insulin only and DMEM medium containing 10% FCS every 2 days for 8 days until the cells were harvested. To examine the effect of Kangen-karyu on adipogenesis, the extract was dissolved in the differentiation medium, and the medium was immediately processed into a sterile container by membrane filtration with a 0.22-μm filter (EMD Millipore, MA, USA).

2.3.2. *MTT assay*

3T3-L1 preadipocytes were seeded at a density of 4×10^3 cells/well in a 96-well plate. After 4 h, Kangen-karyu extract at concentrations of 25, 50, 125, and 250 μg/mL was added to each well and incubated for 24 h. MTT solution (2 mg/mL) was added to each 96-well plate and incubated for 4 h, and then the medium containing MTT solution was removed. The formazan crystals in the viable cells were solubilized with dimethyl sulfoxide (150 μL), and absorbance was determined at 540 nm with a Microplate Reader (Immuno Mini NJ-2300; BioTec, Tokyo, Japan).

2.3.3. *Oil red O staining*

Intracellular lipid accumulation was measured using oil red O staining. The mature 3T3-L1 adipocytes were washed with PBS, fixed with 10% formalin (pH 7.4) for 30 min, and stained with oil red O solution for 1 h. The fat droplets in 3T3-L1 adipocytes were observed by phase contrast microscopy.

2.3.4. *Western blot analysis*

3T3-L1 adipocytes, cultured in 6-well plates, were treated with Kangen-karyu extract for 8 days and harvested using PRO-PREP™ protein extraction solution (iNtRON Biotechnology, Seoul, Korea). Cell debris was removed by centrifugation and the protein quantity in the lysate was determined using Bradford reagent (Bio-Rad Laboratories, Hercules, CA, USA). Cell lysates containing 30 μg of protein were separated using sodium dodecylsulfate polyacrylamide gel (SDS-PAGE) electrophoresis and transferred to nitrocellulose membranes, and the membranes were blocked with a solution of 0.1% Tween 20 in Tris-buffered saline containing 5% skim milk for 1 h at room temperature followed by overnight incubation with primary antibody at 4°C. After overnight incubation, the membranes were incubated with horseradish peroxidase-conjugated secondary antibody for 1 h at room temperature. Finally, protein bands were detected using the chemiluminescent substrate and VisionWorks™LS (Analysis Software, Upland, CA, USA).

2.3.5. *Quantitative real-time polymerase chain reaction (PCR)*

Total RNA was isolated from cells using Tri Reagent (Molecular Research Center, Cincinnati, OH, USA) and quantified using NanoDrop (Thermo Scientific, Wilmington, DE, USA). Fifty ng of isolated RNA was added to a final 30-μl volume of the Diastar™ 2X One Step RT-PCR kit (SolGent, Daejeon, Korea) with each primer: PPARγ, forward sequence 5'-ACC ACT CGC ATT CCT TTG AC-3', reverse sequence 5'-TCA GCG GGA AGG ACT TTA TG-3'; SREBP-1c, forward sequence 5'-CAC TTC TGG AGA CAT CGC AAA C-3', reverse sequence 5'-TGG TAG ACA ACA GCC GCA TC-3'; fatty acid synthase (FAS), forward sequence 5'-CTG CGG AAA CTT CAG GAA ATG-3', reverse sequence 5'-GGT TGC TCG GAA TAT CCA GG-3'. The temperature cycle for the PCR reaction was 50°C for 30 min, 95°C for 15 min, and 30 cycles of [denaturation at 95°C × 1 min, annealing at 58°C (PPARγ, SREBP-1c, and β-actin) and 55°C (FAS) × 1 min and extension at 72°C for 1 min] followed by final denaturation at 72°C for 5 min. β-Actin of the forward sequence 5'-TGC CCA TCT ATG AGG GTT ACG-3', reverse sequence 5'-TAG AAG CAT TTG

CGG TGC ACG-3', and the reaction cycle was as mentioned above. The obtained PCR products were analyzed in nucleic acid staining solution (Red Safe, iNtRON, Korea)-stained agarose (1.5%) gel by using VisionWorks™ LS UVP (Analysis Software, Upland, CA, USA).

2.4. *Animal experiments*

2.4.1. *Experimental animals and treatment*

The 'Guidelines for Animal Experimentation' approved by the University of Toyama were followed in the present study (Registration No.: S-2006 INM-22). Male, 5-wk-old, C57BLKS/J *db*/*db* mice and their age-matched, non-diabetic *m*/*m* littermates were purchased from Japan SLC (Hamamatsu, Japan). They were kept in a plastic-bottomed cage and exposed to a 12-h light/dark cycle. Room temperature (about 25ºC) and humidity (about 60%) were controlled automatically. The mice were allowed free access to laboratory pellet chow (CLEA Japan, Tokyo, Japan, comprising 24.0% protein, 3.5% lipids, and 60.5% carbohydrate) and water was given *ad libitum*. After adaptation, glucose and TG levels of blood taken from the tail vein were measured, and then *db*/*db* mice were divided into three groups. The treatment with Kangen-karyu was initiated after confirming the induction of hyperglycemia and hyperlipidemia in the *db/db* mice, based on the presence of serum glucose 300 ± 10 mg/dL and serum TG 160 ± 5 mg/dL, respectively. The *db*/*db* vehicle group (n = 8) was orally given water, while the other two groups (n = 8 per group) were orally administered Kangen-karyu extract every day for 18 weeks at a dose of 100 mg or 200 mg/kg body weight, respectively. The non-diabetic *m/m* mice (n = 6) as a normal group were compared with the diabetic groups. When the *db/db* mice reached 24 weeks old, they showed reduced blood glucose, β-cell necrosis, and diminished hyperinsulinemia (*21*). Therefore, we decided on the time-point for the cessation of treatment as 24 weeks old in *db/db* mice. Food and water intakes were determined every day during the experimental period. After administration for 18 weeks, blood samples were collected by cardiac puncture from anesthetized mice. Serum was separated immediately by centrifugation. Subsequently, each mouse was perfused with ice-cold physiological saline, and then the liver was harvested, snap-frozen in liquid nitrogen, and stored at –80°C until analyses.

2.4.2. *Measurement of serum parameters*

Glucose, TG, total cholesterol, and non-esterified fatty acids (NEFA) were measured using a commercial kit (Glucose CII-Test, Triglyceride E-Test, Cholesterol E-Test, and NEFA C-Test from Wako Pure Chemical Industries, Osaka, Japan). Leptin and insulin (Morinaga Institute of Biological Science, Yokohama, Japan) levels were measured based on enzyme-linked immunosorbent assays. High-density lipoprotein (HDL), low-density lipoprotein (LDL), and very low-density lipoprotein (VLDL) cholesterol distributions were measured using a BioVision kit (BioVision, Mountain View, CA, USA). Alanine aminotransferase (ALT) and aspartate aminotransferase (AST) were determined using a commercial reagent: GPT-UV Test Wako (Wako Pure Chemical Industries).

2.4.3. *Measurement of hepatic TG content*

The liver of each mouse was homogenized and total lipids of the liver homogenates were extracted with a mixture of chloroform and methanol (2:1, v/v) according to the method of Folch *et al.* (*22*). Then, the amount of TG was determined using commercial kits, as described previously.

2.4.4. *Preparation of nuclear fraction*

To prepare nuclear fractions, hepatic tissues were homogenized with ice-cold lysis buffer containing 5 mM Tris-HCl (pH 7.5), 2 mM $MgCl_2$, 15 mM $CaCl_2$, and 1.5 M sucrose, and then 0.1 M dithiothreitol (DTT) and protease inhibitor cocktail were added. After centrifugation (10,500 × g for 20 min at 4°C), the pellet was suspended with extraction buffer containing 20 mM 2-[4-(2-hydroxyethyl)-1-piperazyl] ethanesulfonic acid (pH 7.9), 1.5 mM $MgCl_2$, 0.42 M NaCl, 0.2 mM EDTA, and 25% (v/v) glycerol, and then 0.1 M DTT and protease inhibitor cocktail were added. The mixture was placed on ice for 30 min. The nuclear fraction was prepared by centrifugation at 20,500 × g for 5 min at 4°C. The protein concentration was determined using a commercial kit (Bio-Rad Laboratories, Hercules, CA, USA).

2.4.5. *Western blot analyses*

For the determination of PPARα and SREBP-1, 10 μg of protein of each nuclear fraction was electrophoresed through 8% SDS-PAGE. Separated proteins were transferred to a nitrocellulose membrane, blocked with 5% (w/v) skim milk solution for 1 h, and then incubated with primary antibodies to PPARα, SREBP-1, and histone, respectively, overnight at 4°C. After the blots were washed, they were incubated with anti-rabbit or anti-mouse IgG horseradish peroxidase-conjugated secondary antibody for 1.5 h at room temperature. Each antigen-antibody complex was visualized using ECL Western Blotting Detection Reagents and detected by chemiluminescence with LAS-4000 (Fujifilm, Tokyo, Japan). Band densities were determined using ATTO Densitograph Software (ATTO Corporation, Tokyo, Japan) and quantified as the ratio to histone. These

protein levels of groups are expressed relative to those of *m/m* mice (represented as 1).

2.4.6. *PCR*

Total RNA was isolated from hepatic tissue using Trizol reagent (Invitrogen Life Technologies, Carlsbad, CA, USA) and quantified using NanoDrop (Thermo Scientific, Wilmington, DE, USA). The cDNAs were synthesized from 5 mg of RNA employing reverse transcriptase (Qiagen, Tokyo, Japan). For the real-time PCR, triplicate aliquots of serially diluted cDNA samples were used in a reaction mixture that contained 1 mM of each primer in a reaction volume of 50 mL employing the SYBR Green Real-time PCR kit (Qiagen) using a fluorometric thermal cycler (Mx3000P^{TM}; Stratagene, La Jolla, CA, USA). Reaction mixtures were incubated for an initial denaturation at 95°C for 15 min, followed by 45 cycles of 94°C for 15 s, 60°C for 30 s, and 72°C for 30 s. Primers used were as follows: acetyl-CoA carboxylase (ACC, sense: CCCAGCAGAATAAAGCTACTTTGG, antisense: TCCTTTTGTGCAACTAGGAACGT), FAS (sense: CCTGGATAGCATTCCGAACCT, antisense: AGCACATCTCGAAGGCTACACA). Glyceraldehyde-3-phosphate dehydrogenase (GAPDH) was used as an endogenous control. The DC_T method was employed for relative quantification. The DC_T value for each sample was determined by calculating the difference between the C_T value of the target gene and that of the GAPDH reference gene. The normalized target gene expression level in the sample was calculated using the formula 2^{-DDCT} as the fold change over the control.

2.5. *Statistical analysis*

Data are expressed as mean values with their standard errors. Statistical comparisons were performed by one-way ANOVA followed by Duncan's multiple-range test. Statistical analysis was conducted using SAS (release 9.2; SAS Institute, Cary, NC, USA) and $p < 0.05$ was considered significant.

3. Results

3.1. *Culture cell experiments*

3.1.1. *Cell viability*

To test the cytotoxic effects, MTT assays were conducted after treatment with various concentrations of Kangen-karyu during the adipogenesis of 3T3-L1 cells. The results of the MTT assay showed that Kangen-karyu did not decrease the cell viability up to the concentration of 250 μg/mL, as shown in Figure 1. Orlistat, which inhibits the absorption of neutral lipids and cholesterol by specifically inhibiting lipase (*23*), at a concentration of 20 μM (10 μg/mL) did not affect the cell viability.

3.1.2. *Lipid accumulation*

As shown in Figure 2A, Kangen-karyu significantly inhibited the accumulation of lipid droplets at a concentration of 50 and 250 μg/mL. As the main components of fat droplets are lipids in the form of TG, the TG contents of cells were determined. As shown in Figure 2B, Kangen-karyu reduced TG accumulation. When the 3T3-L1 cells were treated with orlistat, TG accumulation was reduced by 36% at a concentration of 20 μM.

3.1.3. *PPARγ and aP2 protein expressions*

As shown in Figure 3, the levels of PPARγ (A) and aP2 (B) were significantly inhibited by treatment with both

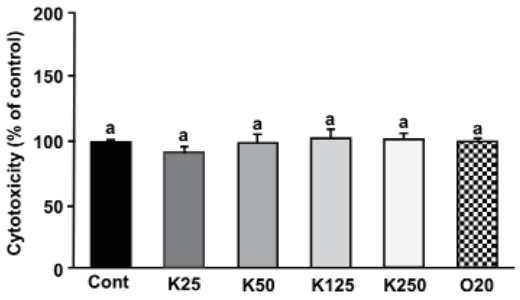

Figure 1. Cell viability. Cont, control; K25, Kangen-karyu 25 μg/mL; K50, Kangen-karyu 50 μg/mL; K125, Kangen-karyu 125 μg/mL; K250, Kangen-karyu 250 μg/mL; O20, orlistat 20 μM. Data are the mean ± S.E.M. Bars with the same letter are not significantly different by Duncan's multiple range tests ($p < 0.05$).

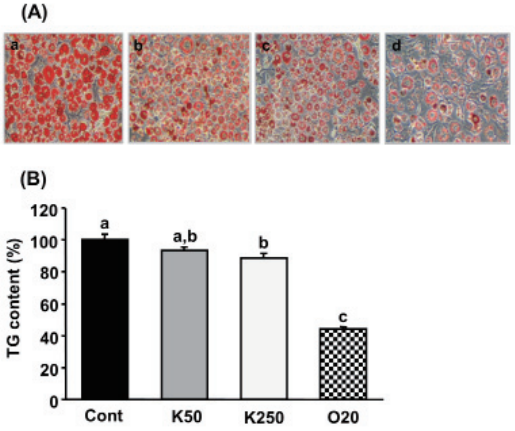

Figure 2. Lipid accumulation in 3T3-L1 adipocytes. Confluent cells were treated with Kangen-karyu or orlistat. **(A)** Cell differentiation was examined on day 8 by oil red O staining. **(B)** The TG content was measured in 3T3-L1 adipocytes. Cont, control; K50, Kangen-karyu 50 μg/mL; K250, Kangen-karyu 250 μg/mL; O20, orlistat 20 μM. Data are the mean ± S.E.M. Bars with the same letter are not significantly different by Duncan's multiple range tests ($p < 0.05$).

50 and 250 μg/mL Kangen-karyu. The effects of Kangen-karyu on PPARγ were more prominent than those of aP2.

3.1.4. *PPARγ, SREBP-1c, and FAS mRNA expressions*

The treatment with Kangen-karyu at 250 μg/mL led to a significant inhibition of PPARγ, SREBP-1c, and FAS mRNA expressions, as shown in Figure 4. In particular, the effect of PPARγ was marked and distinct from those of the other mRNA expressions.

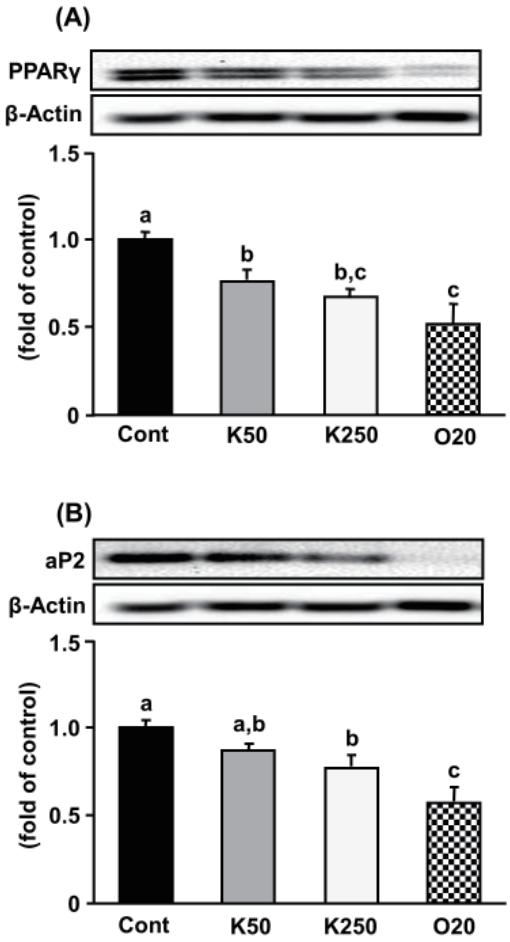

Figure 3. PPARγ and aP2 protein expressions in 3T3-L1 adipocytes. Representative immunoblots for **(A)** PPARγ and **(B)** aP2. Immunoblotting analyses were performed as described in Materials and Methods. Cont, control; K50, Kangen-karyu 50 μg/mL; K250, Kangen-karyu 250 μg/mL; O20, orlistat 20 μM. Data are the mean ± S.E.M. Bars with the same letter are not significantly different by Duncan's multiple range tests ($p < 0.05$).

3.2. *Animal experiments*

3.2.1. *Body weight, food intake, and water intake*

The *db/db* mice displayed typical phenotypes of obesity-induced diabetes with a marked increase in body weight gain, food intake, and water intake, as compared *with m/m* mice (normal control). The gain of body weight in *db/db* mice was non-significantly decreased by Kangen-karyu administration. The food and water intakes in *db/db* mice were significantly decreased by 100 mg/kg of Kangen-karyu treatment.

3.2.2. *Hematological analyses*

All serum constituents were elevated in vehicle-treated *db/db* mice compared with *m/m* mice. As shown in Table 2, Kangen-karyu 200 mg/kg-administered *db/db* mice groups showed decreased serum glucose and leptin, but no alteration of insulin. Furthermore, the administration of Kangen-karyu to *db/db* mice significantly improved TG, LDL/VLDL cholesterol, and NEFA compared with the *db/db* control group. Regarding hepatic function parameters, serum ALT and AST levels in vehicle *db/db* mice were elevated compared with those in *m/m* mice, while, in Kangen-karyu-administered *db/db* mice, these two parameters were slightly decreased.

3.2.3. *Hepatic TG content*

Compared with *m/m* mice, the liver weight of *db/db* mice was significantly augmented, but the administration of Kangen-karyu led to a significant decrease in its weight. Concerning the hepatic content of TG, the *db/db* control group showed a marked increase compared with the *m/m* group. This TG

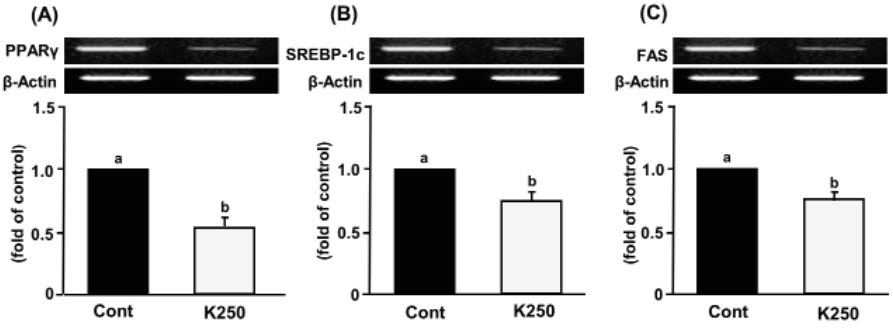

Figure 4. PPARγ, SREBP-1c, and FAS mRNA expressions in 3T3-L1 adipocytes. Representative immunoblots for **(A)** PPARγ, **(B)** SREBP-1c, and **(C)** FAS. Immunoblotting analyses were performed as described in Materials and Methods. Cont, control; K250, Kangen-karyu 250 μg/mL. Data are the mean ± S.E.M. Bars with the same letter are not significantly different by Duncan's multiple range tests ($p < 0.05$).

Table 2. Hematological analyses

Item	*m/m*	*db/db*		
		Veh	K100	K200
Glucose (mg/dL)	134 ± 5***	492 ± 13	434 ± 30	420 ± 17*
Leptin (ng/mL)	1.8 ± 0.1***	21.0 ± 0.8	18.7 ± 1.2	15.8 ± 0.5***
Insulin (ng/mL)	1.57 ± 0.03***	3.36 ± 0.17	3.85 ± 0.30	4.24 ± 0.74
TG (mg/dL)	117 ± 15***	212 ± 12	135 ± 18**	104 ± 14***
Total cholesterol (mg/dL)	78 ± 1***	162 ± 8	159 ± 13	155 ± 15
HDL-C (mg/dL)	42.3 ± 2.9*	52.0 ± 2.8	52.4 ± 1.6	53.7 ± 4.0
LDL / VLDL-C (mg/dL)	9.1 ± 0.3***	20.1 ± 1.3	12.0 ± 1.1***	10.8 ± 1.0***
NEFA (mEq/L)	0.58 ± 0.02***	1.38 ± 0.08	1.05 ± 0.06	1.00 ± 0.05*
ALT (IU/L)	35 ± 2**	98 ± 16	89 ± 8	85 ± 17
AST (IU/L)	11 ± 3***	61 ± 4	55 ± 7	53 ± 4

m/m, Misty mice; *db/db*-Veh, *db/db* vehicle-treated mice; *db/db*-K100, *db/db* Kangen-karyu (100 mg/kg body weight)-treated mice; *db/db*-K200, *db/db* Kangen-karyu (200 mg/kg body weight)-treated mice. Data are the mean ± S.E.M. Significance: * $p < 0.05$, ** $p < 0.01$, *** $p < 0.001$ *vs.* vehicle-treated *db/db* group.

Table 3. Liver weight and TG level

Item	*m/m*	*db/db*		
		Veh	K100	K200
Liver weight (g)	1.44 ± 0.21***	4.11 ± 0.19	3.73 ± 0.16	3.14 ± 0.61
Liver weight (g/100 g body weight)	5.58 ± 0.41**	7.89 ± 0.41	7.03 ± 0.35	5.87 ± 1.14
TG (mg/g tissue)	3.1 ± 0.2***	18.7 ± 1.2	15.3 ± 0.7*	13.4 ± 0.9**

m/m, Misty mice; *db/db*-Veh, *db/db* vehicle-treated mice; *db/db*-K100, *db/db* Kangen-karyu (100 mg/kg body weight)-treated mice; *db/db*-K200, *db/db* Kangen-karyu (200 mg/kg body weight)-treated mice. Data are the mean ± S.E.M. Significance: * $p < 0.05$, ** $p < 0.01$, *** $p < 0.001$ *vs.* vehicle-treated *db/db* group.

content was significantly decreased by Kangen-karyu administration at a dose of 100 and 200 mg/kg body weight/day, as shown in Table 3.

3.2.4. *Hepatic PPARα and SREBP-1 protein expressions*

As shown in Figure 5B, protein expression of hepatic SREBP-1 was markedly increased in the *db/db* control group compared with the *m/m* group. The administration of Kangen-karyu at 100 and 200 mg/kg led to a significant down-regulation of SREBP-1 expression. While, in the case of hepatic PPARα, no significant difference among the groups was observed (Figure 5A).

3.2.5. *Hepatic mRNA expressions involved in TG metabolism*

The effects of Kangen-karyu administration on the mRNA levels of genes involved in lipid metabolism in the hepatic tissue are presented in Figure 6. Over-expressions of ACC and FAS mRNA were seen in hepatic tissue of the *db/db* vehicle group compared with *m/m* group. On the other hand, the administration of Kangen-karyu at a dose of 200 mg/kg body weight/day significantly inhibited the expressions of ACC and FAS in *db/db* mice.

4. Discussion

Dysregulation of the pathways involved in adipogenesis, lipid metabolism, and energy homeostasis can lead to the development of obesity, hepatic steatosis, diabetes, and dyslipidemia. The transcription factors PPARγ and CCAAT/enhancer-binding protein-α (C/EBPα) play a crucial role during adipogenesis. In the later stages of terminal differentiation, proteins such as adipocyte-specific fatty acid-binding protein (aP2), adiponectin, and leptin are expressed. A fine balance between adipocyte hypertrophy and adipogenesis exists to prevent the formation of dysfunctional adipose tissue, since large cells are more likely to be insulin-resistant and, therefore, can influence adipose tissue metabolism.

Adipose tissue, as a metabolic and endocrine organ, plays critical roles in the regulation of energy balance, lipid metabolism, and insulin action. Obesity is a major public health problem involving increased risks of diabetes and cardiovascular disease in many countries. Adipocytes have been emerging as a potential pharmacological target for obesity, diabetes, and cardiovascular diseases (*24-26*). Numerous studies have demonstrated that adipocyte differentiation and the amount of fat accumulation are associated with the occurrence and development of obesity. The findings of this study show that Kangen-karyu plays

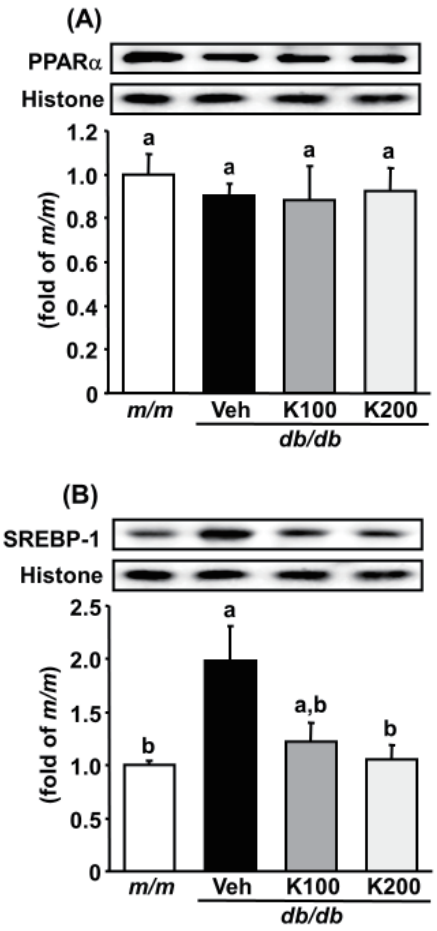

Figure 5. PPARα and SREBP-1 protein expressions in the liver. Representative immunoblots for **(A)** PPARα and **(B)** SREBP-1. Immunoblotting analyses were performed as described in Materials and Methods. *m/m*, Misty mice; *db/db*-Veh, *db/db* vehicle-treated mice; *db/db*-K100, *db/db* Kangen-karyu (100 mg/kg body weight)-treated mice; *db/db*-K200, *db/db* Kangen-karyu (200 mg/kg body weight)-treated mice. Data are the mean ± S.E.M. Bars with the same letter are not significantly different by Duncan's multiple range tests ($p < 0.05$).

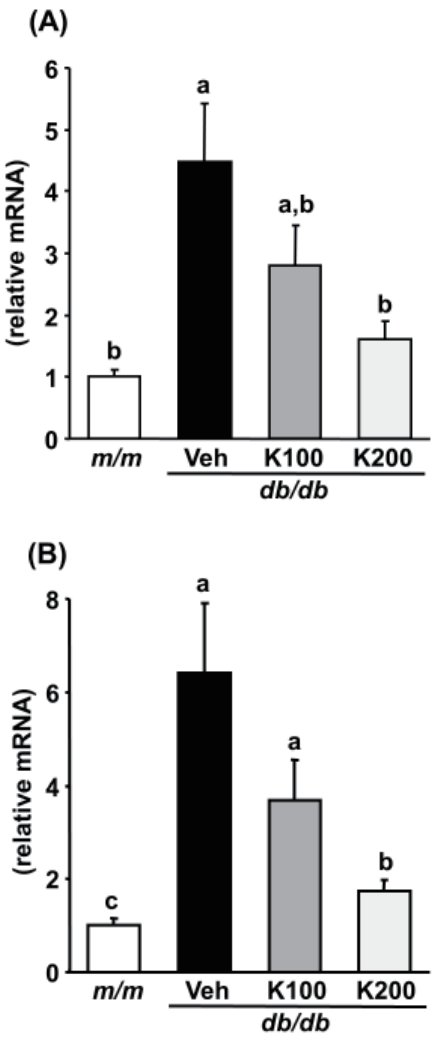

Figure 6. ACC and FAS mRNA expressions in the liver. Representative immunoblots for **(A)** ACC and **(B)** FAS. Immunoblotting analyses were performed as described in Materials and Methods. *m/m*, Misty mice; *db/db*-Veh, *db/db* vehicle-treated mice; *db/db*-K100, *db/db* Kangen-karyu (100 mg/kg body weight)-treated mice; *db/db*-K200, *db/db* Kangen-karyu (200 mg/kg body weight)-treated mice. Data are the mean ± S.E.M. Bars with the same letter are not significantly different by Duncan's multiple range tests ($p < 0.05$).

a significant role in the regulation of energy and lipid metabolism. Our results show that Kangen-karyu significantly inhibited adipocyte differentiation and lipid accumulation. Kangen-karyu significantly reduced TG accumulation, which indicates that it inhibited adipogenesis during adipocyte differentiation, and may have potential anti-dyslipidemia effects.

The differentiation of preadipocytes into adipocytes is regulated by the coordinated expression of various transcription factors, and the induction of metabolic pathways related to lipid metabolism induces the expression of several adipocyte-specific genes like PPARγ, SREBP-1c, and FAS (*27*). In addition, lipid homeostasis is regulated by a family of membrane-bound transcription factors called SREBPs (*28*). SREBP-1 is a key transcription factor that nutritionally regulates the hepatic gene expression of lipogenic enzymes and TG deposition in the liver (*29*). In the present study, Kangen-karyu significantly down-regulated the mRNA levels of PPARγ, SREBP-1c, and FAS, and the protein levels of aP2 and PPARγ in mature adipocytes. These results suggest that Kangen-karyu inhibited adipocyte differentiation and adipogenesis by affecting the transcriptional factor cascade upstream of PPARγ, SREBP-1c, FAS, and aP2, possibly resulting in the inhibition of lipid accumulation by inhibiting adipogenesis.

As an experimental model of dyslipidemia-associated type 2 diabetes mellitus, *db/db* mice are widely used and well-established (*19,30*). C57BLKS/J *db/db* mice develop diabetes due to mutation of the mouse diabetes (*db*) gene that encodes a receptor for leptin. The lack of leptin-receptor signaling results in increased food intake in combination with a phenotype of reduced energy expenditure, reminiscent of the neuroendocrine starvation response (*31*). Consequently, the homozygotes (*db/db*) after birth show unrepressed

eating behavior, become obese, and, by 3-6 months after birth, develop severe insulin resistance associated with hyperinsulinemia, hyperglycemia, and hypertriglyceridemia. Therefore, in this study, we investigated whether Kangen-karyu ameliorates metabolic disorders including hyperlipidemia, using well-established *db/db* type 2 diabetic mice.

The effects of Kangen-karyu on serum lipid levels such as TG, total cholesterol, HDL cholesterol, LDL/VLDL cholesterol, and NEFA were examined. We found that *db/db* mice showed hyperlipidemia. However, the administration of Kangen-karyu reduced hyperlipidemia through lowering TG, LDL/VLDL cholesterol, and NEFA. Also, to investigate the effects of Kangen-karyu on hepatic damage induced by abnormal lipid synthesis, the lipid contents in the liver of *db/db* mice were also examined. The hepatic content of TG was significantly decreased by the administration of Kangen-karyu. These results mean that Kangen-karyu may inhibit fat deposit or lipid output to blood with the regulation of lipid metabolism such as TG synthesis in type 2 diabetes.

Up-regulation of SREBP-1 was reported in leptin-resistant mice, such as *ob/ob* mice and $FVB^{db/db}$ mice (*32,33*). In this study, the increase in hepatic SREBP-1 in *db/db* mice was down-regulated by the administration of Kangen-karyu. This was probably related to the inhibition of hepatic TG accumulations. Furthermore, PPARs, with three isoforms (α, δ, and γ), are also involved in the long-term regulation of lipid metabolism, and their activity is modulated by endogenous lipid-derived ligands. When PPARα is activated, it promotes fatty acid oxidation, ketone body synthesis, and glucose sparing (*34*). In our study, hepatic PPARα was decreased in *db/db* mice; it was increased slightly, but not significantly, by Kangen-karyu administration. However, we found that Kangen-karyu exhibits a significant effect on regulation of SREBP-1. These results suggest that Kangen-karyu has an ameliorating effect on dyslipidemia in type 2 diabetic mice through the regulation of impaired hepatic SREBPs.

It is well known that SREBP-1 primarily controls genes involved in fatty acid synthesis (*29*). These include the genes for ACC and FAS in the fatty acid synthesis pathway (*35*). Type 2 diabetes is associated with increased *de novo* lipogenesis, decreased plasma fatty acid oxidation, and increased fatty acid flux from peripheral tissues to the liver (*36*). Therefore, we examined the effect of Kangen-karyu on regulating lipogenic enzyme genes such as ACC and FAS involved in fatty acid synthesis in the *db/db* mice liver using a real-time quantitative PCR technique. Our results strongly suggest that Kangen-karyu mediates the TG-lowering action by reducing the expression of ACC and FAS, thereby inhibiting fatty acid synthesis in type 2 diabetic mice.

Another finding noted in this study was that Kangen-karyu treatment improved impaired liver function in type 2 diabetic mice. Elevated serum levels of ALT and AST usually indicate hepatocyte damage (*37*). In *db/db* mice, serum ALT and AST were notably increased, but Kangen-karyu treatment showed a tendency to reduce these parameters, suggesting that Kangen-karyu might play an important role in improving liver function.

Thiazolidinediones and fibrate drugs are the most commonly used medications for type 2 diabetes mellitus, hyperlipidemia, and insulin resistance. They bind to and activate PPARs, which results in the upregulation of several genes involved in glucose and lipid metabolism (*38*). PPARs are currently viewed as potential therapeutic targets for the treatment of diabetes and dyslipidemia. PPARγ, predominantly expressed in adipose tissue and macrophages (*39*), affects genes involved in lipid synthesis and storage, and glucose homeostasis. PPARγ agonists, such as thiazolidinediones, control lipid metabolism and insulin sensitivity. However, several concerns such as body weight gain associated with an excess increase of fat mass arise in type 2 diabetes mellitus patients (*40*). Accumulating evidence indicates that the activation of PPARα stimulates lipid consumption by enhancing the expression of fatty acid oxidation genes, resulting in the amelioration of hyperlipidemia (*41*). PPARα agonists, such as fenofibrate used for the treatment of hyperlipidemia and reducing cardiovascular disease, have a potent effect on reducing plasma TG (*42*). Because of these distinct metabolic effects of PPARα and PPARγ agonists on insulin sensitivity and lipid metabolism, new drug development has focused on dual PPARs which possess PPARγ as well as PPARα activity. In this study, we initially assessed the protective effects of Kangen-karyu against type 2 diabetes by investigating specific markers in the serum and hepatic tissue of *db/db* mice, thereby highlighting Kangen-karyu as a promising anti-lipotoxic agent for type 2 diabetes.

References

1. Alberti KGMM, Eckel RH, Grundy SM, Zimmet PZ, Cleeman JI, Donato KA, Fruchart JC, James WPT, Loria CM, Smith Jr. SC. Harmonizing the metabolic syndrome: a joint interim statement of the International Diabetes Federation Task Force on Epidemiology and Prevention; National Heart, Lung, and Blood Institute; American Heart Association; World Heart Federation; International Atherosclerosis Society; and International Association for the Study of Obesity. Circulation. 2009; 120:1640-1645.
2. Eckel RH, Albert KG, Grundy SM, Zimmet PZ. The metabolic syndrome. Lancet. 2010; 375:181-183.
3. Phillips C, Lopez-Miranda J, Perez-Jimenez F, McManus R, Roche HM. Genetic and nutrient determinants of the metabolic syndrome. Curr Opin Cardiol. 2006; 21:185-193.
4. Gregor MF, Hotamisligil GS. Inflammatory mechanisms in obesity. Annu Rev Immunol. 2011; 29:415-445.
5. Hwang JT, Park IJ, Shin JI, Lee YK, Lee SK, Baik

HW, Ha J, Park OJ. Genistein, EGCG, and capsaicin inhibit adipocyte differentiation process via activating AMP-activated protein kinase. Biochem Biophys Res Commun. 2005; 338:694-699.
6. Shepherd PR, Gnudi L, Tozzo E, Yang H, Leach F, Kahn BB. Adipose cell hyperplasia and enhanced glucose disposal in transgenic mice overexpressing GLUT4 selectively in adipose tissue. J Biol Chem. 1993; 268:22243-22246.
7. Sorisky A. From preadipocyte to adipocyte: Differentiation-directed signals of insulin from the cell surface to the nucleus. Crit Rev Clin Lab Sci. 1999; 36:1-34.
8. Lottenberg AM, Afonso Mda S, Lavrador MS, Machado RM, Nakandakare ER. The role of dietary fatty acids in the pathology of metabolic syndrome. J Nutr Biochem. 2012; 23:1027-1040.
9. Hwang HS, Kim SH, Yoo YG, Chu YS, Shon YH, Nam KS, Yun JW. Inhibitory effect of deep-sea water on differentiation of 3T3-L1 adipocytes. Mar Biotechnol. 2009; 11:161-168.
10. Hataguchi Y, Tai H, Nakajima H, Kimata H. Drinking deep-sea water restores mineral imbalance in atopic eczema/dermatitis syndrome. Eur J Clin Nutr. 2005; 59:1093-1096.
11. Bubela T, Boon H, Caulfield T. Herbal remedy clinical trials in the media: A comparison with the coverage of conventional pharmaceuticals. BMC Med. 2008; 6:1-14.
12. Takahashi M, Sugaya K, Kubota K. *Kangenkaryu* prevents the decrease of cholinergic markers following the nucleus basalis magnocellularis lesion. Japan J Pharmacol. 1992; 60:307-310.
13. Gao M, Ikeda K, Noguchi T, Mori K, Yamori Y. Studies on preventive effect of 'Kangenkaryu', Chinese herbal medicine, on stroke in SHR-SP. J Trad Med. 2001; 18:245-250.
14. Makino T, Wakushima H, Okamoto T, Okukubo Y, Saito K, Kano Y. Effects of Kangen-karyu on coagulation system and platelet aggregation in mice. Biol Pharm Bull. 2002; 25:523-525.
15. Cho EJ, Okamoto T, Yokozawa T. Therapeutic efficacy of Kangen-karyu against H_2O_2-induced premature senescence. J Pharm Pharmacol. 2008; 60:1537-1544.
16. Yokozawa T, Cho EJ, Sasaki S, Satoh A, Okamoto T, Sei Y. The protective role of Chinese prescription Kangen-karyu extract on diet-induced hypercholesterolemia in rats. Biol Pharm Bull. 2006; 29:760-765.
17. Yokozawa T, Kim HJ, Yamabe N, Okamoto T, Cho EJ. The protective role of Kangen-karyu against fructose-induced metabolic syndrome in a rat model. J Pharm Pharmacol. 2007; 59:1271-1278.
18. Kim HY, Okamoto T, Yokozawa T. Beneficial effects of Chinese prescription Kangen-karyu on diabetes associated with hyperlipidemia, advanced glycation endproducts, and oxidative stress in streptozotocin-induced diabetic rats. J Ethnopharmacol. 2009; 124:263-269.
19. Hummel KP, Dickie MM, Coleman DL. Diabetes, a new mutation in the mouse. Science. 1966; 153:1127-1128.
20. Park CW, Kim HW, Ko SH, Lim JH, Ryu GR, Chung HW, Han SW, Shin SJ, Bang BK, Breyer MD, Chang YS. Long-term treatment of glucagon-like peptide-1 analog exendin-4 ameliorates diabetic nephropathy through improving metabolic anomalies in *db/db* mice. J Am Soc Nephrol. 2007; 18:1227-1238.
21. Orland MJ, Permutt MA. Quantitative analysis of pancreatic proinsulin mRNA in genetically diabetic (*db/db*) mice. Diabetes. 1987; 36:341-347.
22. Folch J, Lees M, Sloane Stanley GH. A simple method for the isolation and purification of total lipids from animal tissues. J Biol Chem. 1957; 226:497-509.
23. Farrigan C, Pang K. Obesity market overview. Nat Rev Drug Discov. 2002; 1:257-258.
24. Frühbeck G, Gómez-Ambrosi J, Muruzábal FJ, Burrell MA. The adipocyte: A model for integration of endocrine and metabolic signaling in energy metabolism regulation. Am J Physiol Endocrinol Metab. 2001; 280:E827-E847.
25. Kershaw EE, Flier JS. Adipose tissue as an endocrine organ. J Clin Endocrinol Metab. 2004; 89:2548-2556.
26. Zimmet P, Magliano D, Matsuzawa Y, Alberti G, Shaw J. The metabolic syndrome: A global public health problem and a new definition. J Atheroscler Thromb. 2005; 12:295-300.
27. Farmer SR. Transcriptional control of adipocyte formation. Cell Metab. 2006; 4:263-273.
28. Shimano H. SREBPs: physiology and pathophysiology of the SREBP family. FEBS J. 2009; 276:616-621.
29. Yahagi N, Shimano H, Hasty AH, et al. Absence of sterol regulatory element-binding protein-1 (SREBP-1) ameliorates fatty livers but not obesity or insulin resistance in Lep^{ob}/Lep^{ob} mice. J Biol Chem. 2002; 277:19353-19357.
30. Kaku K, Province M, Permutt MA. Genetic analysis of obesity-induced diabetes associated with a limited capacity to synthesize insulin in C57BL/KS mice: evidence for polygenic control. Diagetologia. 1989; 32:636-643.
31. Münzbery H, Myers MG. Molecular and anatomical determinants of central leptin resistance. Nat Neurosci. 2005; 8:566-570.
32. Tobe K, Suzuki R, Aoyama M, Yamauchi T, Kamon J, Kubota N, Terauchi Y, Matsui J, Akanuma Y, Kimura S, Tanaka J, Abe M, Ohsumi J, Nagai R, Kadowaki T. Increased expression of the sterol regulatory element-binding protein-1 gene in insulin receptor substrate-$2^{-/-}$ mouse liver. J Biol Chem. 2001; 276:38337-38340.
33. Wang Z, Jiang T, Li J, Proctor G, McManaman JL, Lucia S, Chua S, Levi M. Regulation of renal lipid metabolism, lipid accumulation, and glomerulosclerosis in $FVB^{db/db}$ mice with type 2 diabetes. Diabetes. 2005; 54:2328-2335.
34. Ferré P. The biology of peroxisome proliferator-activated receptors. Relationship with lipid metabolism and insulin sensitivity. Diabetes. 2004; 53:S43-S50.
35. Girard J, Perdereau D, Foufelle F, Prip-Buus C, Ferré P. Regulation of lipogenic enzyme gene expression by nutrients and hormones. FASEB J. 1994; 8:36-42.
36. Nestel P, Goldrick B. Obesity: Changes in lipid metabolism and the role of insulin. Clin Endocrinol Metab. 1976; 5:313-335.
37. Amacher DE. Serum transaminase elevations as indicators of hepatic injury following the administration of drugs. Regul Toxicol Pharmacol. 1998; 27:119-130.
38. Michalik L, Auwerx J, Berger JP, et al. International union of pharmacology. LXI. Peroxisome proliferator-activated receptors. Pharmacol Rev. 2006; 58:726-741.
39. Vidal-Puig AJ, Considine RV, Jimenez-Liñan M, Werman A, Pories WJ, Caro JF. Peroxisome proliferator-activated receptor gene expression in human tissues. J Clin Invest. 1997; 99:2416-2422.
40. Fonseca V. Effect of thiazolidinediones on body weight in patients with diabetes mellitus. Am J Med. 2003; 115:42S-48S.

41. Bünger M, Hooiveld GJEJ, Kersten S, Müller M. Exploration of PPAR functions by microarray technology: A paradigm for nutrigenomics. Biochim Biophys Acta. 2007; 1771:1046-1064.
42. Bajaj M, Suraamornkul S, Hardies LJ, Glass L, Musi N, DeFronzo RA. Effects of peroxisome proliferator-activated receptor (PPAR)-α and PPAR-γ agonists on glucose and lipid metabolism in patients with type 2 diabetes mellitus. Diabetologia. 2007; 50:1723-1731.

(Received May 7, 2014; Revised June 16, 2014; Accepted June 20, 2014)

Case Report

DOI: 10.5582/ddt.2014.01023

Management of inappropriate sinus tachycardia with ivabradine in a renal transplant recipient

Vipin Kumar Goyal[1,*], Suraj Godara[2], Trilok Chandra Sadasukhi[3], Hoti Lal Gupta[3]

[1] *Department of Anaesthesia and Critical Care, Mahatma Gandhi Medical College and Hospitals, Jaipur, Rajasthan, India;*
[2] *Department of Nephrology, Mahatma Gandhi Medical College and Hospitals, Jaipur, Rajasthan, India;*
[3] *Department of Urology, Mahatma Gandhi Medical College and Hospitals, Jaipur, Rajasthan, India.*

Summary **Inappropriate sinus tachycardia (IST) is a syndrome characterized by unexplained tachycardia (heart rate > 100 beats /min) and related symptoms at rest. We describe a case of a 35 year old male with end stage renal disease who developed IST after renal transplant in the surgical intensive care unit. Management of IST is usually nonspecific and includes bradycardic agents, radiofrequency ablation or surgical ablation of the sinus node. This patient was well managed with ivabradine (I_f pacemaker current inhibitor) after failure and intolerance of β-adrenergic blockers.**

Keywords: Ivabradine, inappropriate sinus tachycardia, renal transplant

1. Introduction

Inappropriate sinus tachycardia (IST) is a very rare cardiac arrhythmia and classified in arrhythmias of supraventricular origin. Etiology is unclear, although sinus node dysfunction or dysautonomia may be the causative factors. Treatment options are very few and mostly ineffective.

2. Case report

We report a case of IST in a 35 year old male who had undergone renal transplant for chronic kidney disease. Patient had a history of chronic kidney disease (grade IV) and was on hemodialysis. No other medical risk factor was present except hypertension for 1 month that was well controlled with tablet amlodipine 5 mg OD. His preoperative routine blood investigations were within normal range except for increased renal function tests and low hemoglobin. Electrocardiogram showed sinus rhythm with heart rate 84 beats/min, ST depression in lead I, V1-V6 and P mitrale. Echocardiography showed ejection fraction 50% with moderate PAH, moderate MR and diastolic dysfunction grade III. Patient's exercise tolerance was good and vital parameters were stable (blood pressure 154/96 mmHg and heart rate 86 beats/min) (Figure 1). Surgery was performed under general anesthesia and patient was shifted to post operative intensive care unit. Hemodynamics were stable throughout intraoperative period. About 10 h after surgery patient developed an episode of sinus tachycardia with heart rate of 120-140 beats/min that was persistent and associated with palpitations, perspiration, sensation of burning in chest and a slight fall in blood pressure (Figure 2). Probable etiologic factors for sinus tachycardia in postoperative period like pain, hypovolemia, hypotension, increased temperature, blood loss, anxiety, and drugs were ruled out. Serum electrolyte and acid base and gas analysis reports were nonsignificant. Repeated injection of metoprolol was tried in an interval but the effect was nonsustained along with a dramatic fall in blood pressure. Calcium channel blockers were not tried in view of interaction of these agents with immunosuppressive agents. Tablet ivabradine 5 mg orally was started as next line of management on a trial and error basis. After half an hour of ivabradine administration, heart rate dropped to 76 - 85 beats/min and remained sustained without significant change in blood pressure. We continued ivabradine 5 mg orally twice a day for 5 days. No further episode of tachycardia was recorded after discontinuation of ivabradine.

**Address correspondence to:*
Dr. Vipin Kumar Goyal, Department of Anaesthesia and Critical Care, Mahatma Gandhi Medical College and Hospitals, Jaipur, Rajasthan, India.
E-mail: dr.vipin28@gmail.com

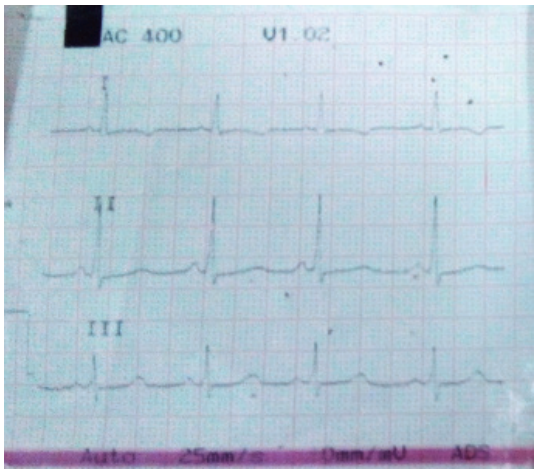

Figure 1. Showing sinus rhythm with heart rate 86 beats/min in preoperative ECG.

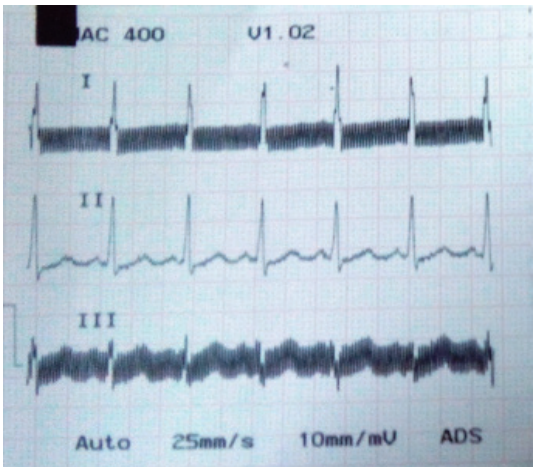

Figure 2. Showing sinus rhythm with heart rate 125 beats/min in postoperative period.

3. Discussion

Sinus tachycardia can be of multiple origins in the postoperative period and is usually well controlled with correction of etiologic factors. Inappropriate sinus tachycardia is a rare entity of unknown origin defined as recurrent or persistent tachycardia with or without associated symptoms. IST is usually associated with symptoms like palpitations, hypotension, dizziness, fatigue, weakness, syncope, etc. Diagnosis is based on 12 lead electrocardiogram and exclusion of other possible etiologic factors like anxiety, pain, medications, fever, anemia, dehydration, hyperthyroidism, pheochromocytoma, pneumothorax, *etc*. Management of IST is a challenge as no clearly defined treatment is present and it is completely based on a trial and error basis. Ivabradine is a selective and specific inhibitor of the hyperpolarization activated pacemaker current (I_f) that controls spontaneous diastolic depolarization in the sinus node and regulates heart rate (*6*). Until now, it was used for treatment of patients with chronic stable angina or chronic heart failure. Ivabradine can be used as an alternative to B blockers and calcium channel blockers for management of IST when these agents are not tolerated or overdose is to be avoided (*1-5*). Only a few research articles and case reports are available mentioning its use to control heart rate in patients with IST.

In our case IST was managed successfully with ivabradine without any untoward adverse effect as seen with β blockers.

References

1. Olshansky B, Sullivan RM. Inappropriate sinus tachycardia. J Am Coll Cardiol. 2013; 61:793-801.
2. Zellerhoff S, Hinterseer M, Felix Krull B, Schulze-Bahr E, Fabritz L, Breithardt G, Kirchhof P, Kaab S. Ivabradine in patients with inappropriate sinus tachycardia. Naunyn Schmiedebergs Arch Pharmacol. 2010; 382:483-486.
3. Calo L, Rebecchi M, Sette A, *et al*. Efficacy of ivabradine administration in patients affected with inappropriate sinus tachycardia. Heart Rhythm. 2010; 7:1318-1323.
4. Schulze V, Steiner S, Hennersdorf M, Strauer B. Ivabradine as an alternative therapeutic trial in the therapy of inappropriate sinus tachycardia. Cardiology. 2008; 110:206-208.
5. Yusuf S, Camm AJ. Sinus tachyarrhythmias and the specific bradycardic agents: A marriage made in heaven? J Cardiovasc Pharmacol Ther. 2003; 8:89-105.
6. DiFrancesco D, Camm JA. Heart rate lowering by specific and selective I(f) current inhibition with ivabradine: A new therapeutic perspective in cardiovascular disease. Drugs. 2004; 64:1757-1765.

(Received May 4, 2014; Accepted June 27, 2014)

Commentary

DOI: 10.5582/ddt.2014.01025

Can gamma-glutamyl transferase levels contribute to a better prognosis for patients with hepatocellular carcinoma?

Zhigang Wang[1,2], Peipei Song[2], Jufeng Xia[2], Yoshinori Inagaki[2], Wei Tang[2,*], Norihoro Kokudo[2]

[1] *Hepato-Biliary-Pancreatic Surgery Division, The Second Affiliated Hospital of Jilin University, Changchun, China;*
[2] *Hepato-Biliary-Pancreatic Surgery Division, Department of Surgery, Graduate School of Medicine, the University of Tokyo, Tokyo, Japan.*

Summary **Hepatocellular carcinoma (HCC) is the most common type of liver cancer. Hepatic resection has long been considered a main treatment option for HCC, but the high rate of recurrence after hepatic resection remains a problem that impacts the prognosis and survival of patients with HCC. Thus, clarifying the factors for survival and risk factors for tumor recurrence after hepatic resection is crucial. Imaging studies are currently emphasized before selecting a treatment and predicting the prognosis for patients with HCC. Recently, laboratory testing of des-gamma-carboxyprothrombin (DCP), alpha-fetoprotein (AFP), indocyanine green 15 min after administration (ICG-R15), and γ-glutamyl transpeptidase (γ-GTP) has garnered attention as a way to select treatment and predict the prognosis of patients with HCC. γ-GTP in particular has critical clinical significance as an indicator of prognosis. This indicator helps to predict prognosis and it helps with the selection of further treatment, as was revealed by studies based on different subgroups of patients published in the past 5 years. The reason for the association between γ-GTP and early recurrence and poor survival is being investigated. Preoperative laboratory results (DCP, AFP, ICG-R15, and γ-GTP) may warrant attention and need to be fully evaluated before selecting a treatment and predicting prognosis in order to improve the prognosis for patients with HCC.**

Keywords: Hepatocellular carcinoma (HCC), laboratory results, γ-glutamyl transpeptidase (γ-GTP), prognosis, recurrence

Hepatocellular carcinoma (HCC) is the fifth most common cancer and the second leading cause of cancer deaths worldwide, accounting for 80-90% of all cases of liver cancer with an estimated global incidence of 782,000 new cases and nearly 746,000 deaths in 2012 (*1*).

Hepatic resection has long been considered a main treatment option for HCC. Improved diagnostic procedures, surgical techniques, and perioperative management have contributed to better outcomes of hepatic resection, even in patients with more advanced, resectable HCC (*2*). However, the high rate of recurrence after hepatic resection remains a problem that impacts the prognosis and survival of patients with HCC, as indicated by a cumulative recurrence rate of 50-60% at 3 years and a cumulative recurrence rate of 60-80% at 5 years (*3-7*). Thus, clarifying the factors for survival and risk factors for tumor recurrence after hepatic resection is crucial. This could help with the selection of an optimal treatment, help with monitoring to reduce the rate of recurrence, and also improve the quality of care for patients with HCC.

As shown in Table 1, imaging studies, pathology, and laboratory results have identified some indices as prognostic factors for patients with HCC (*8-11*). Tumor size, tumor number, and microvascular invasion (MVI) indicated in imaging studies are regarded as factors for survival and risk factors for tumor recurrence, and imaging studies have been emphasized before selecting a treatment and predicting the prognosis for patients with HCC. As some studies have indicated, however,

**Address correspondence to:*
Dr. Wei Tang, Hepato-Biliary-Pancreatic Surgery Division, Department of Surgery, Graduate School of Medicine, the University of Tokyo, Hongo 7-3-1, Bunkyo-ku, Tokyo, 113-8655, Japan.
E-mail: tang-sur@h.u-tokyo.ac.jp

a tumor may recur in about 60.0% of patients with a single tumor smaller than 2.0 cm (*12*). Thus, more approaches to predict prognostic factors are urgently needed in addition to imaging studies. Pathology cannot confirm pathologic changes prior to surgery. In contrast, laboratory testing of des-gamma-carboxyprothrombin (DCP), alpha-fetoprotein (AFP), indocyanine green 15 min after administration (ICG-R15), and γ-glutamyl transpeptidase (γ-GTP) can be performed preoperatively. Thus, these indices warrant further attention as a way to select a treatment and predict prognosis for patients with HCC.

Patients with positive laboratory results for DCP, AFP, ICG-R15, and γ-GTP have a higher risk of recurrence and worse survival (*13-15*). These patients should receive more active treatment including anatomical hepatic resection, liver transplantation, preoperative and postoperative transcatheter arterial chemoembolization (TACE), and closer follow up. Laboratory results for DCP and AFP are related to malignancy features such as vascular invasion and metastasis. ICG-R15 is thought to be related to liver function (*13,16*). Most recently, γ-GTP has been identified as an independent prognostic risk for patients with HCC (*14,17*).

Table 1. Factors related to prognosis for patients with HCC

Examinations	Indicator
Laboratory results	DCP
	AFP
	ICG-R15
	γ-GTP
Imaging studies	Tumor size
	Tumor number
	Vascular invasion
Pathology	Tumor differentiation
	Microvascular invasion
	Intrahepatic metastasis

DCP: des-γ-carboxy-prothrombin, AFP: alpha-fetoprotein, ICG-R15: indocyanine green 15 min after administration, γ-GTP: γ-glutamyl transpeptidase.

γ-GTP is a nearly ubiquitous epithelial enzyme that initiates the degradation of extracellular glutathione and its conjugates, and γ-GTP is correlated with biotransformation, nucleic acid metabolism, and tumorigenesis (*10*). γ-GTP was investigated and utilized as a liver function test or liver enzyme in the 1960s and 1970s (*18*). An increase in γ-GTP can be detected in patients with hepatitis, liver cirrhosis, or primary or secondary liver cancer (*19,20*). γ-GTP was used as a diagnostic tumor marker for liver disease with a high sensitivity of 83-100% but a low specificity of 32% (*21*). Thus, for a long time γ-GTP was not considered to be a useful tumor marker for the detection of liver disease. However, γ-GTP has critical clinical significance as an indicator of prognosis. This indicator helps to predict prognosis and it helps to select further treatment, as was revealed by studies based on different subgroups of patients published in the past 5 years (*10,22-29*).

As shown in Table 2, patients with high levels of γ-GTP had a greater risk of early recurrence and shorter

Table 2. Investigation of γ-GTP as a prognostic factor based on different subgroups of patients with HCC

Authors (Year)	Patients with HCC	Treatment	Results	*Ref.*
Ju *et al*. (2009)	219 patients with HBV-related HCC (2002-2006)	hepatic resection	Preoperative γ-GTP was independently associated with survival	(*22*)
Liu *et al*. (2012)	428 HCC cases	hepatic resection	Long-term outcomes for patients with γ-GTP > 80 U/L were poor	(*23*)
Zhao *et al*. (2012)	162 patients with multi-nodular HCC and Child-Pugh class A liver function	hepatic resection	γ-GTP > 64 U/L was a significant predictive factor for 1-year survival	(*24*)
Zhao *et al*. (2013)	266 patients with multi-nodular HCC	hepatic resection	γ-GTP > 130 U/L was a preoperative predictor for microvascular invasion	(*25*)
Faber *et al*. (2013)	148 patients with HCC and no liver cirrhosis or extrahepatic metastases	hepatic resection	γ-GTP > 50 U/L could be a poor prognostic factor for cumulative survival	(*26*)
Carr *et al*. (2010)	413 patients with biopsy-proven unresectable HCC and low AFP levels	–	γ-GTP ≥ 110 U/L was one of the most significant factors for survival	(*27*)
Zhang *et al*. (2011)	277 patients with intermediate HCC	TACE	γ-GTP > 50 U/L was an independent prognostic factor for overall survival	(*10*)
Guiu *et al*. (2011)	88 patients with HCC	TACE	γ-GTP ≥ 165 U/L as an independent predictor associated with OS	(*28*)
Nishikawa *et al*. (2013)	74 patients with HBV-related HCC	entecavir	γ-GTP ≥ 50 U/L was significant predictive factor linked to recurrence-free survival	(*29*)

TACE: transcatheter arterial chemoembolization.

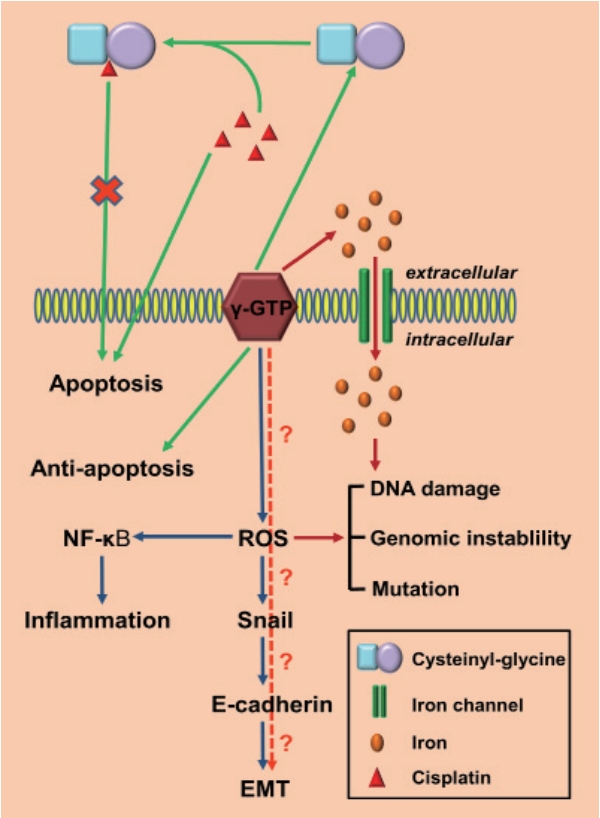

Figure 1. The molecular mechanism of γ-GTP in cancer cells. γ-GTP can promote chemotherapy resistance by increasing cysteinyl-glycine, which complexes with cisplatin. Ion channels are overactivated by γ-GTP to induce damage at the genetic level. Moreover, γ-GTP plays a role in countering apoptosis in lymphoma cells. In addition, ROS is elevated by γ-GTP and subsequently leads to damage at the genetic level, inflammation, invasion, and metastasis.

overall survival, including patients with HBV-related HCC, those with HCC and low AFP levels, those with non-cirrhotic HCC, multi-nodular HCC, and those who underwent TACE. Curative hepatic resection and a close follow-up are suggested for these patients. The combination of γ-GTP and other prognostic factors, such as tumor size, tumor number, microvascular invasion, or laboratory results for AFP and DCP, warrants further attention when selecting a treatment and predicting the prognosis for patients with HCC.

The reason why γ-GTP is significantly associated with early recurrence and poor survival has yet to be clearly indicated. There are two possible reasons: *i*) γ-GTP may be associated with worse liver function *via* induction of DNA instability and subsequent oncogenesis; *ii*) γ-GTP may be associated with the degree of malignancy of HCC, such as vascular invasion, tumor metastasis, or worse tumor differentiation.

A growing number of studies have described mechanisms of γ-GTP over the last two decades. One study suggested that γ-GTP promoted DNA damage, genomic instability, and genetic mutation by increasing the uptake of iron (*30*), and the role of iron in carcinogenesis was reviewed by Weinberg (*31*). This mechanism is thought to lead to the death of normal liver cells or the loss of normal liver function. The pro-oxidant role of γ-GTP has been reported and the subsequent production of reactive oxygen species (ROS) may promote certain intra- and extracellular molecular signals (*32*). Recently, ROS were reported to promote epithelial-to-mesenchymal transition *via* the Snail-E-cadherin pathway (*33*) and to induce inflammation and invasion *via* the NF-κB pathway (*34,35*). A study of U937 lymphoma cells found that γ-GTP may play a role in anti-apoptotic signaling (*36*). A study has confirmed that cysteinyl-glycine, which is catalyzed by γ-GTP, is able to form complexes with cisplatin and that such adducts are not readily transported through the cell membrane (*37*). These mechanisms are thought to account for the progression of HCC. Although the molecular-biological significance of γ-GTP to worse liver function and the progression of HCC is suggested (Figure 1), this significance should be clarified in further studies.

In conclusion, preoperative laboratory results (DCP, AFP, ICG-R15, and γ-GTP) should be fully evaluated before selecting a treatment and predicting prognosis in order to improve the prognosis for patients with HCC. Recent studies have identified γ-GTP as an independent prognostic factor for patients with HCC, and further studies of the reason for the association between γ-GTP and early recurrence and poor survival are urgently needed.

Acknowledgements

This work was supported by Grants-in-Aid from the Ministry of Education, Science, Sports, and Culture of Japan.

References

1. World Health Organization. GLOBOCAN 2012: Estimated Cancer Incidence, Mortality and Prevalence Worldwide in 2012. *http://globocan.iarc.fr/Pages/fact_sheets_cancer.aspx* (accessed May 3, 2014)
2. Rahbari NN, Mehrabi A, Mollberg NM, Müller SA, Koch M, Büchler MW, Weitz J. Hepatocellular carcinoma: Current management and perspectives for the future. Ann Surg. 2011; 253:453-469.
3. Laurent C, Blanc JF, Nobili S, Sa Cunha A, le Bail B, Bioulac-Sage P, Balabaud C, Capdepont M, Saric J. Prognostic factors and longterm survival after hepatic resection for hepatocellular carcinoma originating from noncirrhotic liver. J Am Coll Surg. 2005; 201:656-662.
4. Nagasue N, Ono T, Yamanoi A, Kohno H, El-Assal ON, Taniura H, Uchida M. Prognostic factors and survival after hepatic resection for hepatocellular carcinoma without cirrhosis. Br J Surg. 2001; 88:515-522.
5. Yeh CN, Chen MF, Lee WC, Jeng LB. Prognostic factors of hepatic resection for hepatocellular carcinoma with cirrhosis: Univariate and multivariate analysis. J Surg

Oncol. 2002; 81:195-202.
6. Zhu WJ, Huang CY, Li C, Peng W, Wen TF, Yan LN, Li B, Wang WT, Xu MQ, Yang JY, Jiang L. Risk factors for early recurrence of HBV-related hepatocellular carcinoma meeting Milan criteria after curative resection. Asian Pac J Cancer Prev. 2013; 14:7101-7106.
7. Naito S, Imamura H, Tukada A, Matsuyama Y, Yoshimoto J, Sugo H, Ishizaki Y, Kawasaki S. Postoperative recurrence pattern and prognosis of patients with hepatocellular carcinoma, with particular reference to the hepatitis viral infection status. Liver Int. 2014; 34:802-813.
8. Shindoh J, Hasegawa K, Inoue Y, Ishizawa T, Nagata R, Aoki T, Sakamoto Y, Sugawara Y, Makuuchi M, Kokudo N. Risk factors of post-operative recurrence and adequate surgical approach to improve long-term outcomes of hepatocellular carcinoma. HPB (Oxford). 2013; 15:31-39.
9. Park SK, Jung YK, Chung DH, Kim KK, Park YH, Lee JN, Kwon OS, Kim YS, Choi DJ, Kim JH. Factors influencing hepatocellular carcinoma prognosis after hepatectomy: A single-center experience. Korean J Intern Med. 2013; 28:428-438.
10. Zhang JB, Chen Y, Zhang B, Xie X, Zhang L, Ge N, Ren Z, Ye SL. Prognostic significance of serum gamma-glutamyl transferase in patients with intermediate hepatocellular carcinoma treated with transcatheter arterial chemoembolization. Eur J Gastroenterol Hepatol. 2011; 23:787-793.
11. Shirabe K, Kajiyama K, Harimoto N, Masumoto H, Fukuya T, Ooya M, Maehara Y. Prognosis of hepatocellular carcinoma accompanied by microscopic portal vein invasion. World J Gastroenterol. 2009; 15:2632-2637.
12. Yamashita Y, Tsuijita E, Takeishi K, Fujiwara M, Kira S, Mori M, Aishima S, Taketomi A, Shirabe K, Ishida T, Maehara Y. Predictors for microinvasion of small hepatocellular carcinoma ≤ 2 cm. Ann Surg Oncol. 2012; 19:2027-2034.
13. Kaibori M, Matsui Y, Yanagida H, Yokoigawa N, Kwon AH, Kamiyama Y. Positive status of alpha-fetoprotein and des-gamma-carboxy prothrombin: important prognostic factor for recurrent hepatocellular carcinoma. World J Surg. 2004; 28:702-707.
14. Sawada T, Kubota K, Kita J, Kato M, Shiraki T, Park K, Shimoda M. Clinical outcome of hepatectomy for hepatocellular carcinomas ≤ 2 cm. World J Surg. 2011; 35:377-385.
15. Fukuda S, Itamoto T, Amano H, Kohashi T, Ohdan H, Tashiro H, Asahara T. Clinicopathologic features of hepatocellular carcinoma patients with compensated cirrhosis surviving more than 10 years after curative hepatectomy. World J Surg. 2007; 31:345-352.
16. Nobuoka D, Kato Y, Gotohda N, Takahashi S, Nakagohri T, Konishi M, Kinoshita T, Nakatsura T. Postoperative serum alpha-fetoprotein level is a useful predictor of recurrence after hepatectomy for hepatocellular carcinoma. Oncol Rep. 2010; 24:521-528.
17. Kim SH, Choi SB, Lee JG, Kim SU, Park MS, Kim do Y, Choi JS, Kim KS. Prognostic factors and 10-year survival in patients with hepatocellular carcinoma after curative hepatectomy. J Gastrointest Surg. 2011; 15:598-607.
18. Whitfield JB. Gamma glutamyl transferase. Crit Rev Clin Lab Sci. 2001; 38:263-355.
19. Sheehan M, Haythorn P. Predictive values of various liver function tests with respect to the diagnosis of liver disease. Clin Biochem. 1979; 12:262-263.
20. Braun JP, Bardies J, Thouvenot JP, Benard P, Rico AG. Serum gamma-glutamyltransferase in equids: Reference physiologic values. Am J Vet Res. 1982; 43:339-340.
21. Ellis G, Worthy E, Goldberg DM. Lack of value of serum gamma-glutamyl transferase in the diagnosis of hepatobiliary disease. Clin Biochem. 1979; 12:142-145.
22. Ju MJ, Qiu SJ, Fan J, Zhou J, Gao Q, Cai MY, Li YW, Tang ZY. Preoperative serum gamma-glutamyl transferase to alanine aminotransferase ratio is a convenient prognostic marker for Child-Pugh A hepatocellular carcinoma after operation. J Gastroenterol. 2009; 44:635-642.
23. Liu H, Zhang A, Qian N, Gao L, Xu L, Zhang W, Jiang K, Cai S, Huang Z, Dong J. Postoperative transarterial chemoembolization benefits patients with high gamma-glutamyl transferase levels after curative hepatectomy for hepatocellular carcinoma: A survival stratification analysis. Tohoku J Exp Med. 2012; 227:269-280.
24. Zhao WC, Zhang HB, Yang N, Fu Y, Qian W, Chen BD, Fan LF, Yang GS. Preoperative predictors of short-term survival after hepatectomy for multinodular hepatocellular carcinoma. World J Gastroenterol. 2012; 18:3272-3281.
25. Zhao WC, Fan LF, Yang N, Zhang HB, Chen BD, Yang GS. Preoperative predictors of microvascular invasion in multinodular hepatocellular carcinoma. Eur J Surg Oncol. 2013; 39:858-864.
26. Faber W, Sharafi S, Stockmann M, Denecke T, Sinn B, Puhl G, Bahra M, Malinowski MB, Neuhaus P, Seehofer D. Long-term results of liver resection for hepatocellular carcinoma in noncirrhotic liver. Surgery. 2013; 153:510-517.
27. Carr BI, Pancoska P, Branch RA. Low alpha-fetoprotein hepatocellular carcinoma. J Gastroenterol Hepatol. 2010; 25:1543-1549.
28. Guiu B, Deschamps F, Boulin M, Boige V, Malka D, Ducreux M, Hillon P, de Baère T. Serum gamma-glutamyl-transferase independently predicts outcome after transarterial chemoembolization of hepatocellular carcinoma: External validation. Cardiovasc Intervent Radiol. 2012; 35:1102-1108.
29. Nishikawa H, Nishijima N, Arimoto A, Inuzuka T, Kita R, Kimura T, Osaki Y. Prognostic factors in patients with hepatitis B virus-related hepatocellular carcinoma undergoing nucleoside analog antiviral therapy. Oncol Lett. 2013; 6:1213-1218.
30. Corti A, Duarte TL, Giommarelli C, De Tata V, Paolicchi A, Jones GD, Pompella A. Membrane gamma-glutamyl transferase activity promotes iron-dependent oxidative DNA damage in melanoma cells. Mutat Res. 2009; 669:112-121.
31. Weinberg ED. The role of iron in cancer. Eur J Cancer Prev. 1996; 5:19-36.
32. Stark AA, Russell JJ, Langenbach R, Pagano DA, Zeiger E, Huberman E. Localization of oxidative damage by a glutathione-gamma-glutamyl transpeptidase system in preneoplastic lesions in sections of livers from carcinogen-treated rats. Carcinogenesis. 1994; 15:343-348.
33. Larue L, Bellacosa A. Epithelial-mesenchymal transition in development and cancer: Role of phosphatidylinositol 3' kinase/AKT pathways. Oncogene. 2005; 24:7443-7454.
34. Javed S, Mejías-Luque R, Kalali B, Bolz C, Gerhard M. Helicobacter bilis gamma-glutamyltranspeptidase

enhances inflammatory stress response *via* oxidative stress in colon epithelial cells. PLoS One. 2013; 8:e73160.
35. Wu Y, Zhou BP: TNF-α/NF-κB/Snail pathway in cancer cell migration and invasion. Br J Cancer. 2010; 102:639-644.
36. Moon DO, Kim BY, Jang JH, Kim MO, Jayasooriya RG, Kang CH, Choi YH, Moon SK, Kim WJ, Ahn JS, Kim GY. K-RAS transformation in prostate epithelial cell overcomes H_2O_2-induced apoptosis *via* upregulation of gamma-glutamyltransferase-2. Toxicol In Vitro. 2012; 26:429-434.
37. Paolicchi A, Sotiropuolou M, Perego P, Daubeuf S, Visvikis A, Lorenzini E, Franzini M, Romiti N, Chieli E, Leone R, Apostoli P, Colangelo D, Zunino F, Pompella A. gamma-Glutamyl transpeptidase catalyses the extracellular detoxification of cisplatin in a human cell line derived from the proximal convoluted tubule of the kidney. Eur J Cancer. 2003; 39:996-1003.

(Received May 3, 2014; Accepted June 22, 2014)

DD&T
Drug Discoveries & Therapeutics

Guide for Authors

1. Scope of Articles

Drug Discoveries & Therapeutics welcomes contributions in all fields of pharmaceutical and therapeutic research such as medicinal chemistry, pharmacology, pharmaceutical analysis, pharmaceutics, pharmaceutical administration, and experimental and clinical studies of effects, mechanisms, or uses of various treatments. Studies in drug-related fields such as biology, biochemistry, physiology, microbiology, and immunology are also within the scope of this journal.

2. Submission Types

Original Articles should be well-documented, novel, and significant to the field as a whole. An Original Article should be arranged into the following sections: Title page, Abstract, Introduction, Materials and Methods, Results, Discussion, Acknowledgments, and References. Original articles should not exceed 5,000 words in length (excluding references) and should be limited to a maximum of 50 references. Articles may contain a maximum of 10 figures and/or tables.

Brief Reports definitively documenting either experimental results or informative clinical observations will be considered for publication in this category. Brief Reports are not intended for publication of incomplete or preliminary findings. Brief Reports should not exceed 3,000 words in length (excluding references) and should be limited to a maximum of 4 figures and/or tables and 30 references. A Brief Report contains the same sections as an Original Article, but the Results and Discussion sections should be combined.

Reviews should present a full and up-to-date account of recent developments within an area of research. Normally, reviews should not exceed 8,000 words in length (excluding references) and should be limited to a maximum of 100 references. Mini reviews are also accepted.

Policy Forum articles discuss research and policy issues in areas related to life science such as public health, the medical care system, and social science and may address governmental issues at district, national, and international levels of discourse. Policy Forum articles should not exceed 2,000 words in length (excluding references).

Case Reports should be detailed reports of the symptoms, signs, diagnosis, treatment, and follow-up of an individual patient. Case reports may contain a demographic profile of the patient but usually describe an unusual or novel occurrence. Unreported or unusual side effects or adverse interactions involving medications will also be considered. Case Reports should not exceed 3,000 words in length (excluding references).

News articles should report the latest events in health sciences and medical research from around the world. News should not exceed 500 words in length.

Letters should present considered opinions in response to articles published in Drug Discoveries & Therapeutics in the last 6 months or issues of general interest. Letters should not exceed 800 words in length and may contain a maximum of 10 references.

3. Editorial Policies

Ethics: Drug Discoveries & Therapeutics requires that authors of reports of investigations in humans or animals indicate that those studies were formally approved by a relevant ethics committee or review board.

Conflict of Interest: All authors are required to disclose any actual or potential conflict of interest including financial interests or relationships with other people or organizations that might raise questions of bias in the work reported. If no conflict of interest exists for each author, please state "There is no conflict of interest to disclose".

Submission Declaration: When a manuscript is considered for submission to Drug Discoveries & Therapeutics, the authors should confirm that 1) no part of this manuscript is currently under consideration for publication elsewhere; 2) this manuscript does not contain the same information in whole or in part as manuscripts that have been published, accepted, or are under review elsewhere, except in the form of an abstract, a letter to the editor, or part of a published lecture or academic thesis; 3) authorization for publication has been obtained from the authors' employer or institution; and 4) all contributing authors have agreed to submit this manuscript.

Cover Letter: The manuscript must be accompanied by a cover letter signed by the corresponding author on behalf of all authors. The letter should indicate the basic findings of the work and their significance. The letter should also include a statement affirming that all authors concur with the submission and that the material submitted for publication has not been published previously or is not under consideration for publication elsewhere. The cover letter should be submitted in PDF format. For example of Cover Letter, please visit http://www.ddtjournal.com/downcentre.php (Download Centre).

Copyright: A signed JOURNAL PUBLISHING AGREEMENT (JPA) must be provided by post, fax, or as a scanned file before acceptance of the article. Only forms with a hand-written signature are accepted. This copyright will ensure the widest possible dissemination of information. A form facilitating transfer of copyright can be downloaded by clicking the appropriate link and can be returned to the e-mail address or fax number noted on the form (Please visit Download Centre). Please note that your manuscript will not proceed to the next step in publication until the JPA form is received. In addition, if excerpts from other copyrighted works are included, the author(s) must obtain written permission from the copyright owners and credit the source(s) in the article.

Suggested Reviewers: A list of up to 3 reviewers who are qualified to assess the scientific merit of the study is welcomed. Reviewer information including names, affiliations, addresses, and e-mail should be provided at the same time the manuscript is submitted online. Please do not suggest reviewers with known conflicts of interest, including participants or anyone with a stake in the proposed research; anyone from the same institution; former students, advisors, or research collaborators (within the last three years); or close personal contacts. Please note that the Editor-in-Chief may accept one or more of the proposed reviewers or may request a review by other qualified persons.

Language Editing: Manuscripts prepared by authors whose native language is not English should have their work proofread by a native English speaker before submission. If not, this might delay the publication of your manuscript in Drug Discoveries & Therapeutics.

The Editing Support Organization can provide English proofreading, Japanese-English translation, and Chinese-English translation services to authors who want to publish in Drug Discoveries & Therapeutics and need assistance before submitting a manuscript. Authors can visit this organization directly at http://www.iacmhr.com/iac-eso/support.php?lang=en. IAC-ESO was established to facilitate manuscript preparation by researchers whose native language is not English and to help edit works intended for international academic journals.

4. Manuscript Preparation

Manuscripts should be written in clear, grammatically correct English and submitted as a Microsoft Word file in a single-column format. Manuscripts must be paginated and typed in 12-point Times New Roman font with 24-point line spacing. Please do not embed figures in the text. Abbreviations should be used as little as possible and should be explained at first mention unless the term is a well-known abbreviation (*e.g.* DNA). Single words should not be abbreviated.

Title page: The title page must include 1) the title of the paper (Please note the title should be short, informative, and contain the major key words); 2) full name(s) and affiliation(s) of the author(s), 3) abbreviated names of the author(s), 4) full name, mailing address, telephone/fax numbers, and e-mail address of the corresponding author; and 5) conflicts of interest (if you have an actual or potential conflict of interest to disclose, it must be included as a footnote on the title page of the manuscript; if no conflict of interest exists for each author, please state "There is no conflict of interest to disclose"). Please visit Download Centre and refer to the title page of the manuscript sample.

Abstract: The abstract should briefly state the purpose of the study, methods, main findings, and conclusions. For article types including Original Article, Brief Report, Review, Policy Forum, and Case Report, a one-paragraph abstract consisting of no more than 250 words must be included in the manuscript. For News and Letters, a brief summary of main content in 150 words or fewer should be included in the manuscript. Abbreviations must be kept to a minimum and non-standard abbreviations explained in brackets at first mention. References should be avoided in the abstract. Key words or phrases that do not occur in the title should be included in the Abstract page.

Introduction: The introduction should be a concise statement of the basis for the study and its scientific context.

Materials and Methods: The description should be brief but with sufficient detail to enable others to reproduce the experiments. Procedures that have been published previously should not be described in detail but appropriate references should simply be cited. Only new and significant modifications of previously published procedures require complete description. Names of products and manufacturers with their locations (city and state/country) should be given and sources of animals and cell lines should always be indicated. All clinical investigations must have been conducted in accordance with Declaration of Helsinki principles. All human and animal studies must have been approved by the appropriate institutional review board(s) and a specific declaration of approval must be made within this section.

Results: The description of the experimental results should be succinct but in sufficient detail to allow the experiments to be analyzed and interpreted by an independent reader. If necessary, subheadings may be used for an orderly presentation. All figures and tables must be referred to in the text.

Discussion: The data should be interpreted concisely without repeating material already presented in the Results section. Speculation is permissible, but it must be well-founded, and discussion of the wider implications of the findings is encouraged. Conclusions derived from the study should be included in this section.

Acknowledgments: All funding sources should be credited in the Acknowledgments section. In addition, people who contributed to the work but who do not meet the criteria for authors should be listed along with their contributions.

References: References should be numbered in the order in which they appear in the text. Citing of unpublished results, personal communications, conference abstracts, and theses in the reference list is not recommended but these sources may be mentioned in the text. In the reference list, cite the names of all authors when there are fifteen or fewer authors; if there are sixteen or more authors, list the first three followed by *et al*. Names of journals should be abbreviated in the style used in PubMed. Authors are responsible for the accuracy of the references. Examples are given below:

Example 1 (Sample journal reference):
Nakata M, Tang W. Japan-China Joint Medical Workshop on Drug Discoveries and Therapeutics 2008: The need of Asian pharmaceutical researchers' cooperation. Drug Discov Ther. 2008; 2:262-263.

Example 2 (Sample journal reference with more than 15 authors):
Darby S, Hill D, Auvinen A, *et al*. Radon in homes and risk of lung cancer: Collaborative analysis of individual data from 13 European case-control studies. BMJ. 2005; 330:223.

Example 3 (Sample book reference):
Shalev AY. Post-traumatic stress disorder: Diagnosis, history and life course. In: Post-traumatic Stress Disorder, Diagnosis, Management and Treatment (Nutt DJ, Davidson JR, Zohar J, eds.). Martin Dunitz, London, UK, 2000; pp. 1-15.

Example 4 (Sample web page reference):
World Health Organization. The World Health Report 2008 – primary health care: Now more than ever. *http://www.who.int/whr/2008/whr08_en.pdf* (accessed September 23, 2010).

Tables: All tables should be prepared in Microsoft Word or Excel and should be arranged at the end of the manuscript after the References section. Please note that tables should not in image format. All tables should have a concise title and should be numbered consecutively with Arabic numerals. If necessary, additional information should be given below the table.

Figure Legend: The figure legend should be typed on a separate page of the main manuscript and should include a short title and explanation. The legend should be concise but comprehensive and should be understood without referring to the text. Symbols used in figures must be explained.

Figure Preparation: All figures should be clear and cited in numerical order in the text. Figures must fit a one- or two-column format on the journal page: 8.3 cm (3.3 in.) wide for a single column, 17.3 cm (6.8 in.) wide for a double column; maximum height: 24.0 cm (9.5 in.). Please make sure that artwork files are in an acceptable format (TIFF or JPEG) at minimum resolution (600 dpi for illustrations, graphs, and annotated artwork, and 300 dpi for micrographs and photographs). Please provide all figures as separate files. Please note that low-resolution images are one of the leading causes of article resubmission and schedule delays. All color figures will be reproduced in full color in the online edition of the journal at no cost to authors.

Units and Symbols: Units and symbols conforming to the International System of Units (SI) should be used for physicochemical quantities. Solidus notation (*e.g.* mg/kg, mg/mL, mol/mm^2/min) should be used. Please refer to the SI Guide www.bipm.org/en/si/ for standard units.

Supplemental data: Supplemental data might be useful for supporting and enhancing your scientific research and Drug Discoveries & Therapeutics accepts the submission of these materials which will be only published online alongside the electronic version of your article. Supplemental files (figures, tables, and other text materials) should be prepared according to the above guidelines, numbered in Arabic numerals (*e.g.*, Figure S1, Figure S2, and Table S1, Table S2) and referred to in the text. All figures and tables should have titles and legends. All figure legends, tables and supplemental text materials should be placed at the end of the paper. Please note all of these supplemental data should be provided at the time of initial submission and note that the editors reserve the right to limit the size and length of Supplemental Data.

5. Submission Checklist

The Submission Checklist will be useful during the final checking of a manuscript prior to sending it to Drug Discoveries & Therapeutics for review. Please visit Download Centre and download the Submission Checklist file.

6. Online submission

Manuscripts should be submitted to Drug Discoveries & Therapeutics online at http://www.ddtjournal.com. The manuscript file should be smaller than 5 MB in size. If for any reason you are unable to submit a file online, please contact the Editorial Office by e-mail at office@ddtjournal.com

7. Accepted manuscripts

Proofs: Galley proofs in PDF format will be sent to the corresponding author *via* e-mail. Corrections must be returned to the editor (proof-editing@ddtjournal.com) within 3 working days.

Offprints: Authors will be provided with electronic offprints of their article. Paper offprints can be ordered at prices quoted on the order form that accompanies the proofs.

Page Charge: A page charge of $140 will be assessed for each printed page of an accepted manuscript. The charge for printing color figures is $340 for each page. Under exceptional circumstances, the author(s) may apply to the editorial office for a waiver of the publication charges at the time of submission.

(Revised February 2013)

Editorial and Head Office:

Pearl City Koishikawa 603
2-4-5 Kasuga, Bunkyo-ku
Tokyo 112-0003
Japan
Tel: +81-3-5840-9697
Fax: +81-3-5840-9698
E-mail: office@ddtjournal.com

DD&T
Drug Discoveries & Therapeutics

JOURNAL PUBLISHING AGREEMENT (JPA)

Manuscript No.:

Title:

Corresponding author:

The International Advancement Center for Medicine & Health Research Co., Ltd. (IACMHR Co., Ltd.) is pleased to accept the above article for publication in Drug Discoveries & Therapeutics. The International Research and Cooperation Association for Bio & Socio-Sciences Advancement (IRCA-BSSA) reserves all rights to the published article. Your written acceptance of this JOURNAL PUBLISHING AGREEMENT is required before the article can be published. Please read this form carefully and sign it if you agree to its terms. The signed JOURNAL PUBLISHING AGREEMENT should be sent to the Drug Discoveries & Therapeutics office (Pearl City Koishikawa 603, 2-4-5 Kasuga, Bunkyo-ku, Tokyo 112-0003, Japan; E-mail: office@ddtjournal.com; Tel: +81-3-5840-9697; Fax: +81-3-5840-9698).

1. Authorship Criteria

As the corresponding author, I certify on behalf of all of the authors that:

1) The article is an original work and does not involve fraud, fabrication, or plagiarism.
2) The article has not been published previously and is not currently under consideration for publication elsewhere. If accepted by Drug Discoveries & Therapeutics, the article will not be submitted for publication to any other journal.
3) The article contains no libelous or other unlawful statements and does not contain any materials that infringes upon individual privacy or proprietary rights or any statutory copyright.
4) I have obtained written permission from copyright owners for any excerpts from copyrighted works that are included and have credited the sources in my article.
5) All authors have made significant contributions to the study including the conception and design of this work, the analysis of the data, and the writing of the manuscript.
6) All authors have reviewed this manuscript and take responsibility for its content and approve its publication.
7) I have informed all of the authors of the terms of this publishing agreement and I am signing on their behalf as their agent.

2. Copyright Transfer Agreement

I hereby assign and transfer to IACMHR Co., Ltd. all exclusive rights of copyright ownership to the above work in the journal Drug Discoveries & Therapeutics, including but not limited to the right 1) to publish, republish, derivate, distribute, transmit, sell, and otherwise use the work and other related material worldwide, in whole or in part, in all languages, in electronic, printed, or any other forms of media now known or hereafter developed and the right 2) to authorize or license third parties to do any of the above.

I understand that these exclusive rights will become the property of IACMHR Co., Ltd., from the date the article is accepted for publication in the journal Drug Discoveries & Therapeutics. I also understand that IACMHR Co., Ltd. as a copyright owner has sole authority to license and permit reproductions of the article.

I understand that except for copyright, other proprietary rights related to the Work (*e.g.* patent or other rights to any process or procedure) shall be retained by the authors. To reproduce any text, figures, tables, or illustrations from this Work in future works of their own, the authors must obtain written permission from IACMHR Co., Ltd.; such permission cannot be unreasonably withheld by IACMHR Co., Ltd.

3. Conflict of Interest Disclosure

I confirm that all funding sources supporting the work and all institutions or people who contributed to the work but who do not meet the criteria for authors are acknowledged. I also confirm that all commercial affiliations, stock ownership, equity interests, or patent-licensing arrangements that could be considered to pose a financial conflict of interest in connection with the article have been disclosed.

Corresponding Author's Name (Signature):

Date: